ENERGY DISSIPATION IN TURBULENCE

by

Ali Pakzad

B.S. in pure Mathematics

Bahounar University, 2006

Submitted to the Graduate Faculty of

the Kenneth P. Dietrich School of Arts and Sciences in partial

fulfillment

of the requirements for the degree of

Doctor of Philosophy

University of Pittsburgh

2018

UNIVERSITY OF PITTSBURGH

DIETRICH SCHOOL OF ARTS AND SCIENCES

This dissertation was presented

by

Ali Pakzad

It was defended on

May 10, 2018

and approved by

Prof. William Layton, Dietrich School of Arts and Sciences, University of Pittsburgh

Prof. Gautam Iyer, Department of Mathematical Sciences, Carnegie Mellon University

Prof. Michael Neilan, Dietrich School of Arts and Sciences, University of Pittsburgh

Prof. Catalin Trenchea, Dietrich School of Arts and Sciences, University of Pittsburgh

Dissertation Director: Prof. William Layton, Dietrich School of Arts and Sciences, University of Pittsburgh

ENERGY DISSIPATION IN TURBULENCE

Ali Pakzad, PhD

University of Pittsburgh, 2018

The accurate simulation of turbulent flows is a central computational challenge in many important applications, including global climate change estimation, environmental science, ocean and atmosphere dynamics, energy efficiency improvement and optimization of industrial processes. As an example, turbulence predictions are key to limiting damage of hurricanes (estimated to be hundreds of billions of dollars in 2017). These are fundamentally non-linear problems that probed in this thesis through numerical computations and supporting mathematical analysis. The accuracy of turbulence models depends on their turbulent dissipation. The dissipation is studied and it is utilized to validate results with the *Statistical Equilibrium Law* as the benchmark:

- In Chapter 3, the energy dissipation in a turbulence model discretized on an under-resolved mesh is delineated. This is the first connection between computational experience and mathematical analysis in this direction [63].
- It is rigorously proved in Chapter 4 that the over-dissipation (wrong accuracy) of a turbulence model can be corrected using van Driest damping [62]. This had been an open question (e.g. [5] p. 78) since 1963.
- The temperature in natural convection is uniformly bounded in time. Although the problem has been studied for a long time, no better bounds for the approximate temperature than an exponential growth in time were obtained e.g. [78, 79, 87]. In Chapter 5, it is proved that the temperature approximation is bounded sub-linearly in time by introducing a new interpolation [19].

TABLE OF CONTENTS

LIST OF FIGURES

DEDICATION

Foremost, I would like to offer my gratitude to my supervisor Dr. William Layton from whom I have learned so much not only about fluid dynamics, but also about life. He is someone you instantly love and never forget once you meet him. Without his extraordinary insight and support, this dissertation would have been a distant dream. I always admire the way he has encouraged me and pushed me to succeed. He always says: "Never rest, until good is better and better is best."

I am also deeply grateful to Dr. Catalin Trenchea for his support and many valuable discussions and suggestions in my research. I also wish to thank Dr. Gautam Iyer and Dr. Michael Neilan for serving on my committee and for their insightful comments on this thesis.

I want to express to my gratitude to Dr. Peyman Givi for his stimulating lectures on various topics in computational fluid dynamics, from which my research has greatly benefited. A special thanks goes to Dr. John Chadam and Dr. Satish Iyengar for their willingness to discuss and support from the beginning.

I will forever be thankful to my dear cousin Dr. Reza Pakzad, who initially introduced the attractive world of Mathematics to me. His contributions to my success extend beyond availability for discussions.

I always owe my deepest gratitude to my beloved mother and father. My hard-working parents have sacrificed their lives for my sister and myself and provided us an unconditional love and care.

Eventually, I would also like to extend my special regards and loves to my lovely wife, Maryam, who encourage and support me during this challenging journey. As she has dedicated herself to supporting my dreams, I cannot sufficiently thank her, but I dedicate this work to her and our beautiful daughter, Johnna.

1.0 INTRODUCTION

The accurate simulation of turbulent flows is a central computational challenge in many important applications, including global climate change estimation, environmental science, ocean and atmosphere dynamics, energy efficiency improvement and optimization of industrial processes. As two examples, turbulence predictions are key to limiting damage of hurricanes (estimated to be hundreds of billions of dollars in 2017). In addition, 85% of the energy in the US is generated by combustion for which accurate simulation of turbulent mixing is critical for energy efficiency optimization.

One of the most fascinating features in turbulent flows is the emergence of complicated chaotic structures involving a wide range of length scales behind which typical flow patterns are still recognizable [73]. The state of motion is too complex to allow for a detailed description of the fluid velocity and experimental or numerical measurements. One of the main challenges in fluid dynamics is thus the derivation of quantitative statements on turbulent flows to validate a result from a model. In this thesis the time-averaged energy dissipation rate is employed as a **benchmark** (e.g. [58] and [35]) to check the results' accuracy and validate the model's simulation. The classical **Statistical Equilibrium Law** is based on the concept of the energy cascade. Considering U and L as the global velocity and length scales, time-averaged energy dissipation rate $\langle\varepsilon\rangle$ scales as (Kolmogorov 1941)

$$\langle\varepsilon\rangle \simeq \frac{U^3}{L}.$$

Saffman 1968 [70] addressed this estimate and wrote:

This result is fundamental to an understanding of turbulence and yet still lacks theoretical support.

As was predicted by Richardson [69] and Kolmogorov [43], in turbulent flows and in the limit of the high Reynolds number, the energy dissipation rate is often observed to approach a limit independent of the viscosity [20]. In the 1990s, Doering and Constantin [15] and Doering and Foias [17] estimated the energy dissipation rigorously and directly from the equations of motion, $\langle\varepsilon\rangle \leq C\,\frac{U^3}{L}$. Similar estimations have been proven by Marchiano [53], Wang [85] and Kerswell [42] in more generality. There are many numerical (e.g. [7] and [61]) and experimental (e.g. [81] and [75]) evidence to support the Statistical Equilibrium Law.

These are the fundamentally non-linear problems that have been probed in this thesis through numerical computations and supporting mathematical analysis. The accuracy of turbulence models depends on their turbulent dissipation. This dissipation is investigated here and it is utilized to validate results with the Statistical Equilibrium Law as the benchmark.

Although all chapters are related conceptually, each chapter is written such that it can be read independently.

In Chapter 2, we introduce some fundamental concepts and motivations used extensively in this thesis.

In Chapter 3, upper bounds are derived on the *computed* time-averaged energy dissipation rate, $\langle\varepsilon(u^h)\rangle$, for an under-resolved mesh h for turbulent shear flow [63]. Because of the limitations of computers, we are forced to struggle with the meaning of the under-resolved flow simulation. Turbulence models are introduced to account for sub-mesh scale effects, when solving fluid flow problem numerically on an under-resolved spatial mesh size h [47]. One key in getting a good approximation for a turbulence model is to correctly calibrate the energy dissipation $\varepsilon(u)$ in the model on the under-resolved mesh and understand how the energy dissipation rates for different scales depend on the physical parameters [46]. The energy dissipation rates of various turbulence models have been analyzed assuming infinite resolution (i.e. for the continuous model e.g. [15], [45], [46], [53], [62] and [85]), but not coarse resolution. The unexplored question is: What is the time-averaged energy dissipation rate $\langle\varepsilon(u^h)\rangle$, when u^h is an approximation of u on a coarse mesh h, associated with the computational cost?

In Chapter 4, we study the time-averaged energy dissipation rate $\langle\varepsilon_{SMD}(u)\rangle$ for the

combination of the Smagorinsky model and a damping function. The Smagorinsky model is well known to over-damp [71]. One common correction is to include damping functions that reduce the effects of model viscosity near walls [67]. There has been many numerical tests but no analytic support of this fact since 1956 (cited in [5] p.78). Mathematical analysis is given in Chapter 4 that allows the evaluation of $\langle \varepsilon_{SMD}(u) \rangle$ for any damping function. Moreover, the analysis motivates a modified van Driest damping. We rigorously prove that the combination of the Smagorinsky model with this modified damping function does not over dissipate and is also consistent with Kolmogorov phenomenology [62].

In Chapter 5, we improve the stability estimates for the velocity, temperature and pressure approximation in the natural convection problem. Natural convection of a fluid driven by heating a wall is a classical problem in fluid mechanics that is still of technological and scientific importance (e.g. [11] and [26]). The temperature in natural convection problems is, under mild data assumptions, uniformly bounded in time. This property has not yet been proven for the standard finite element method (FEM) approximation of natural convection problems with nonhomogeneous Dirichlet boundary conditions, e.g., the differentially heated vertical wall and Rayleigh-Bénard problems. However, when this often analyzed problem is approximated by standard FEM, all available stability bounds for the temperature exhibit exponential growth in time, e.g. [78, 79, 87]. Even in the stationary case, stability estimates can yield extremely restrictive mesh conditions $h = \mathcal{O}(Ra^{-10})$ [12], when Ra is the dimensionless Rayleigh number. We prove that provided the first mesh line in the finite element mesh is within $\mathcal{O}(Ra^{-1})$ of the heated wall, the computed velocity, pressure, and temperature in the natural convection problems are stable allowing for sub-linear growth in time [19].

2.0 BACKGROUND

In this chapter we are going to provide mathematical preliminaries on the Navier-Stokes equations. We briefly describe the Richardson energy cascade, and from there, we discuss the motivation behind a turbulence model in Large Eddy Simulation. We end the chapter by introducing the most classical turbulence model in LES, the Smagorinsky model.

2.1 THE NAVIER-STOKES EQUATIONS

Consider the flow of an incompressible fluid with the kinematic viscosity ν. The velocity and pressure (u, p) satisfy the Navier-Stokes equations for $0 < t < \infty$ in the bounded and regular flow domain Ω in $\mathbb{R}^3$

$$u_t + u \cdot \nabla u - \nu \Delta u + \nabla p = f(x,t) \quad \text{and} \quad \nabla \cdot u = 0 \quad \text{in } \Omega, \tag{2.1.1}$$

subject to the no-slip condition on $\partial\Omega$, initial conditions and pressure normalization conditions

$$u = 0 \quad \text{on } \partial\Omega \times (0,\infty), \;\; u(x,0) = u_0(x) \quad \text{in } \Omega \text{ and } \int_\Omega p(x,t)dx = 0. \tag{2.1.2}$$

Here $f(x,t) \in L^\infty(0,\infty; L^2(\Omega)^3)$ is the force and $u_0 \in L^2(\Omega)^3$ is a weakly divergence-free initial condition. The Navier-Stokes equations (NSE) which describe the motion of viscous Newtonian fluids should be solved forward in time for $u(x,t)$ and $p(x,t)$, starting from an initial divergence-free velocity field $u_0(x)$. Moreover, (2.1.1) is nothing more than the Newton's second law of motion when $u_t + u \cdot \nabla u$ is acceleration of a fluid element and $\nu \bigtriangledown u - \nabla p$ is the force per unit mass density due to the neighboring elements [15].

Although there has been considerable progress since the NSE was presented in 1840 by French engineer Claude Louis Marie Henri Navier, a number of fundamental questions about its solutions remain, and several constitute grand challenges for the mathematics community. Indeed, it is not known whether the three-dimensional Navier-Stokes equations possess unique smooth solutions at high Reynolds number. This problem is one of the seven most important open problems in mathematics for which the Clay Mathematics institute has offered a one-million-dollar prize for a proof or a counterexample.

2.1.1 Mathematical Preliminaries, Notations and Definitions

We use the standard notations $L^p(\Omega), W^{k,p}(\Omega), H^k(\Omega) = W^{k,2}(\Omega)$ for the Lebesgue and Sobolev spaces respectively. The inner product in the space $L^2(\Omega)$ will be denoted by $(\cdot,\cdot)$ and its norm by $||\cdot||$ for scalar, vector and tensor quantities. Norms in Sobolev spaces $H^k(\Omega), k > 0$, are denoted by $||\cdot||_{H^k}$ and the usual L^p norm is denoted by $||\cdot||_p$. The symbols C and C_i for $i = 1, 2, 3$ stand for generic positive constant independent of ν, L and U. In addition, ∇u is the gradient tensor $(\nabla u)_{ij} = \frac{\partial u_j}{\partial x_i}$ for $i, j = 1, 2, 3$. $\mathbf{D}(u) := \frac{1}{2}(\nabla u + \nabla u^\top)$ denotes the deformation tensor. L is the characteristic length of the domain and U is the characteristic velocity. The *Reynolds number* is defined as

$$\mathcal{R}e = \frac{UL}{\nu}.$$

In fluid dynamics, the Reynolds number plays an important role to help predict similar flow patterns in different fluid flow situations. It is roughly defined as the ratio of inertial forces to viscous forces. If $\mathcal{R}e$ is small, then the viscous forces are dominant and the flow tends to be smooth and move slowly (laminar flow). For very large $\mathcal{R}e$ the flow is dominated by the inertial forces and featured by instabilities and chaotic small-scales motions (turbulence).

The following function spaces will be used to define the weak solution of the NSE in Definition 2.1.3.

$$H(\Omega) := \{v \in L^2(\Omega);\ \nabla \cdot v = 0 \quad \text{and} \quad v \cdot \hat{n} = 0 \quad \text{on} \quad \partial\Omega\},$$

$$Q := L_0^2 = \{q \in L^2(\Omega);\ \int_\Omega q\, dx = 0\},$$

$$V := \{v \in H_0^1;\ (q, \nabla \cdot v) = 0 \quad \forall q \in Q\},$$

$$L^2(0,T;V) := \{v(t) : [0,T] \to V;\ \int_0^T \|\nabla v\|^2 < \infty\},$$

$$L^\infty(0,T;H(\Omega)) := \{v(t); [0,T] \to H(\Omega);\ \text{ess sup}_{0<t<T}\|v\| < \infty\}.$$

Definition 2.1.1. (Energy Dissipation Rate) The energy dissipation rate per unit volume of the flow at time t is

$$\varepsilon(u) := \frac{\nu}{|\Omega|}\|\nabla u(\cdot,t)\|^2,$$

and the time-averaged of the quantity g is

$$\langle g \rangle := \limsup_{T\to\infty} \frac{1}{T}\int_0^T g(\cdot,t)dt.$$

The time-averaged energy dissipation rate per unit mass is

$$\langle \varepsilon(u) \rangle := \limsup_{T\to\infty} \frac{1}{T}\int_0^T \varepsilon(u)dt = \frac{\nu}{|\Omega|}\limsup_{T\to\infty} \frac{1}{T}\int_0^T \|\nabla u\|^2 dt = \frac{\nu}{|\Omega|}\langle \|\nabla u\|^2 \rangle. \tag{2.1.3}$$

The *energy dissipation rate* is one of the most critical quantities in the theory of turbulence. Upper bounds yield estimates on the small length scales in the solutions. Moreover, the system's global attractor, if it exists, is also controlled by this quantity [85]. The work done by forces such as drag are balanced by the energy dissipation rate in steady-state problems. Upper bounds for the energy dissipation rate are applied to estimate length scales and, in particular, overall complexity of turbulent flow simulation [46]. Moreover, it is usual to compute time-averaged flow statistics in practical simulations of fluid dynamic and match them against benchmark averages; see, e.g. [34] or [35].

Definition 2.1.2. (Trilinear from) Define the trilinear form b on $H^1 \times H^1 \times H^1$ as,

$$b(u,v,w) := \frac{1}{2}(u \cdot \nabla v, w) - \frac{1}{2}(u \cdot \nabla w, v).$$

2.1.2 Variational Formulation and Continuous-in-Time Finite Element Discretization of NSE

The weak solutions of NSE, introduced by Leray [48], satisfies not only the Navier-Stokes equations in the weak sense but also the energy inequality (for details on the distinction between weak and strong solution see [13]).

Definition 2.1.3. (Weak solution of NSE) Let $u_0 \in H(\Omega)$, $f \in L^2(\Omega \times (0,T))$. A measurable function $u(x,t) : \Omega \times [0,T] \to \mathbb{R}^d$ is a weak solution of NSE if

1. $u \in L^2(0,T;V) \cap L^\infty(0,T;H(\Omega))$,
2. $u(x,t)$ satisfies the integral relation

$$\int_0^T (u_t, v) + \nu(\nabla u, \nabla v) + (u \cdot \nabla u, v) - (p, \nabla \cdot v)\, dt = \int_0^T (f, v)\, dt \qquad \forall v \in C_0^\infty(\Omega \times (0,T)),$$

3. $u(x,t')$ satisfies the energy inequality for all $t \in [0,T]$

$$\frac{1}{2}||u(t')||^2 + \nu \int_0^t ||\nabla u(t')||^2\, dt' \leq \frac{1}{2}||u_0||^2 + \int_0^t (u(t'), f(t'))\, dt',$$

4. $\lim_{t\to 0} ||u(t) - u_0|| = 0$.

These are integrated versions of equations (2.1.1) that make sense for velocity fields $u(x,t)$ that may not be smooth enough to be differentiated as required to satisfy the partial differential equations (2.1.1) pointwise in space and time. The basic idea behind the construction of weak solutions is to start with an appropriately regularized approximation to the Navier-Stokes equations to which solutions may be shown to exist for all times and then consider the limit of these approximate solutions as the regularization is removed [15]. In two dimensions, it is known that a weak solution exists and is unique. In $3d$, it is proven that weak solution exist, Leray [48], but it is not known if weak solutions are unique.

To discretize the NSE, let T_h be a quasiuniform tetrahedral or 3-D rectangular mesh of Ω with mesh size $h \in (0,1)$. Consider $X^h \subset H_0^1(\Omega)$ be the Lagrange finite element space including continuous piecewise linear functions associated with the mesh T_h. We shall assume throughout the thesis that the pressure finite element space $Q^h \subset L_0^2(\Omega)$ is conforming, has

approximation properties typical of finite element spaces commonly in use and satisfies the following discrete inf-sup condition where $\beta^h > 0$ uniformly in h as $h \to 0$

$$\inf_{q^h \in Q^h} \sup_{v^h \in X^h} \frac{(q^h, \nabla \cdot v^h)}{||\nabla v^h|| ||q^h||} \geq \beta^h > 0. \tag{2.1.4}$$

The approximate velocity and pressure are maps: $u^h : [0,T] \longrightarrow X^h$, $p^h : (0,T] \longrightarrow Q^h$ satisfying

$$\begin{aligned} (u_t^h, v^h) + \nu(\nabla u^h, \nabla v^h) + b(u^h, u^h, v^h) - (p^h, \nabla \cdot v^h) &= (f, v^h) \quad \forall v^h \in X^h, \\ (\nabla \cdot u^h, q^h) &= 0 \qquad \forall q^h \in Q^h, \\ (u^h(x,0) - u_0(x), v^h) &= 0 \qquad \forall v^h \in X^h. \end{aligned} \tag{2.1.5}$$

By choosing a basis for (X^h, Q^h) and expanding (u^h, q^h) in terms of the basis, the above equations (2.1.5) reduce to a nonlinear system of ODE's in t with a linear side condition. Then approximate velocities and pressures can be computed by using a time stepping method (for more details see [27] or [29]). Under the inf-sup condition (2.1.4) the pressure can be eliminated temporarily from the system by restricting v^h in (2.1.5) to the space of discretely divergence free function V^h

$$V^h := \{v^h \in X^h : (q^h, \nabla \cdot v^h) = 0, \forall q^h \in Q^h\}.$$

Moreover, under the discrete inf-sup condition (2.1.4), system (2.1.5) is equivalent to: find $u^h : [0,T] \longrightarrow V^h$ which satisfies

$$(u_t^h, v^h) + \nu(\nabla u^h, \nabla v^h) + b(u^h, u^h, v^h) = (f, v^h) \qquad \forall v^h \in V^h. \tag{2.1.6}$$

Remark 2.1.1. The inf-sup condition (2.1.4) plays the key role of ensuring that, given a unique velocity, there is a corresponding pressure. It is also critical to bounding the fluid pressure and showing the pressure is stable [23].

2.2 ENERGY CASCADE

Turbulent flow is observed to consist of a cascade of three-dimensional eddies of various sizes. The picture of the energy cascade was first described by Richardson [69] as follows. Energy is input into the largest scales of the flow. The large eddies are unstable and break up. There is an intermediate range (inertial range) in which non-linearity drives energy into smaller scales and conserves the global energy because dissipation is negligible. These smaller eddies undergo a similar break up process, and transfer their energy to yet smaller eddies. This energy cascade, in which energy is transferred to successively smaller and smaller eddies, continues until the Reynolds number is sufficiently small and dissipation is non negligible. The molecular viscosity is then effective in dissipating the kinetic energy and the energy in those smallest eddies decays to zero exponentially fast (Figure 1). $E(K)$ and K are kinetic energy and wave number respectively in Figure 1. The data were gathered from 17 different flow by Saddoughi and Veeravalli (1994) are perfectly consistent with the described energy cascade and Figure 1 (see p. 235 of [67]).

Solutions of the NSE exhibit this energy cascade. This fact has been understood since the work of L. F. Richardson and A. N. Kolmororov and is based on a few fundamental properties of solutions of the NSE (see the details on [47]). One reason that the above description is of importance is that it places dissipation at the end of a sequence of processes. Therefore, the rate of dissipation is determined by the first process in the sequence, which is the transfer of energy from the largest eddies. These largest eddies have energy of order U^2 and timescale $\tau = \frac{L}{U}$, so the rate of transfer of energy can be scaled as $\frac{U}{\tau} = \frac{U^3}{L}$. This implies the **Equilibrium Dissipation Law** for time-averaged energy dissipation rate $\langle\varepsilon\rangle$ (Kolmogorov 1941); $\langle\varepsilon\rangle \simeq \frac{U^3}{L}$.

2.3 LARGE EDDY SIMULATION

In Kolmogorov's description of the eddies in turbulent flow in 1941, the large eddies are deterministic in nature. Those below a critical size die quickly due to viscous forces [20].

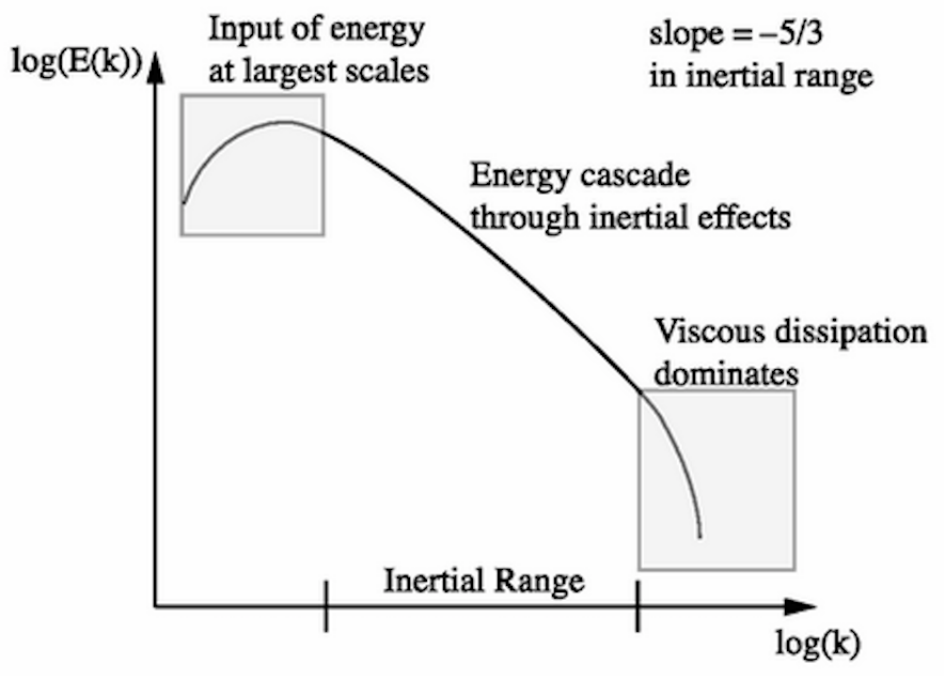

Figure 1: A diagram of the energy cascade at very high Reynolds number.

This critical length scale, *Kolmogorov microscale*, is $\eta = \mathcal{O}(\mathcal{R}e^{-\frac{3}{4}})$ and $\mathcal{O}(\mathcal{R}e^{-\frac{1}{2}})$ in three and two dimensions respectively. To simulate properly the persistent eddies in a three-dimensional flow, $\mathcal{O}(\mathcal{R}e^{\frac{9}{4}})$ mesh points in space per time-step are required. For example for a small airplane with $\mathcal{R}e = 2 \times 10^7$, 10^{16} mesh points are required. This number increases to at least 10^{20} mesh points for an atmospheric flow. Such a procedure is called a *direct numerical simulation* (DNS) and is not practical (at the present time!) for many interesting flows.

One approach to the simulation of turbulent flow is called *Large Eddy Simulation* (LES). The aim is to simulate accurately the motion of those eddies of size $\geq \delta$. From the numerical point of view, δ is associated with the mesh size h ($\simeq$ computational cost). Once a coarse mesh ($\gg$ Kolmogorov microscale) is selected, the mean effects of small eddies (smaller than the coarse mesh size) on the large eddies should be modeled. Regarding the energy cascade, small eddies act to drain energy from the large eddies. Therefore, it is required to model the energy lost to the resolved scales.

2.3.1 Models in Large Eddy Simulation

According to the LES and from the point of view of applications, only those flow structures above a certain length scale $\delta = \mathcal{O}(h)$ can be computed or represented. The mathematical derivation of any LES model from the NSE proceeds as follows. Consider the length scale $\delta > 0$ and a smooth function $g(x) = (\frac{6}{\pi})^{\frac{3}{2}} \exp(-6|x|^2)$. The mollifier $g_\delta(x)$ is defined by:

$$g_\delta(x) := \delta^{-3}\, g(\frac{x}{\delta}).$$

The local spacial filter is defined by convolution with g_δ. Given $u(x)$ define:

$$\bar{u}(x) := (g_\delta \star u)(x) = \int_{\mathbb{R}^3} g_\delta(x-y)u(y)dy,$$

where u is extended by zero outside of Ω. This convolution eliminates any local oscillations smaller than $\mathcal{O}(\delta)$. Ignoring boundaries for the moment and averaging the incompressible Navier-Stokes equations (2.1.1) with constant filter width δ (i.e. take $g_\delta\star$ NSE(u)) gives:

$$\bar{u}_t + \bar{u}\cdot\nabla\bar{u} - \nu\Delta\bar{u} + \nabla\bar{p} + \nabla\cdot\mathbf{R}(u,u) = \bar{f} \quad \text{and} \quad \nabla\cdot\bar{u} = 0 \quad \text{in } \Omega, \tag{2.3.1}$$

where $\mathbf{R}(u,u)$ denotes the *sub-filter scale stress tensor*

$$\mathbf{R}(u,u) := \overline{u\,u} - \bar{u}\,\bar{u}.$$

Since $\mathbf{R}$ is a function of u and $\bar{u}$, system (2.3.1) is not closed. The simplest closure assumption is that the turbulent stress is a linear function of the large scale's deformation tensor $\mathbf{D}(\bar{u})$ [67]. This assumption denotes the *Eddy Viscosity Hypothesis* and is quite old in fluid mechanics. It is based on the energy cascade and the fact that "the small eddies act to drain energy from the large eddies." This model is given by:

$$\nabla\cdot\mathbf{R}(u,u) \sim -\nabla\cdot(2\nu_T\mathbf{D}(\bar{u})), \tag{2.3.2}$$

where ν_T is the turbulent viscosity coefficient and is required to be modeled [1].

[1]The substitution (2.3.2) is not strictly correct. In fact, $\mathbf{R}$ must be split into two parts

$$\mathbf{R} = \big(\mathbf{R} - \frac{1}{3}\text{trace}(\mathbf{R})\mathbf{I}\big) + \frac{1}{3}\text{trace}(\mathbf{R})\mathbf{I}.$$

2.3.2 The Smagorinsky Model

In 1963 Joseph Smagorinsky [2] proposed the following model for the turbulent viscosity coefficient,

$$\nu_T = (C_s\delta)^2|\mathbf{D}(u)|. \tag{2.3.3}$$

In (2.3.3) C_s is the standard model parameter whose correct value is still under debate [5]. Using Körn's inequality for $1 < p < \infty$ [31], it can be shown that $\|\mathbf{D}(u)\|_p \simeq \|\nabla u\|_p$. Therefore, for simplification in the energy calculation, one can replace $\nabla \cdot (2(C_s\delta)^2|\mathbf{D}(u)|\mathbf{D}(u))$ by $\nabla \cdot ((C_s\delta)^2|\nabla u|\nabla u)$ in the model. Although in this thesis we focus on the following version of the Smagorisky model, the analysis herein holds for both by the same argument.

$$u_t + u \cdot \nabla u - \nu\Delta u + \nabla p - \nabla \cdot ((C_s\delta)^2|\nabla u|\nabla u) = f. \tag{2.3.4}$$

In general, the eddy viscosity term $\nabla \cdot ((C_s\delta)^2|\nabla u|\nabla u)$ with $\delta = \mathcal{O}(h)$ is added to the Navier-Stokes equations to model the extra dissipation which cannot be captured by the NSE viscous term on an under-resolved mesh. The Smagorinsky model has proved to be the workhorse in the large eddy simulation of flow. The model was used in 1967 to develop the first coupled atmosphere - ocean climate models for studies of global warming, emphasizing the important differences between the equilibrium and transient responses to increasing carbon dioxide.

The average of the stresses, $\frac{1}{3}\text{trace}(\mathbf{R})\mathbf{I}$, is incorporated into the turbulent pressure in (2.3.1). i.e.

$$\bar{p} + \frac{1}{3}\text{trace}(\mathbf{R})\mathbf{I} \Longrightarrow \bar{p}.$$

The trace free part of $\mathbf{R}$ is then modeled by the turbulent diffusion,

$$\nabla \cdot \left(\mathbf{R} - \frac{1}{3}\text{trace}(\mathbf{R})\mathbf{I}\right) \sim -\nabla \cdot (2\nu_T\mathbf{D}(\bar{u})).$$

[2] Joseph Smagorinsky was a leader in the 1950's in using numerical methods and mathematical models to predict trends in weather and climate. He was the first to show that practical forecasting could really be done by solving the Navier-Stokes equations.

3.0 ANALYSIS OF MESH EFFECTS ON TURBULENT FLOW STATISTICS

Because of the limitations of computers, we are forced to struggle with the meaning of under-resolved flow simulations. Turbulence models are introduced to account for sub-mesh scale effects, when solving fluid flow problems numerically. One key in getting a good approximation for a turbulent model is to correctly calibrate the energy dissipation $\varepsilon(u)$ in the model on an under-resolved mesh [46]. The energy dissipation rates of various turbulent models have been analyzed assuming infinite resolution (i.e. for the continuous model e.g. [15], [45], [46], [53], [62] and [85]). The question explored herein is: What is the time-averaged energy dissipation rate $\langle\varepsilon(u^h)\rangle$, when u^h is an approximation of u on a given mesh h (fixed computational cost) for the Smagorinsky model?

Numerical simulations of turbulent flows include only the motion of eddies above some length scale δ (which depends on attainable resolution). The state of motion in turbulence is too complex to allow for a detailed description of the fluid velocity. Benchmarks are required to validate simulations' accuracy. Two natural benchmarks for numerical simulations are the kinetic energy in the eddies of size $> \mathcal{O}(\delta)$ and the energy dissipation rates of eddies in size $> \mathcal{O}(\delta)$ (e.g. [58] and [35]). Motivated from here, we focus on the calculation of the time-averaged energy dissipation rates of motions larger than δ. In the large-eddy simulation (LES), predicting how flow statistics (e.g. time-averaged) depend on the grid size h and the filter size δ is listed as one of ten important questions by Pope [66].

$$\begin{aligned} u_t + u\cdot\nabla u - \nu\Delta u + \nabla p - \nabla\cdot((C_s\delta)^2|\nabla u|\nabla u) = 0, \\ \nabla\cdot u = 0 \qquad \text{and} \quad u(x,0) = u_0 \quad \text{in } \Omega. \end{aligned} \tag{3.0.1}$$

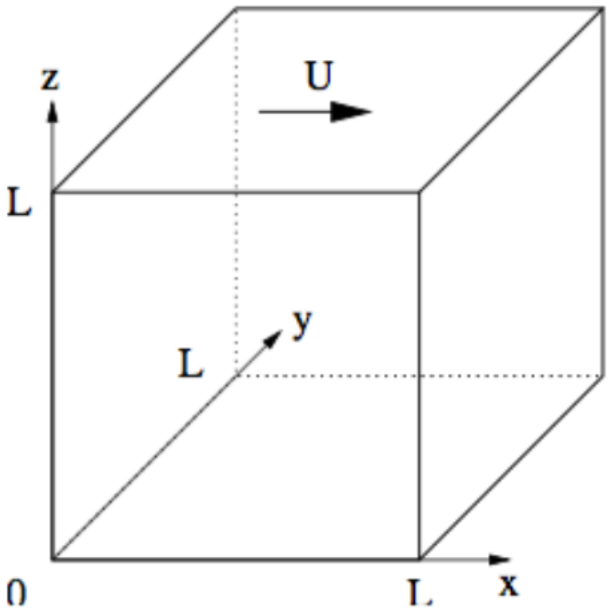

Figure 2: Shear flow boundary condition.

Consider the Smagorinsky model (3.0.1) subject to a boundary-induced shear (3.0.2) in the flow domain $\Omega = (0, L)^3$,

In (3.0.1) u is the velocity field, p is the pressure, ν is the kinematic viscosity, δ is the turbulence-resolution length scale (associated with the mesh size h) and $C_s \simeq 0.1$ is the standard model parameter (see Lilly [50] for more details). We consider shear flow, containing a turbulent boundary layer, in a domain that is simplified to permit more precise analysis. L-periodic boundary conditions in x and y directions are imposed. $z = 0$ is a fixed wall and the wall $z = L$ moves with velocity U (Figure 2),

$$\begin{aligned} &L - \text{periodic boundary condition in } \ x \text{ and } \ y \text{ direction,} \\ &u(x, y, 0, t) = (0, 0, 0)^\top \quad \text{and} \quad u(x, y, L, t) = (U, 0, 0)^\top. \end{aligned} \tag{3.0.2}$$

To disregard the effects of the time discretization on dissipation, we consider (3.0.1) continuous in time and discretized in space (see (3.1.6)) by a standard finite element method

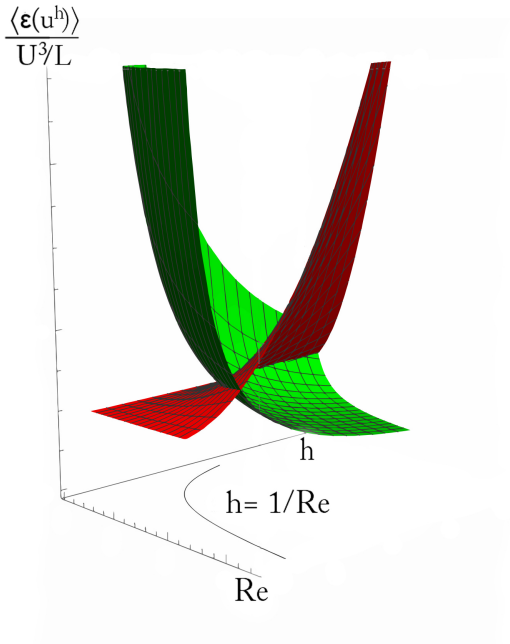

Figure 3: Dissipation vs. h and $\mathcal{R}e$.

since the effects of the spatial discretization, and not the time discretization, on dissipation is the subject of study here. In Theorem 3.2.1, we first estimate $\langle \varepsilon(u^h) \rangle$ for fine enough mesh that no model to be necessary ($h < \mathcal{O}(\mathcal{R}e^{-1})\, L$). Since models are used for meshes coarser than a DNS, we next investigate (3.0.1) on an arbitrary coarse mesh. Theorem 3.2.3 presents the analysis of $\langle \varepsilon(u^h) \rangle$ on an under-resolved mesh. The results in Theorems 3.2.1 and 3.2.3 can be summarized as,

$$\frac{\langle \varepsilon(u^h) \rangle}{U^3/L} \simeq \begin{cases} 1 + (\frac{c_s \delta}{L})^2\, \mathcal{R}e^2 & \text{for} \quad h < \mathcal{O}(\mathcal{R}e^{-1})\, L \\ \frac{1}{\mathcal{R}e}\, \frac{L}{h} + (\frac{C_s\, \delta}{h})^2 + \frac{L^5}{(C_s \delta)^4\, h} + \frac{L^{\frac{5}{2}}}{(C_s\, \delta)^4}\, h^{\frac{3}{2}} & \text{for} \quad h \geq \mathcal{O}(\mathcal{R}e^{-1})\, L \end{cases} . \tag{3.0.3}$$

Considering $\delta = h$ in (3.0.3), which is the common choice in LES [66], we speculate that $\frac{\langle \varepsilon(u^h) \rangle}{U^3/L}$ varies with $\mathcal{R}e$ and h as depicted qualitatively in figure 3.

Remark 3.0.1. Shear flow has two natural microscales. The Kolmogorov microscale is $\eta \simeq \mathcal{R}e^{-\frac{3}{4}}\, L$, and describes the size of the smallest persistent motion away from walls. The second

length is $\mathcal{R}e^{-1}\,L$ which denotes the turbulent boundary layer. Our analysis here, and (3.0.3), indicates this latter scale is the more important one for shear flow.

In (3.0.3), $\langle\varepsilon(u^h)\rangle$ scales as $\frac{U^3}{L}$ as predicted by Richardson and Kolmogorov. For the fully-resolved case, this estimate is consistent as $\mathcal{R}e \to \infty$ and $\delta = h \simeq \mathcal{O}(\mathcal{R}e^{-1})$ with the rate proven for the Navier-Stokes equations in [15]. On the other hand, the weak $\mathcal{R}e$ dependence in the under-resolved case (that vanishes as $\mathcal{R}e \to \infty$) is consistent with Figure 4, adopted from [20]. This figure shows how the dissipation coefficient varies with Reynolds number for a circular cylinder based on experimental data quoted in [82]. Tritton [82] observed that the dissipation coefficient behaves as $\mathcal{R}e^{-1}$ for small $\mathcal{R}e$, and at high Reynolds number stays approximately constant independent of the viscosity. Theorem 3.2.3 is also consistent with the recent results in [56] derived through structure function theories of turbulence. Corollaries 3.2.6 and 3.2.8 show that the estimate (3.0.3) suggests over-dissipation of the model for any choice of $C_s > 0$ and $\delta > 0$. In other words, the constant C_s causes excessive damping of large-scale fluctuation, which agrees the computational experience (p.247 of Sagaut [71]). There are several model refinements to reduce this over-dissipation such as the damping function [62].

In Sections 3.1, we collect necessary mathematical tools. In Section 3.2, the major results are proven. We end this chapter with numerical illustrations and conclusions in Sections 3.3 and 3.4.

3.0.1 Motivation and Related Works

In turbulence, dissipation predominantly occurs at small scales. Once a mesh (of size h) is selected, an eddy viscosity term $\nabla\cdot((C_s\delta)^2|\nabla u|\nabla u)$ in (3.0.1) with $\delta = \mathcal{O}(h)$ is added to the Navier-Stokes equations (NSE), $C_s = 0$ in (3.0.1), to model this extra dissipation which can not be captured by the NSE viscous term on an under-resolved mesh.

Turbulence is about prediction of velocities' averages rather than the point-wise velocity. One commonly used average in turbulent flow modeling is time-averaging. Time averages seem to be predictable even when dynamic flow behavior over bounded time intervals is irregular [20]. Time averaging is defined in terms of the limit superior (lim sup) of a function

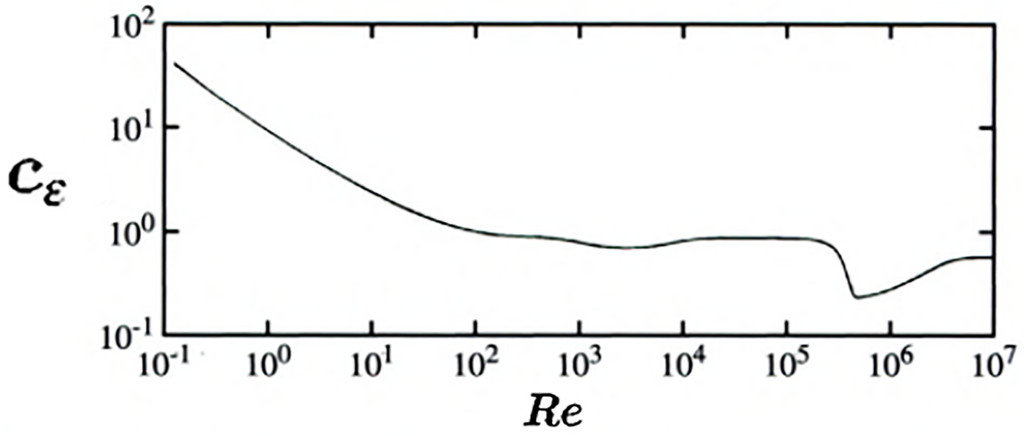

Figure 4: Variation of dissipation coefficient with Reynolds number for circular cylinder.

as,

$$\langle \psi \rangle = \limsup_{T \to \infty} \frac{1}{T} \int_0^T \psi(t)\, dt.$$

The classical **Statistical Equilibrium Law** is based on the concept of the energy cascade. Energy is input into the largest scales of the flow, then the kinetic energy cascade from large to small scale of motions. When it reaches a scale small enough for the viscous dissipation to be effective, it dissipates mostly into heat (Richardson 1922, [69]). Since viscous dissipation is negligible through this cascade, the energy dissipation rate is related then to the power input to the largest scales at the first step in the cascade. These largest eddies have energy $\frac{1}{2}U^2$ and time scale $\tau = \frac{L}{U}$, this implies the equilibrium dissipation law for time-averaged energy dissipation rate $\langle \varepsilon \rangle$ (Kolmogorov 1941),

$$\langle \varepsilon \rangle = \mathcal{O}(\frac{U^2}{\tau}) \simeq C_\varepsilon \frac{U^3}{L},$$

with C_ε = constant. Saffman 1968 [70], addressing the estimate of the energy dissipation rates, $\langle \varepsilon \rangle \simeq \frac{U^3}{L}$, and wrote that,

This result is fundamental to an understanding of turbulence and yet still lacks theoretical support.

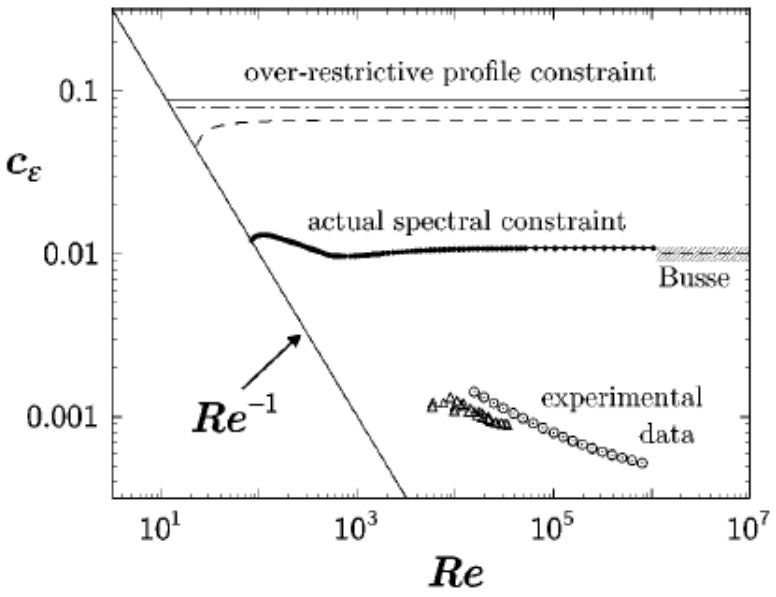

Figure 5: C_ϵ versus $\mathcal{R}e$, adopted from [60].

Information about C_ε carries interesting information about the structure of the turbulent flow. Therefore mathematically rigorous upper bounds on C_ε are of high relevance. There are many analytical ([15], [53] and [85]), numerical [7] and experimental [75] evidence to support the equilibrium dissipation law; some of them are mentioned below.

Taylor [81] considered C_ε to be constant for geometrically similar boundaries. His work led to the question "If C_ε depends on geometry, boundary and inlet conditions". Since then, a multitude of laboratory experiments [75] and numerical simulations [7] concerned with isotropic homogeneous turbulence seem to confirm that C_ε is independent of Reynolds number in the limit of high Reynolds number, but are not conclusive as to whether C_ε is universal at such high Reynolds number values. In fact, the high Reynolds number values of C_ε seem to differ from flow to flow. The first results in 3D obtained for turbulent shear flow between parallel plates by Howard [33] and Busse [10] under assumptions that the flow is statistically stationary. There is an asymptotic non-zero upper bound, $C_\epsilon \simeq 0.01$ as $\mathcal{R}e \to \infty$, first derived by Busse [10] (Joining dashed line in Figure 5). The lower bound on C_ε is already given for laminar flow by Doering and Constantin, $\frac{1}{\mathcal{R}e} \leq C_\varepsilon$ (solid slanted

straight line in Figure 5). Rigorous asymptotic $\mathcal{R}e \to \infty$ dissipation rate bounds of the form $\langle \varepsilon \rangle \leq C_\varepsilon \frac{U^3}{L}$, with $C_\epsilon \simeq 0.088$ (topmost horizontal solid line in Figure 5), were derived for a number of boundary-driven flows during the 1990s (Doering and Constantin [15]). The residual dissipation bound like this appeared for a shear layer turbulent Taylor-Couette flow- where L was the layer thickness and U was the overall velocity drop across the layer. The upper bound has been confirmed with higher precision in [61] as $C_\epsilon \simeq 0.01087$ (Heavy dots in Figure 5). The corresponding experimental data measured by Reichardt [68] for the plane Couette flow (Triangles in Figure 5) and by Lathrop, Fineberg, and Swinney [44] for the small-gap Taylor-Couette system (Circles in Figure 5).

3.0.2 Why the Eddy Viscosity model and not the Navier- Stokes Equations?

A shear flow is one where the boundary condition is tangential. The flow problem with the boundary condition like (3.0.2) becomes very close to the flow between rotating cylinders. Flow between rotating cylinders is one of the classic problems in experimental fluid dynamics (e.g. [20]).

Consider the Navier Stokes equations, $C_s = 0$ in (3.0.1), with the boundary condition (3.0.2). The difficulty in the analysis of the energy dissipation of the shear flow appears due to the effect of the non-homogeneous boundary condition on the flow. The classical approach is required to construct a careful and non-intuitive choice of background flow Φ known as the Hopf extension [32].

Definition 3.0.1. Let $\Phi(x, y, z) := (\phi(z), 0, 0)$, where,

$$\phi(z) = \begin{cases} 0 & \text{if } z \in [0, L-h] \\ \frac{U}{h}(z - L + h) & \text{if } z \in [L-h, L] \end{cases}. \tag{3.0.4}$$

The strategy is to subtract off the inhomogeneous boundary conditions (3.0.2). Consider $v = u - \Phi$, then v satisfies homogeneous boundary conditions. Substituting $u = v + \Phi$ in the NSE yields,

$$v_t + v \cdot \nabla v - \nu \Delta v + \nabla p + \phi(z) \frac{\partial v}{\partial x} + v_3 \phi'(z)(1, 0, 0) = \nu \phi''(z)(1, 0, 0), \tag{3.0.5}$$

$$\nabla \cdot v = 0.$$

The key idea in making progress in the mathematical understanding of the energy dissipation rate is the energy inequality. Taking inner product (3.0.5) with $v = (v_1, v_2, v_3)$ and integrating over Ω gives,

$$\frac{1}{2}\frac{\partial}{\partial t}||v||^2 + \nu||\nabla v||^2 + \int_\Omega \left(\phi(z)\frac{\partial v}{\partial x}\cdot v + v_1 v_3 \phi'(z)\right) dx = \int_\Omega \nu\phi''(z)v_1\, dx. \tag{3.0.6}$$

However the NSE are rewritten to make the viscous term easy to handle, the nonlinear term changes and must again be wrestled with. To calculate the energy dissipation, the non-linear terms should be controlled by the diffusion term. Since both terms are quadratic in u, considering current tools in analysis, this control is doable only by assuming h in Definition 3.0.1 being small. Doering and Constantin [15] used the NSE to find an upper bound on the time-averaged energy dissipation rate for shear driven turbulence, assuming $h \simeq \mathcal{R}e^{-1}$. Similar estimations have been proven by Marchiano [53], Wang [85] and Kerswell [42] in more generality. For the semi-discrete NSE, John, Layton and Manica [39] show that assuming infinite resolution near the boundaries, computed time-averaged energy dissipation rate $\langle\varepsilon(u^h)\rangle$ for the shear flow scales as predicted for the continuous flow by the Kolmogorov theory,

$$\langle\varepsilon(u^h)\rangle \simeq \frac{U^3}{L}.$$

Now the question arises: How to find $\langle\varepsilon(u^h)\rangle$ for shear driven turbulence without any restriction on the mesh size? With current analysis tools, the effort seems to be hopeless. Therefore the p-laplacian term,

$$\nabla\cdot(|\nabla u|^{p-2}\,\nabla u), \tag{3.0.7}$$

was added to the NSE. This modification will lead to the $p^{\text{th}}-$ degree term on the left side of the energy inequality. Then applying appropriate Young's inequality on the non-linear term, we will absorb it on the $p^{\text{th}}-$ degree term without any restriction on h. Herein, we focus on $p = 3$ (the Smagorinsky model (3.0.1)), but the analysis for $p > 3$ remains as an interesting problem.

3.1 MATHEMATICAL PRELIMINARIES, NOTATIONS AND DEFINITIONS

We use the standard notations $L^p(\Omega), W^{k,p}(\Omega), H^k(\Omega) = W^{k,2}(\Omega)$ for the Lebesgue and Sobolev spaces respectively. The inner product in the space $L^2(\Omega)$ will be denoted by $(\cdot,\cdot)$ and its norm by $||\cdot||$ for scalar, vector and tensor quantities. Norms in Sobolev spaces $H^k(\Omega), k > 0$, are denoted by $||\cdot||_{H^k}$ and the usual L^p norm is denoted by $||\cdot||_p$. The symbols C and C_i for $i = 1, 2, 3$ stand for generic positive constant independent of the ν, L and U. In addition, ∇u is the gradient tensor $(\nabla u)_{ij} = \frac{\partial u_j}{\partial x_i}$ for $i, j = 1, 2, 3$.

The Reynolds number is $\mathcal{R}e = \frac{UL}{\nu}$. The time-averaged energy dissipation rate for model (3.0.1) includes dissipation due to the viscous forces and the turbulent diffusion. It is given by,

$$\langle \varepsilon(u) \rangle = \limsup_{T\to\infty} \frac{1}{T} \int_0^T \left(\frac{1}{|\Omega|} \int_\Omega \nu |\nabla u|^2 + (c_s \delta)^2 |\nabla u|^3 dx \right) dt. \tag{3.1.1}$$

Definition 3.1.1. The velocity at a given time t is sought in the space

$$\mathbb{X}(\Omega) := \{u \in H^1(\Omega) : u(x, y, 0) = (0, 0, 0),\ u(x, y, L) = (U, 0, 0),$$
$$u \text{ is } L\text{-periodic in } x \text{ and } y \text{ direction}\}.$$

The test function space is

$$\mathbb{X}_0(\Omega) := \{u \in H^1(\Omega) : u(x, y, 0) = (0, 0, 0),\ u(x, y, L) = (0, 0, 0),$$
$$u \text{ is } L\text{-periodic in } x \text{ and } y \text{ direction}\}.$$

The pressure at time t is sought in

$$Q(\Omega) := L^2_0(\Omega) = \{q \in L^2(\Omega) :\ \textstyle\int_\Omega q dx = 0\}.$$

And the space of divergence-free functions is denoted by

$$V(\Omega) := \{u \in \mathbb{X}(\Omega) :\ (\nabla \cdot u, q) = 0\ \forall q \in Q\}.$$

Lemma 3.1.1. Φ in Definition 3.0.1 satisfies,

a) $\|\Phi\|_\infty \le U$, b) $\|\nabla\Phi\|_\infty \le \frac{U}{h}$, c) $\|\Phi\|^2 \le \frac{U^2L^2h}{3}$,

d) $\|\nabla\Phi\|^2 \le \frac{U^2L^2}{h}$, e) $\|\nabla\Phi\|_3^3 \le \frac{U^3L^2}{h^2}$, f) $||\nabla\Phi||_{\frac{3}{2}}^{\frac{3}{2}} = \frac{U^3L^4}{h}$.

Proof. They all are the immediate consequences of the Definition 3.0.1. □

Remark 3.1.2. Φ extends the boundary conditions (3.0.2) to the interior of Ω. Moreover, it is a divergence-free function. $h \in (0, L)$ stands for the spatial mesh size.

Using a standard scaling argument in the next lemma shows how the constant C_ℓ in the Sobolev inequality $||u||_6 \leq C_\ell ||\nabla u||_3$ depends on the geometry in $\mathbb{R}^3$.

Lemma 3.1.3. Consider the Sobolev inequality $||u||_6 \leq C_\ell ||\nabla u||_3$, then C_ℓ is the order of $L^{\frac{1}{2}}$ when the domain is $\Omega = [0, L]^3$, i.e.

$$||u||_6 \leq C\, L^{\frac{1}{2}} ||\nabla u||_3.$$

Proof. Let $\Omega = [0, L]^3$, $\hat{\Omega} = [0, 1]^3$ and for simplicity $x = (x_1, x_2, x_3)$ and $\hat{x} = (\hat{x}_1, \hat{x}_2, \hat{x}_3)$. Consider the change of variable $\eta : \hat{\Omega} \longrightarrow \Omega$ by $\eta(\hat{x}) = L\,\hat{x} = x$. If $u(L\hat{x}) = \hat{u}(\hat{x})$, using the chain rule gives,

$$\frac{d}{d\hat{x}_i}(\hat{u}(\hat{x})) = \frac{d}{d\hat{x}_i}(u(L\hat{x})) = L\frac{du}{dx_i}(L\hat{x}),$$

for $i = 1, 2, 3$ and since $L\hat{x} = x$ we have,

$$\frac{1}{L}\frac{d\hat{u}}{d\hat{x}_i} = \frac{du}{dx_i}. \tag{3.1.2}$$

Using (3.1.2) and the change of variable formula, one can show,

$$||\frac{\partial u_i}{\partial x_j}||_3^3 = \int_\Omega |\frac{\partial u_i}{\partial x_j}|^3\, dx = \int_{\hat{\Omega}} \frac{1}{L^3} |\frac{\partial \hat{u}_i}{\partial \hat{x}_j}|^3\, L^3 d\hat{x} = ||\frac{\partial \hat{u}_i}{\partial \hat{x}_j}||_3^3,$$

therefore,

$$||\nabla u||_3^3 = \sum_{i,j=1}^{3} ||\frac{\partial u_i}{\partial x_j}||_3^3 = \sum_{i,j=1}^{3} ||\frac{\partial \hat{u}_i}{\partial \hat{x}_j}||_3^3 = ||\hat{\nabla}\hat{u}||_3^3. \tag{3.1.3}$$

Again by applying the change of variable formula, we have,

$$||u||_{L^6(\Omega)} = (\int_\Omega |u|^6 dx)^{\frac{1}{6}} = (\int_{\hat{\Omega}} L^3\, |\hat{u}|^6 d\hat{x})^{\frac{1}{6}} = L^{\frac{1}{2}} ||\hat{u}||_{L^6(\hat{\Omega})},$$

using the Sobolev inequality and also inequality (3.1.3) on the above equality leads to,

$$||\hat{u}||_{L^6(\hat{\Omega})} = L^{-\frac{1}{2}} ||u||_{L^6(\Omega)} \leq L^{-\frac{1}{2}} C_\ell ||\nabla u||_3 = L^{-\frac{1}{2}} C_\ell ||\hat{\nabla}\hat{u}||_3, \tag{3.1.4}$$

therefore as claimed $C_\ell = \mathcal{O}(L^{\frac{1}{2}})$. □

We will need the well-known dependence of the Poincaré -Friedrichs inequality constant on the domain. A straightforward argument in the thin domain $\mathcal{O}_h$ implies Lemma 3.1.4.

Lemma 3.1.4. Let $\mathcal{O}_h = \{(x, y, z) \in \Omega : L - h \leq z \leq L\}$ be the region close to the upper boundary. Then we have

$$\|u - \Phi\|_{L^2(\mathcal{O}_h)} \leq h\|\nabla(u - \Phi)\|_{L^2(\mathcal{O}_h)}. \tag{3.1.5}$$

Proof. The proof is standard. For details see Lemma 4.1.3. □

3.1.1 Variational Formulation and Discretization

The variational formulation is obtained by taking the scalar product $v \in \mathbb{X}_0$ and $q \in L^2_0$ with (3.0.1) and integrating over the space Ω.

$$\begin{aligned}(u_t, v) + \nu(\nabla u, \nabla v) + (u \cdot \nabla u, v) - (p, \nabla \cdot v) + ((C_s\delta)^2|\nabla u|\nabla u, \nabla v) = 0 \quad \forall v \in \mathbb{X}_0,\\ (\nabla \cdot u, q) = 0 \quad \forall q \in L^2_0,\\ (u(x, 0) - u_0(x), v) = 0 \quad \forall v \in \mathbb{X}_0.\end{aligned} \tag{3.1.6}$$

To discretize the SM, consider two finite-dimensional spaces $\mathbb{X}^h \subset \mathbb{X}$ and $\mathbb{Q}^h \subset \mathbb{Q}$ satisfying the following discrete inf-sup condition where $\beta^h > 0$ uniformly in h as $h \to 0$,

$$\inf_{q^h \in \mathbb{Q}^h} \sup_{v^h \in X^h} \frac{(q^h, \nabla \cdot v^h)}{||\nabla v^h||||q^h||} \geq \beta^h > 0. \tag{3.1.7}$$

The inf-sup condition (3.1.7) plays a significant role in studies of the finite-element approximation of the Navier-Stokes equations. It is usually taken as a criterion of whether or not the families of finite-element spaces yield stable approximations. In the other words, it ensures given the unique velocity, there is a corresponding pressure. It is also critical to bounding the fluid pressure and showing the pressure is stable [29].

Consider a subspace $V^h \subset \mathbb{X}^h$ defined by:

$$V^h := \{v^h \in X^h : (q^h, \nabla \cdot v^h) = 0, \forall q^h \in \mathbb{Q}^h\}.$$

Note that most often $V^h \not\subset V$ and $\nabla \cdot u^h \neq 0$ for any $u^h \in V^h$. Thus we need an extension of the trilinear from $(u \cdot \nabla v, w)$ as follows.

Definition 3.1.2. (Trilinear from) Define the trilinear form b on $\mathbb{X} \times \mathbb{X} \times \mathbb{X}$ as:

$$b(u, v, w) := \frac{1}{2}(u \cdot \nabla v, w) - \frac{1}{2}(u \cdot \nabla w, v).$$

Lemma 3.1.5. The nonlinear term $b(\cdot, \cdot, \cdot)$ is continuous on $\mathbb{X} \times \mathbb{X} \times \mathbb{X}$ (and thus on $V \times V \times V$ as well). Moreover, we have the following skew-symmetry properties for $b(\cdot, \cdot, \cdot)$,

$$b(u, v, w) = (u \cdot \nabla v, w) \quad \forall u \in V \text{ and } v, w \in \mathbb{X},$$

Moreover,

$$b(u, v, v) = 0 \quad \forall u, v \in \mathbb{X}.$$

Proof. The proof is standard, see p.114 of Girault and Raviart [27]. □

The semi-discrete/continuous-in-time finite element approximation continues by selecting finite element spaces $\mathbb{X}_0^h \subset \mathbb{X}_0$. The approximate velocity and pressure of the Smagorinsky problem (3.0.1) are $u^h : [0, T] \longrightarrow \mathbb{X}^h$ and $p^h : (0, T] \longrightarrow \mathbb{Q}^h$ such that,

$$\begin{aligned}
(u_t^h, v^h) + \nu(\nabla u^h, \nabla v^h) + b(u^h, u^h, v^h) - (p^h, \nabla \cdot v^h) + (C_s\delta)^2|\nabla u^h|\nabla u^h, \nabla v^h) = 0 \quad \forall v^h \in \mathbb{X}_0^h, \\
(\nabla \cdot u^h, q^h) = 0 \quad \forall q^h \in \mathbb{Q}^h, \\
(u^h(x, 0) - u_0(x), v^h) = 0 \quad \forall v^h \in \mathbb{X}_0^h.
\end{aligned} \tag{3.1.8}$$

3.2 THEOREMS AND PROOFS

In this section, we present upper bounds on the *computed* time-averaged energy dissipation rate for the Smagorinsky model (3.0.1) subject to the shear flow boundary condition (3.0.2). Theorem 3.2.1 considers the case when the mesh size is fine enough $h < \mathcal{O}(\mathcal{R}e^{-1})\, L$. The restriction on the mesh size arises from the mathematical analysis of constructible background flow in finite element space.

On the other hand, Theorem 3.2.3 investigates $\langle \varepsilon(u^h) \rangle$ for any mesh size $0 < h < L$. We then take a minimum of two bounds to find the optimal upper bound in (3.0.3) with respect to current analysis.

Theorem 3.2.1. **(fully-resolved mesh)** Suppose $u_0 \in L^2(\Omega)$ and mesh size $h < (\frac{1}{5}\mathcal{R}e^{-1})L$. Then $\langle \varepsilon(u^h) \rangle$ satisfies,

$$\langle \varepsilon(u^h) \rangle \leq C \left[1 + (\frac{C_s\delta}{L})^2\, \mathcal{R}e^2\right] \frac{U^3}{L}.$$

Proof. Let $h = \gamma L$ in Definition 3.0.1 for $0 < \gamma < L$. Take $v^h = u^h - \Phi \in \mathbb{X}_0^h$ in (3.1.8). Since $b(\cdot,\cdot,\cdot)$ is skew-symmetric (Lemma 3.1.5) and $\nabla \cdot \Phi = 0$, we have,

$$(u_t^h, u^h - \Phi) + \nu(\nabla u^h, \nabla u^h - \nabla\Phi) + b(u^h, u^h, u^h - \Phi) + ((C_s\delta)^2 |\nabla u^h| \nabla u^h, \nabla u^h - \nabla\Phi) = 0,$$

and integrate in time to get,

$$\begin{aligned} &\frac{1}{2}\|u^h(T)\|^2 - \frac{1}{2}\|u^h(0)\|^2 + \nu\int_0^T \|\nabla u^h\|^2 dt + \int_0^T (\int_\Omega (C_s\delta)^2 |\nabla u^h|^3 dx) dt = (u^h(T), \Phi) \\ &- (u^h(0), \Phi) + \int_0^T b(u^h, u^h, \Phi) dt + \nu\int_0^T (\nabla u^h, \nabla\Phi) dt + (C_s\delta)^2 \int_0^T (|\nabla u^h| \nabla u^h, \nabla\Phi) dt. \end{aligned} \tag{3.2.1}$$

Using the Cauchy-Schwarz-Young's inequality and Lemma 3.1.1 for $h = \gamma L$ to bound the right-hand side of the above energy equality:

$$(u^h(T), \Phi) \leq \frac{1}{2}\|u^h(T)\|^2 + \frac{1}{2}\|\Phi\|^2 = \frac{1}{2}\|u^h(T)\|^2 + \frac{U^2\gamma L^3}{6}. \tag{3.2.2}$$

$$(u^h(0), \Phi) \leq \|u^h(0)\| \|\Phi\| = \sqrt{\frac{\gamma}{3}} U L^{\frac{3}{2}} \|u^h(0)\|. \tag{3.2.3}$$

$$\nu \int_0^T (\nabla u^h, \nabla \Phi) dt \leq \frac{\nu}{2} \int_0^T \|\nabla u^h\|^2 + \|\nabla \Phi\|^2 dt = \frac{\nu}{2} \int_0^T \|\nabla u^h\|^2 dt + \frac{\nu}{2} \frac{U^2 L}{\gamma} T. \tag{3.2.4}$$

Next, the nonlinear term $b(\cdot, \cdot, \cdot)$ in (3.2.1) can be rewritten as,

$$\begin{aligned} b(u^h, u^h, \Phi) &= b(u^h - \Phi, u^h - \Phi, \Phi) + b(\Phi, u^h - \Phi, \Phi) \\ &= \frac{1}{2} b(u^h - \Phi, u^h - \Phi, \Phi) - \frac{1}{2} b(u^h - \Phi, \Phi, u^h - \Phi) \\ &+ \frac{1}{2} b(\Phi, u^h - \Phi, \Phi) - \frac{1}{2} b(\Phi, \Phi, u^h - \Phi). \end{aligned} \tag{3.2.5}$$

Each term in (3.2.5) is estimated separately as follows using Lemma 3.1.4 and the Cauchy-Schwarz-Young's inequality. For the first term in (3.2.5) we have,

$$\begin{aligned} &b(u^h - \Phi, u^h - \Phi, \Phi) \leq \|\Phi\|_{L^\infty} \|u^h - \Phi\|_{L^2} \|\nabla (u^h - \Phi)\|_{L^2} \leq \gamma L U \|\nabla (u^h - \Phi)\|_{L^2}^2 \\ &\leq \gamma L U \|\nabla u^h - \nabla \Phi\|_{L^2}^2 \leq U L \gamma (\|\nabla u^h\| + \|\nabla \Phi\|)^2 \leq U L \gamma (2\|\nabla u^h\|^2 + 2\|\nabla \Phi\|^2) \\ &\leq U L \gamma (2\|\nabla u^h\|^2 + 2\frac{U^2 L}{\gamma}) = 2U L \gamma \|\nabla u^h\|^2 + 2U^3 L^2. \end{aligned} \tag{3.2.6}$$

For the second term we have,

$$\begin{aligned} &b(u^h - \Phi, \Phi, u^h - \Phi) \leq \|\nabla \Phi\|_{L_\infty} \|u^h - \Phi\|^2 \leq \frac{U}{\gamma L} \gamma^2 L^2 \|\nabla (u^h - \Phi)\|^2 \\ &\leq \gamma^2 L^2 \frac{U}{\gamma L} (2\|\nabla u^h\|^2 + 2\frac{U^2 L}{\gamma}) = 2\gamma L U \|\nabla u^h\|^2 + 2U^3 L^2. \end{aligned} \tag{3.2.7}$$

The third one is estimated as,

$$\begin{aligned} &b(\Phi, u^h - \Phi, \Phi) \leq \|\Phi\|_{L^\infty} \|\nabla (u^h - \Phi)\|_{L^2} \|\Phi\|_{L^2} \leq U \sqrt{\frac{U^2 \gamma L^3}{3}} (\|\nabla u^h\| + \|\nabla \Phi\|) \\ &\leq U \sqrt{\frac{U^2 \gamma L^3}{3}} (\|\nabla u^h\| + \sqrt{\frac{U^2 L}{\gamma}}) \leq \frac{U^2 \gamma^{\frac{1}{2}} L^{\frac{3}{2}}}{\sqrt{3}} \|\nabla u^h\| + \frac{U^3 L^2}{\sqrt{3}} \\ &= [\frac{U^{\frac{3}{2}} L}{\sqrt{3}}] \ [(U\gamma L)^{\frac{1}{2}} \|\nabla u^h\|] + \frac{U^3 L^2}{\sqrt{3}} \leq (\frac{U^3 L^2}{6}) + \frac{1}{2} U L \gamma \|\nabla u^h\|^2 + \frac{U^3 L^2}{\sqrt{3}} \\ &= \frac{1}{2} U L \gamma \|\nabla u^h\|^2 + (\frac{\sqrt{3}}{3} + \frac{1}{6}) U^3 L^2. \end{aligned} \tag{3.2.8}$$

And finally the last one satisfies,

$$
\begin{aligned}
&b(\Phi,\Phi,u^h-\Phi)\le\|\Phi\|_{L^\infty}\|\nabla\Phi\|_{L^2}\|u^h-\Phi\|_{L^2}\le U\sqrt{\frac{U^2L}{\gamma}}\gamma L\|\nabla(u^h-\Phi)\|_{L^2}\\
&\le U^2\gamma^{\frac12}L^{\frac32}(\|\nabla u^h\|+\|\nabla\Phi\|)\le U^2\gamma^{\frac12}L^{\frac32}(\|\nabla u^h\|+(\frac{U^2L}{\gamma})^{\frac12})\\
&=U^2\gamma^{\frac12}L^{\frac32}\|\nabla u^h\|+U^3L^2=[U^{\frac32}L]\ [(UL\gamma)^{\frac12}\|\nabla u^h\|]+U^3L^2\\
&\le\frac12(U^3L^2)+\frac12UL\gamma\|\nabla u^h\|^2+U^3L^2=\frac12UL\gamma\|\nabla u^h\|^2+\frac32U^3L^2.
\end{aligned}
\tag{3.2.9}
$$

Use (3.2.6), (3.2.7), (3.2.8) and (3.2.9) in (3.2.5) gives the final estimation for the non-linear term as below,

$$
|b(u^h,u^h,\Phi)|\le\frac52UL\gamma\|\nabla u^h\|^2+\frac{19}{6}U^3L^2. \tag{3.2.10}
$$

Finally, using Hölder's inequality and Young's inequality for $p=\frac32$ and $q=3$ and lemma 3.1.3 on the last term gives,

$$
\begin{aligned}
|(|\nabla u^h|\nabla u^h,\nabla\Phi)|&\le\int_\Omega|\nabla u^h|^2\cdot\nabla\Phi\,dx\\
&\le(\int_\Omega|\nabla u^h|^3)^{\frac23}(\int_\Omega|\nabla\Phi|^3)^{\frac13}\\
&\le\frac23(\int_\Omega|\nabla u^h|^3)+\frac13(\int_\Omega|\nabla\Phi|^3)\le\frac23(\int_\Omega|\nabla u^h|^3)+\frac13\frac{U^3}{\gamma^2}.
\end{aligned}
\tag{3.2.11}
$$

Inserting (3.2.2), (3.2.3), (3.2.4), (3.2.10) and (3.2.11) in (3.2.1) implies,

$$
\begin{aligned}
(\frac{\nu}{2}-\frac52\gamma LU)\int_0^T\|\nabla u^h\|^2dt+\frac13\int_0^T(\int_\Omega(C_s\delta)^2|\nabla u^h|^3dx)dt\le\frac12\|u^h(0)\|^2+\frac16U^2\gamma L^3\\
+\sqrt{\frac{\gamma}{3}}UL^{\frac32}\|u^h(0)\|+\frac{19}{6}U^3L^2T+\frac{\nu}{2\gamma}LU^2T+\frac13(C_s\delta)^2\frac{U^3T}{\gamma^2}.
\end{aligned}
\tag{3.2.12}
$$

Dividing (3.2.12) by T and $|\Omega|=L^3$ and taking limsup as $T\to\infty$ lead to,

$$
min\{\frac12-\frac52\frac{\gamma LU}{\nu},\frac13\}\langle\varepsilon(u^h)\rangle\le\frac{19}{6}\frac{U^3}{L}+\frac{\nu}{2\gamma}\frac{U^2}{L^2}+\frac13(C_s\delta)^2\frac{U^3}{\gamma^2L^3}.
$$

Let $\gamma<\frac15\mathcal{R}e^{-1}$, then $min\{\frac12-\frac52\frac{\gamma LU}{\nu},\frac13\}>0$ and the above estimate becomes,

$$
\langle\varepsilon(u^h)\rangle\le C\left[1+(\frac{C_s\delta}{L})^2\mathcal{R}e^2\right]\frac{U^3}{L},
$$

which proves the theorem.

□

Remark 3.2.2. The kinetic energy, $\frac{1}{2}\|u^h\|^2$, is not required in the proof to be uniformly bounded in time since it was canceled out from both sides after inserting (3.2.2) in (3.2.1).

The estimate in Theorem 3.2.1 goes to $\frac{U^3}{L}$ for fixed $\mathcal{R}e$ as $C_s\,\delta \to 0$, which is consistent with the rate proven for NSE by Doering and Constantin [15]. But it over dissipates for fixed δ as $\mathcal{R}e \to \infty$ as derived for the continuous case by Layton [46]. To fix this issue, one can suggest a super fine filter size $\delta \simeq \frac{1}{\mathcal{R}e}$ which is not practical due to the computation cost. From here, we are motivated to study the following under-resolved case.

Theorem 3.2.3. **(under-resolved mesh)** Suppose $u_0 \in L^2(\Omega)$. Then for any given mesh size $0 < h < L$, $\langle \varepsilon(u^h) \rangle$ satisfies,

$$\langle \varepsilon(u^h) \rangle \leq C \left[\frac{1}{\mathcal{R}e}\,\frac{L}{h} + (\frac{C_s\,\delta}{h})^2 + \frac{L^5}{(C_s\delta)^4\,h} + \frac{L^{\frac{5}{2}}}{(C_s\,\delta)^4}\,h^{\frac{3}{2}} \right] \frac{U^3}{L}.$$

Proof. The proof is very similar to the one of Theorem 3.2.1, except the estimation on the nonlinear term. Let $h \in (0, L)$ be fixed from the beginning. The strategy is to subtract off the inhomogeneous boundary conditions (3.0.2). The proof arises as well by taking $v^h = u^h - \Phi$ in the finite element problem (3.1.8). Then after integrating with respect to time, we get (3.2.1). The proof continues by estimating each term on the right-hand side of (3.2.1). Using Lemma 3.1.1 and the Cauchy-Schwarz-Young's inequality, the first three terms on the RHS of the energy equality (3.2.1) can be estimated as,

$$(u^h(T), \Phi) \leq \frac{1}{2}\|u^h(T)\|^2 + \frac{1}{2}\|\Phi\|^2 = \frac{1}{2}\|u^h(T)\|^2 + \frac{1}{6}L^2U^2h. \tag{3.2.13}$$

$$(u^h(0), \Phi) \leq \|u^h(0)\|\|\Phi\| = \sqrt{\frac{h}{3}}UL\|u^h(0)\|. \tag{3.2.14}$$

$$\nu \int_0^T (\nabla u^h, \nabla \Phi)dt \leq \frac{\nu}{2}\int_0^T \|\nabla u^h\|^2 + \|\nabla \Phi\|^2 dt = \frac{\nu}{2}\int_0^T \|\nabla u^h\|^2 dt + \frac{\nu}{2}\frac{U^2L^2}{h}T. \tag{3.2.15}$$

Next applying the Young's inequality,

$$ab \leq \frac{1}{p}a^p + \frac{1}{q}b^q,$$

for conjugate $p = \frac{3}{2}$ and $q = 3$ on $a = |\nabla u^h|^2$ and $b = |\nabla \Phi|$ gives,

$$\begin{aligned} |\int_\Omega |\nabla u^h| \nabla u^h \nabla \Phi \, dx| \leq \int_\Omega |\nabla u^h|^2 |\nabla \Phi| \, dx &\leq \int_\Omega \big(\frac{2}{3}|\nabla u^h|^3 + \frac{1}{3}|\nabla \Phi|^3\big) \, dx \\ &\leq \frac{2}{3}\int_\Omega |\nabla u^h|^3 dx + \frac{1}{3}\frac{U^3 L^2}{h^2}. \end{aligned} \tag{3.2.16}$$

Inserting (3.2.13), (3.2.14), (3.2.15) and (3.2.16) in (3.2.1) implies,

$$\begin{aligned} &\frac{1}{2}\|u^h(T)\|^2 - \frac{1}{2}\|u^h(0)\|^2 + \nu\int_0^T \|\nabla u^h\|^2 dt + (C_s\delta)^2 \int_0^T (\int_\Omega |\nabla u^h|^3 dx) dt \\ &\leq \frac{1}{2}\|u^h(T)\|^2 + \frac{1}{6}L^2U^2h + \sqrt{\frac{h}{3}}UL\|u^h(0)\| + \frac{\nu}{2}\int_0^T \|\nabla u^h\|^2 dt + \frac{\nu}{2}\frac{U^2L^2}{h}T \\ &+ \int_0^T b(u^h, u^h, \Phi) dt + \frac{2}{3}(C_s\delta)^2 \int_0^T (\int_\Omega |\nabla u^h|^3 dx) dt + \frac{1}{3}(C_s\delta)^2 \frac{U^3L^2}{h^2}T. \end{aligned} \tag{3.2.17}$$

Finally the nonlinear term $b(u^h, u^h, \Phi)$ is estimated as follow. First from Definition 3.1.2, we have,

$$|b(u^h, u^h, \Phi)| \leq \frac{1}{2}|(u^h \cdot \nabla u^h, \Phi)| + \frac{1}{2}|(u^h \cdot \nabla \Phi, u^h)|. \tag{3.2.18}$$

The first term on (3.2.18) can be estimated using Hölder's inequality[1] for $p = 3, q = 6$ and $r = 2$,

$$|(u^h \cdot \nabla u^h, \Phi)| \leq \int_\Omega |u^h \nabla u^h \Phi| dx \leq ||\nabla u^h||_3 \, ||u^h||_6 \, ||\Phi||_2,$$

then applying the following Young's inequality [2] for conjugate exponents $p = 3$ and $q = \frac{3}{2}$,

$$ab \leq \frac{\epsilon}{3}a^3 + \frac{\epsilon^{-\frac{1}{2}}}{\frac{3}{2}}b^{\frac{3}{2}}, \tag{3.2.19}$$

when $a = ||\nabla u^h||_3$, $b = ||u^h||_6 \, ||\Phi||_2$ and $\epsilon = \frac{(C_s\delta)^2}{4}$ leads to,

[1] $\int_\Omega |f\, g\, h| dx \leq ||f||_p \, ||g||_q \, ||h||_r$ for $\frac{1}{p} + \frac{1}{q} + \frac{1}{r} = 1$.

[2] More generally, for conjugate ($\frac{1}{p} + \frac{1}{q} = 1$) exponents $a \geq 0, b \geq 0 : ab \leq \frac{\epsilon}{p}a^p + \frac{\epsilon^{-\frac{q}{p}}}{q}b^q$ for any $\epsilon \geq 0$.

$$|b(u^h,u^h,\Phi)| \leq \frac{1}{12}(C_s\delta)^2||\nabla u^h||_3^3 + \frac{2}{3}(\frac{(C_s\delta)^2}{4})^{-\frac{1}{2}}\,||\Phi||_2^{\frac{3}{2}}\,||u^h||_6^{\frac{3}{2}}.$$

From Lemma 3.1.3 we have $||u^h||_6 \leq C\,L^{\frac{1}{2}}||\nabla u^h||_3$, it follows that

$$|b(u^h,u^h,\Phi)| \leq \frac{1}{12}(C_s\delta)^2||\nabla u^h||_3^3 + \frac{2}{3}(\frac{(C_s\delta)^2}{4})^{-\frac{1}{2}}\,||\Phi||_2^{\frac{3}{2}}\,CL^{\frac{3}{4}}||\nabla u^h||_3^{\frac{3}{2}}.$$

Again apply the general Young's inequality for conjugate exponents $p=2$ and $q=2$ to the second term of the above inequality when $\epsilon = \frac{(C_s\delta)^2}{6}$,

$$|(u^h\cdot\nabla u^h,\Phi)| \leq \frac{1}{6}(C_s\delta)^2||\nabla u^h||_3^3 + \frac{1}{12}(C_s\delta)^2||\nabla u^h||_3^3 + C\frac{8}{3}L^{\frac{3}{2}}(C_s\delta)^{-4}||\Phi||_2^3.$$

Use $||\Phi||_2^3 = (\frac{h}{3})^{\frac{3}{2}}L^3U^3$ from the Lemma 3.1.1 on the above inequality and then,

$$|(u^h\cdot\nabla u^h,\Phi)| \leq \frac{1}{6}(C_s\delta)^2||\nabla u^h||_3^3 + C\,L^{\frac{3}{2}}(C_s\delta)^{-4}h^{\frac{3}{2}}L^3U^3. \tag{3.2.20}$$

The second term $|(u^h\cdot\nabla\Phi,u^h)|$ on (3.2.18) can be bounded first using Hölder's inequality for $p=6, q=\frac{3}{2}$ and $r=6$,

$$|(u^h\cdot\nabla\Phi,u^h)| \leq \int_\Omega |u^h\,\nabla\Phi\,u^h|dx \leq ||\nabla\Phi||_{\frac{3}{2}}\,||u^h||_6^2.$$

Using $||u^h||_6 \leq L^{\frac{1}{2}}||\nabla u^h||_3$, Lemma 3.1.3, we have:

$$|(u^h\cdot\nabla\Phi,u^h)| \leq \int_\Omega |u^h\,\nabla\Phi\,u^h|dx \leq ||\nabla\Phi||_{\frac{3}{2}}\,L\,||\nabla u^h||_3^2,$$

then use Young's inequality (3.2.19) with $a=||\nabla u^h||_3^2$ and $b=||\nabla\Phi||_{\frac{3}{2}}\,L$ for $p=\frac{3}{2}, q=3$ and $\epsilon=\frac{3}{16}(C_s\delta)^2$,

$$|(u^h\cdot\nabla\Phi,u^h)| \leq \frac{(C_s\delta)^2}{8}||\nabla u^h||_3^3 + \frac{16}{27}\frac{1}{(C_s\delta)^4}||\nabla\Phi||_{\frac{3}{2}}^3\,L^3.$$

Since $||\nabla\Phi||_{\frac{3}{2}}^3 = \frac{U^3L^4}{h}$, Lemma 3.1.1, the above inequality turns to be,

$$|(u^h\cdot\nabla\Phi,u^h)| \leq \frac{(C_s\delta)^2}{8}||\nabla u^h||_3^3 + \frac{16}{27}\frac{U^3\,L^7}{(C_s\delta)^4\,h}. \tag{3.2.21}$$

Combining (3.2.20) and (3.2.21) in (3.2.18), we have the following estimate on the non-linearity,

$$|b(u^h, u^h, \Phi)| \leq \frac{7}{24}(C_s\delta)^2||\nabla u^h||_3^3 + \frac{U^3\,L^7}{(C_s\delta)^4\,h} + \frac{L^{\frac{3}{2}}h^{\frac{3}{2}}L^3U^3}{(C_s\delta)^4}. \tag{3.2.22}$$

Inserting (3.2.22) in (3.2.17) yields:

$$\begin{aligned}\frac{1}{2}\int_0^T \nu\|\nabla u^h\|^2 dt + \frac{1}{2}\int_0^T (\int_\Omega (C_s\delta)^2|\nabla u^h|^3 dx)dt \leq \frac{1}{2}\|u^h(0)\|^2 + \frac{1}{6}L^2U^2h \\ + \sqrt{\frac{h}{3}}UL\|u^h(0)\| + \frac{\nu}{2}\frac{U^2L^2}{h}T + \frac{1}{3}(C_s\delta)^2\frac{U^3L^2}{h^2}T + \frac{U^3\,L^7}{(C_s\delta)^4\,h}\,T + \frac{L^{\frac{3}{2}}h^{\frac{3}{2}}L^3U^3}{(C_s\delta)^4}\,T.\end{aligned} \tag{3.2.23}$$

Note that the above inequality can justify the fact that the computed time-averaged of the energy dissipation of the solution (3.0.1) is uniformly bounded and hence $\langle\varepsilon(u^h)\rangle$ is well-defined.

Dividing both sides of the inequality (3.2.23) by $|\Omega| = L^3$ and T, taking lim Sup as $T \longrightarrow \infty$ leads to,

$$\frac{1}{2}\langle\varepsilon(u^h)\rangle \leq \frac{1}{2}\,\frac{\nu U^2}{hL} + \frac{1}{3}(C_s\delta)^2\frac{U^3}{h^2L} + \frac{L^4\,U^3}{(C_s\delta)^4\,h} + \frac{h^{\frac{3}{2}}\,L^{\frac{3}{2}}\,U^3}{(C_s\delta)^4},$$

which can be written as

$$\langle\varepsilon(u^h)\rangle \leq C\left[\frac{1}{\mathcal{R}e}\,\frac{L}{h} + (\frac{C_s\,\delta}{h})^2 + \frac{L^5}{(C_s\delta)^4\,h} + \frac{L^{\frac{5}{2}}}{(C_s\,\delta)^4}\,h^{\frac{3}{2}}\right]\frac{U^3}{L}, \tag{3.2.24}$$

and the theorem is proved.

□

Remark 3.2.4. The estimate in Theorem 3.2.3 is for a coarse mesh $h \geq \mathcal{O}(\mathcal{R}e^{-1})\,L$. For the fully-resolved case $h \to \mathcal{R}e^{-1}$ (or equivalently $C_s\delta \to 0$), the other estimate in Theorem 3.2.1 takes over. Moreover, the estimate is independent of the viscosity at high Reynolds number. It is also dimensionally consistent.

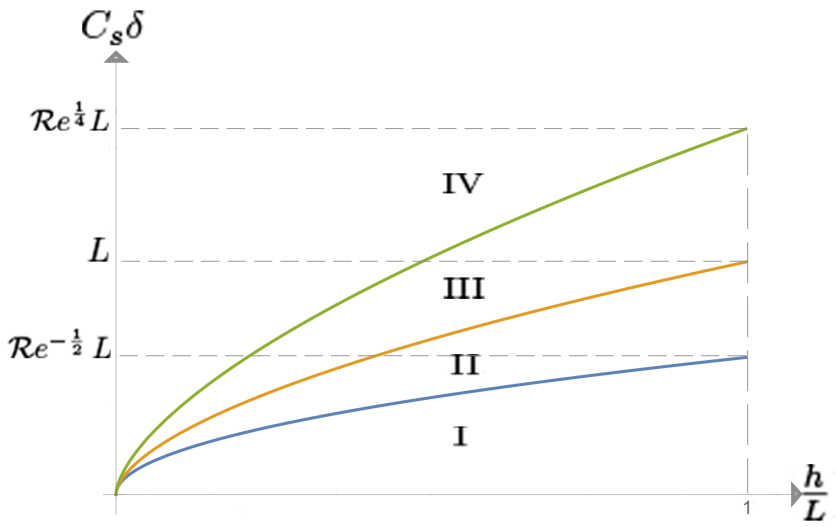

Figure 6: Level Sets.

The value of $\langle \varepsilon(u^h) \rangle$ in Theorem 3.2.3 depends on three discretization parameters; the turbulence resolution length scale δ, the Smagorinsky constant C_s and the numerical resolution h. These affect $\langle \varepsilon(u^h) \rangle$, but have no impact on the underlying velocity field $u(x,t)$, and hence they have no effect upon $\langle \varepsilon(u) \rangle$.

Consider the upper bound on $\frac{\langle \varepsilon(u^h) \rangle}{U^3/L}$ in (3.2.24) as function of $(C_s\delta)$ and h, when $\mathcal{R}e \gg 1$ and L are being fixed. The expression includes three main terms. The terms in the estimate are associated with physical effects as follows,

1. $\lambda_1(h, C_s\delta) = \frac{1}{\mathcal{R}e}\frac{L}{h}$ $\quad\Longrightarrow\quad$ Viscosity,
2. $\lambda_2(h, C_s\delta) = (\frac{C_s\delta}{h})^2$ $\quad\Longrightarrow\quad$ Model Viscosity,
3. $\lambda_3(h, C_s\delta) = \frac{L^5}{(C_s\delta)^4\, h} + \frac{L^{\frac{5}{2}}}{(C_s\,\delta)^4}\, h^{\frac{3}{2}}$ $\quad\Longrightarrow\quad$ Non-linearity.

Tracking back the proof of Theorem 3.2.3, λ_1, λ_2 and λ_3 correspond to the viscosity term $\nu\Delta u$, model viscosity $\nabla\cdot((C_s\delta)^2|\nabla u|\nabla u)$ and non-linear term $u\cdot\nabla u$ respectively. The three level sets of $\lambda_1 = \lambda_2, \lambda_2 = \lambda_3$ and $\lambda_1 = \lambda_3$ are respectively denoted by the curves ζ_1, ζ_2 and ζ_3 in the Figure 6, which are calculated as,

1. $\zeta_1 : \lambda_1 = \lambda_2 \Longrightarrow C_s\delta = \mathcal{R}e^{-\frac{1}{2}}\, L\, (\frac{h}{L})^{\frac{1}{2}}$,
2. $\zeta_2 : \lambda_2 = \lambda_3 \Longrightarrow C_s\delta = L\left[(\frac{h}{L})^{\frac{7}{2}} + \frac{h}{L}\right]^{\frac{1}{6}}$,
3. $\zeta_2 : \lambda_1 = \lambda_3 \Longrightarrow C_s\delta = \mathcal{R}e^{\frac{1}{4}} L\left[1 + (\frac{h}{L})^{\frac{5}{2}}\right]^{\frac{1}{4}}$.

Remark 3.2.5. In Figure 6, consider the horizontal axis to be $\frac{h}{L}$ and the vertical one to be $C_s\delta$. The three level sets divide the $(\frac{h}{L})\,(C_s\delta)$ - plane into the four regions. The four regions $\mathrm{I}, \mathrm{II}, \mathrm{III}$ and IV are identified with respect to the comparative magnitudes of λ_1, λ_2 and λ_3 on the $(\frac{h}{L})\,(C_s\delta)$ - plane. After comparing the magnitude of these three functions on each separate region, it can be seen that below the curve ζ_2 (regions I and II) the effect of non-linearity term $u \cdot \nabla u$ on the energy dissipation, corresponding to λ_3, dominates the other terms. But above the curve ζ_2 (regions III and IV) the model viscosity term, corresponding to λ_2, dominates. Surprisingly, the viscosity term $\nu\Delta u$ is never bigger than the other two terms for any choice of h, δ and C_s.

The Smagorinsky coefficient C_s can be calibrated for a given class of flows. Its value varies from flow to flow and from domain to domain (see e.g. Page 23 of Galperin and Orszag [22] who quote a range $0.000744 \leq C_s \leq 0.020$). In the next corollary the optimal value, with respect the current analysis, of C_s in the Theorem 3.2.3 is investigated, considering $\delta = h$ which is a common choice [66].

Corollary 3.2.6. Let $\delta = h \geq \mathcal{O}(\mathcal{R}e^{-1})\, L$ be fixed. Then for any choice of $C_s > 0$, the upper estimate on $\frac{\langle \varepsilon(u^h)\rangle}{U^3/L}$ in the Theorem 3.2.3 is larger than the dissipation coefficient C_ϵ in Figure 5.

Proof. Letting $\delta = h$, Theorem 3.2.3 suggests,

$$\frac{\langle \varepsilon(u^h)\rangle}{U^3/L} \simeq \frac{1}{\mathcal{R}e}\,\frac{L}{h} + {C_s}^2 + \frac{1}{C_s^4}\big[(\frac{L}{h})^5 + (\frac{L}{h})^{\frac{5}{2}}\big]. \tag{3.2.25}$$

Solving the minimization problem $(C_s)_{\min} = \arg\min_{C_s} F(C_s)$, the minimum of the function,

$$F(C_s) = \frac{1}{\mathcal{R}e}\,\frac{L}{h} + {C_s}^2 + \frac{1}{C_s^4}\big[(\frac{L}{h})^5 + (\frac{L}{h})^{\frac{5}{2}}\big], \tag{3.2.26}$$

occurs at

$$F_{\min} = \frac{1}{\mathcal{R}e}\,\frac{L}{h} + 2\big[(\frac{L}{h})^5 + (\frac{L}{h})^{\frac{5}{2}}\big]^{\frac{1}{3}}, \tag{3.2.27}$$

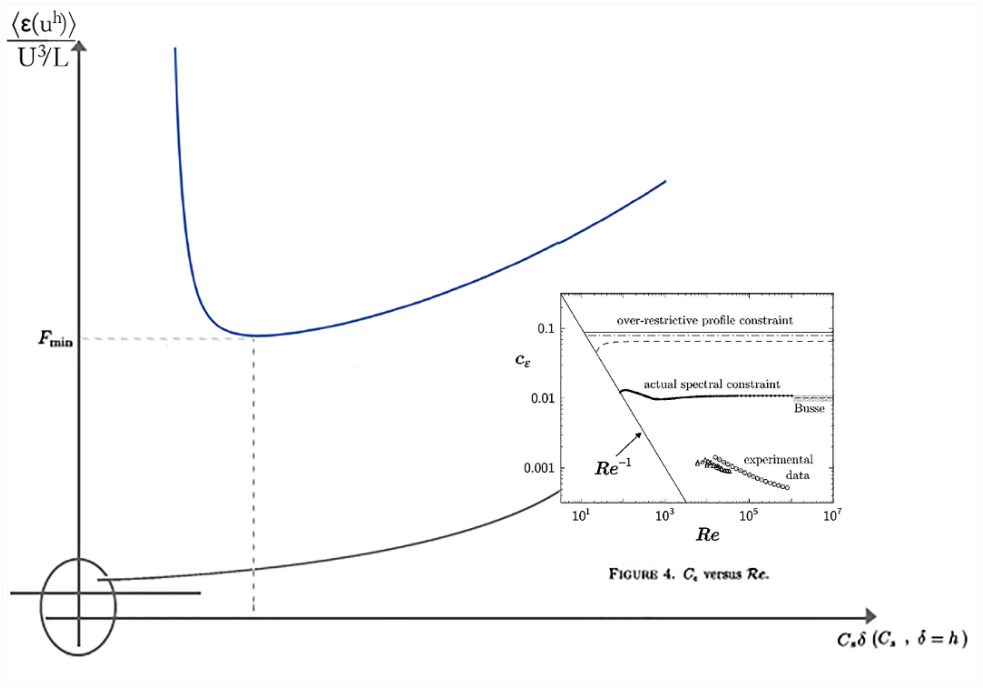

FIGURE 4. C_ϵ versus $\mathcal{R}e$.

Figure 7: Theorem 3.2.3 vs experimental results in Figure 5.

for $(C_s)_{\min} = \sqrt[6]{2}\,[(\frac{L}{h})^5 + (\frac{L}{h})^{\frac{5}{2}}]^{\frac{1}{6}}$, assuming $\mathcal{O}(\mathcal{R}e^{-1}) < \frac{h}{L} < 1$ is fixed. This minimum amount (3.2.27) dramatically exceeds the range of C_ϵ in Figure 5 for any typical choice of h in LES. □

Remark 3.2.7. Corollary 3.2.6 indicates over-dissipation of $\langle \varepsilon(u^h) \rangle$ for any choice of $C_s > 0$. As an example, let $\frac{h}{L} = 0.01$, then $F_{\min} \simeq 2000$ in (3.2.27) as $\mathcal{R}e \to \infty$. It is much larger than the experimental range of C_s in Figure 5, $\frac{1}{\mathcal{R}e} \le C_\epsilon \le 0.1$, see Figure 7.

However δ is taken $\mathcal{O}(h)$ in many literature [66], the relationship between the grid size h and the filter size δ has been made based on heuristic instead of a sound numerical analysis (p.26 of [5]). Therefore for an LES of fixed computational cost (i.e. fixed h) and fixed length scale L, one can ask how the artificial parameter $C_s\,\delta$ should be selected such that the statistics of the model be consistent with numerical and experimental evidence summarized in Figure 5. To answer this question, the inequality (3.2.24) takes over in the next corollary for under-resolved spatial mesh $h \ge \mathcal{O}(\mathcal{R}e^{-1})\,L$, since no model is used when (at much

greater cost) a DNS is performed with $\frac{h}{L} \simeq \mathcal{R}e^{-1}$.

Corollary 3.2.8. Let the mesh size $h \geq \mathcal{O}(\mathcal{R}e^{-1})\, L$ be fixed. Then for any choice of $C_s > 0$ and $\delta > 0$, the upper estimate on $\frac{\langle \varepsilon(u^h)\rangle}{U^3/L}$ in the Theorem 3.2.3 is larger than the dissipation coefficient C_ϵ in Figure 5.

Proof. Solving the minimization problem $(C_s\delta)_{\min} = \arg\min_{C_s\delta} G(C_s\delta)$, the minimum of the function,

$$G(C_s\delta) = \frac{1}{\mathcal{R}e}\,\frac{L}{h} + (\frac{C_s\,\delta}{h})^2 + \frac{L^5}{(C_s\delta)^4\,h} + \frac{L^{\frac{5}{2}}}{(C_s\,\delta)^4}\,h^{\frac{3}{2}}, \tag{3.2.28}$$

occurs at,

$$F_{\min} = \frac{1}{\mathcal{R}e}\,\frac{L}{h} + 2\big[(\frac{L}{h})^5 + (\frac{L}{h})^{\frac{5}{2}}\big]^{\frac{1}{3}},$$

for $(C_s\delta)_{\min} = \sqrt[6]{2}\,h\,[(\frac{L}{h})^5 + (\frac{L}{h})^{\frac{5}{2}}]^{\frac{1}{6}}$ assuming h and L are fixed. This minimum amount which is much larger than the experimental range of C_ϵ, $\frac{1}{\mathcal{R}e} \leq C_\epsilon \leq 0.1$, leads to over-dissipation of the model, Figure 7. □

Remark 3.2.9. The extra dissipation in the Corollary 3.2.6 and 3.2.8, which is consistent with experience with the Smagorinsky model (e.g., Iliescu and Fischer [35] and Moin and Kim [57]), can laminarize the numerical approximation of a turbulent flow and prevent the transition to turbulence.

Remark 3.2.10. In the limit of high Reynolds number and for a fixed computational cost $h \geq \mathcal{O}(\mathcal{R}e^{-1})\, L$, the estimate in Theorem 3.2.3 is the function of $C_s\delta$,

$$\frac{\langle \varepsilon(u^h)\rangle}{U^3/L} \simeq (\frac{C_s\,\delta}{h})^2 + \frac{1}{(C_s\delta)^4}\,[\frac{L^5}{h} + L^{\frac{5}{2}}\,h^{\frac{3}{2}}],$$

which consists of two major parts. First,

$$\lambda_2 = \mathcal{O}((C_s\delta)^2)$$

is derived from the eddy viscosity term and is quadratic in $(C_s\delta)$. The latter,

$$\lambda_3 = \mathcal{O}((C_s\delta)^{-4})$$

is derived from the non-linearity term and is inversely proportional to $(C_s\delta)^4$. Therefore, the behavior of the graph $\frac{\langle\varepsilon(u^h)\rangle}{U^3/L}$ in Figure 7 is decided by the competition between the increasing function λ_2 and the decreasing function λ_3. This observation suggests model over-dissipation is due to the action of the model viscosity, which is also consistent with [45]. Analysis in [45] suggested that the model over-dissipation is due to the action of the model viscosity in boundary layers rather than in interior small scales generated by the turbulent cascade.

3.3 NUMERICAL SIMULATIONS

The test is a comparison between simulation of the NSE and the Smagorinsky model for two dimensional time-dependent shear flow between two cylinders, motivated by the classic problem of flow between rotating cylinders. The domain is a disk with a smaller center obstacle inside. The flow is driven by the rotational force at the outer circle in the absence of body force, with no-slip boundary conditions suppressed on the inner circle. Note that in the absence of body force here, most of the interesting structures are expected to be due to the interaction of the flow with the boundaries. The tests were performed using FreeFEM++ [30], with Taylor-Hood elements (continuous piecewise quadratic polynomials for the velocity and continuous linear polynomials for the pressure) in all tests. The under-resolved mesh is parameterized by the number of mesh points m = 60 around the outer circle and n = 20 mesh points around the immersed circle and extended to all of the domain as a Delaunay mesh, Figure 8. We take $\mathcal{R}e = 3000$, final time $T = 10$ and time step $\Delta t = 0.01$. The initial condition u_0 is generated by solving the steady Stokes problem with the same condition described above on the same geometry, this gives an initial condition that is divergence free and satisfies the boundary conditions. The Backward Euler method is utilized for time discretization.

In the NSE (Figure 9), as it is expected, flow does not approach a steady state and the chaotic behavior of the velocity field especially near the boundaries can be seen. To verify the code works properly, $C_s = 0.00001$ (i.e. $C_s \to 0$) is considered once in the SM. The same chaotic behavior as the NSE is observed in this scenario and the result is quite identical,

which is consistent with the fact that SM $\to$ NSE as $C_s \to 0$ (Figure 10).

To run the test on the Smagorinsky model, providing all other conditions hold, consider $C_s = 0.17$ [50]. Motivated by Corollaries 4.2.2 and 4.2.4, consider $\delta = h$ (Figure 11) and $\delta = h^{\frac{1}{6}}$ (Figure 12). In all cases, the model predicts the flow will quickly reach a nonphysical equilibrium, which is clearly over-dissipated. This extra dissipation laminarizes the approximation of the flow and prevents the transition to turbulence.

3.4 CONCLUSION

We investigate the computed time-averaged energy dissipation $\langle \varepsilon(u^h) \rangle$ here for shear flow turbulence on the under-resolved mesh. $\langle \varepsilon(u^h) \rangle$ scales as the equilibrium dissipation law, $\frac{U^3}{L}$, for an under-resolved mesh independent of ν at high Reynolds number being considered. The upper bound in Theorem 3.2.3 does not give the correct dissipation for any choice of the Smagorinsky constant $C_s > 0$ and filter size $\delta > 0$, which is consistent with the numerical evidence. In addition, it is shown that the viscosity term $\nu \Delta u$ does not affect $\langle \varepsilon(u^h) \rangle$ for any choice of discretization parameters. The next important step would be analyzing the computed energy dissipation rate for other turbulent models, e.g. dynamic subgrid-scale model, on an under-resolved spatial mesh.

The analysis here indicates that the model over-dissipation is due to the action of the eddy viscosity term $\nabla \cdot ((C_s \delta) |\nabla u| \nabla u)$. The classical approach to correct the over-dissipation of the Smagorinsky model is to multiply the eddy viscosity term with a damping function. The mathematical analysis in [62] shows that the combination of the Smagorinsky with a modified van Driest damping does not over dissipate assuming infinite resolution (i.e. continues case). The unexplored question is: What is the statistics of this combination on an under-resolved mesh size?

In this report, the Smagorinsky model is used instead of the NSE. One can try to calculate the energy dissipation rate for the discretized NSE on the coarse mesh. The key part of the success is to prove the boundedness of the kinetic energy of the approximate velocity, $||u^h||^2$, for the NSE without any restriction on the mesh size h.

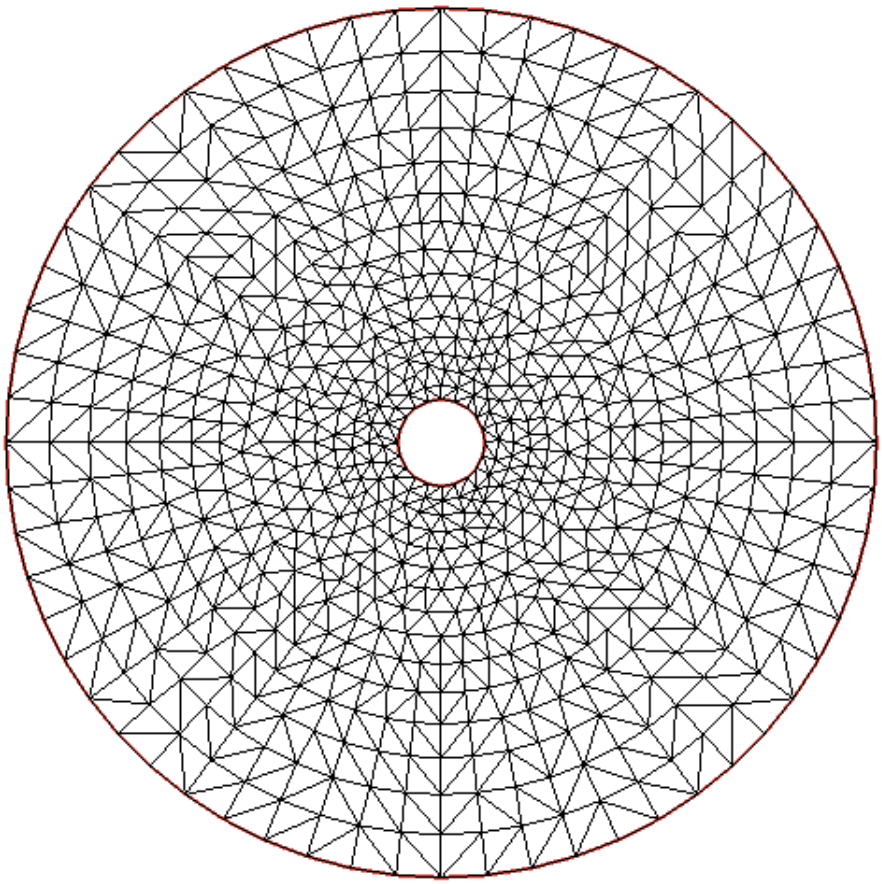

Figure 8: Coarse mesh with 60 mesh points on the outer and 20 points on the inner circle.

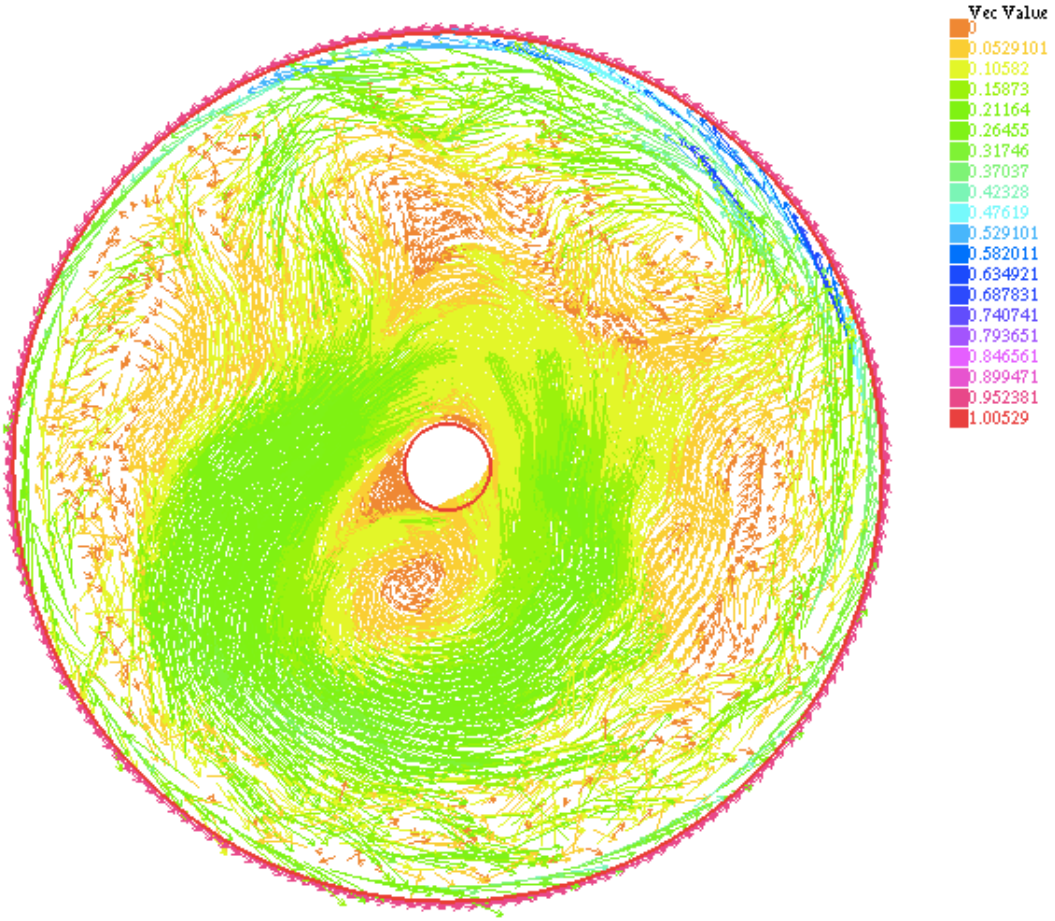

Figure 9: NSE; Chaotic velocity field near the boundary.

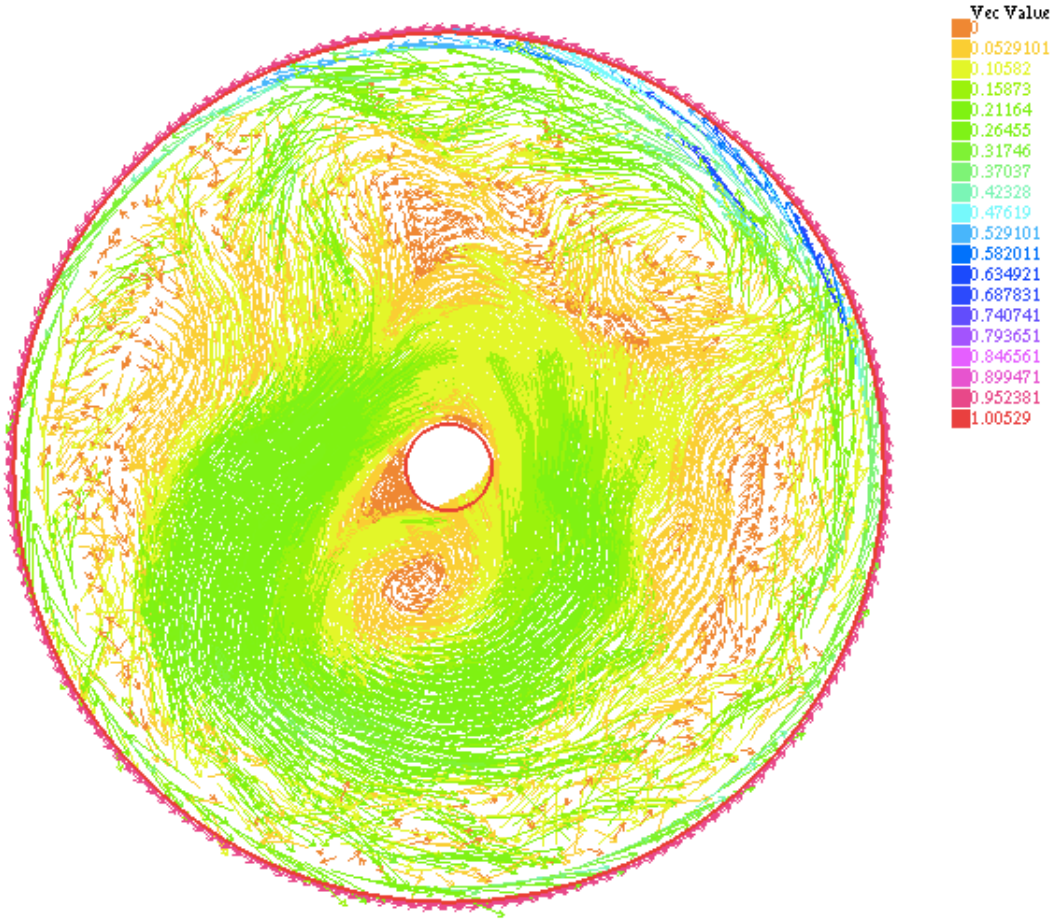

Figure 10: SM $\to$ NSE as $C_s \to 0$.

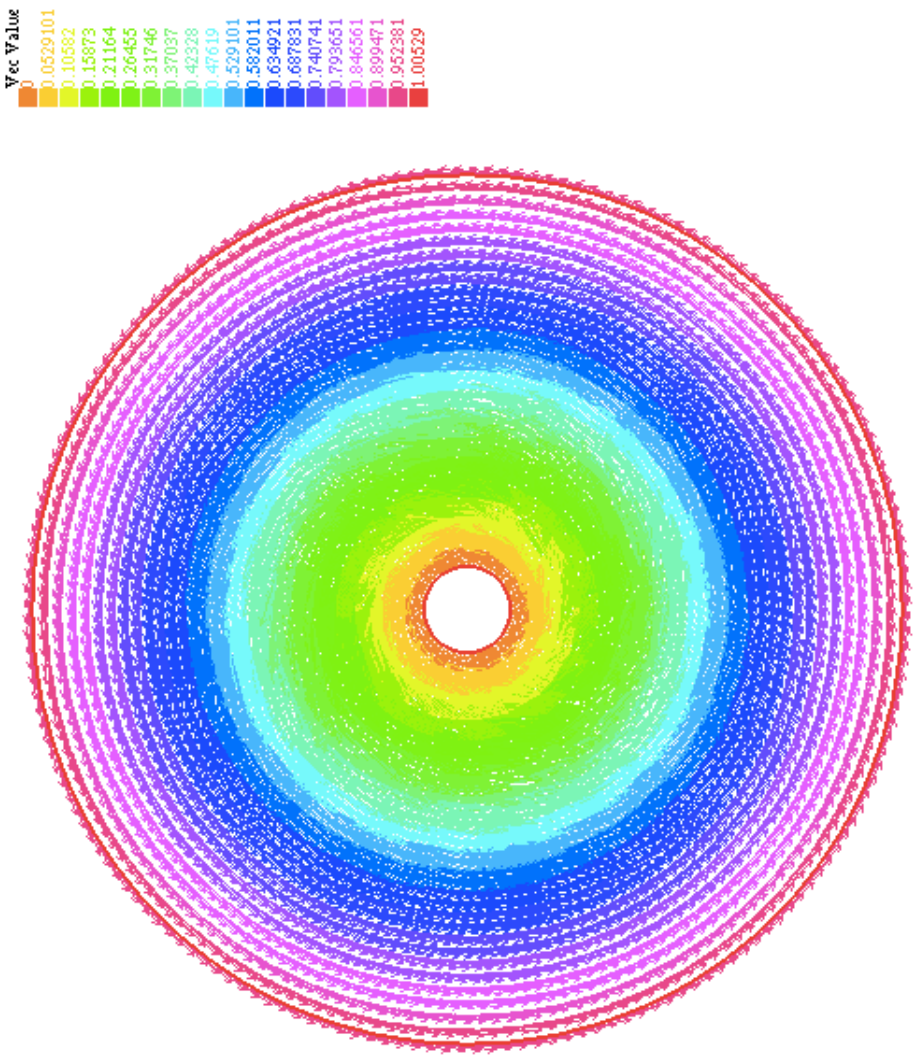

Figure 11: SM where $\delta = h$ for any $C_s > 0$; Flow reaches nonphysical equilibrium.

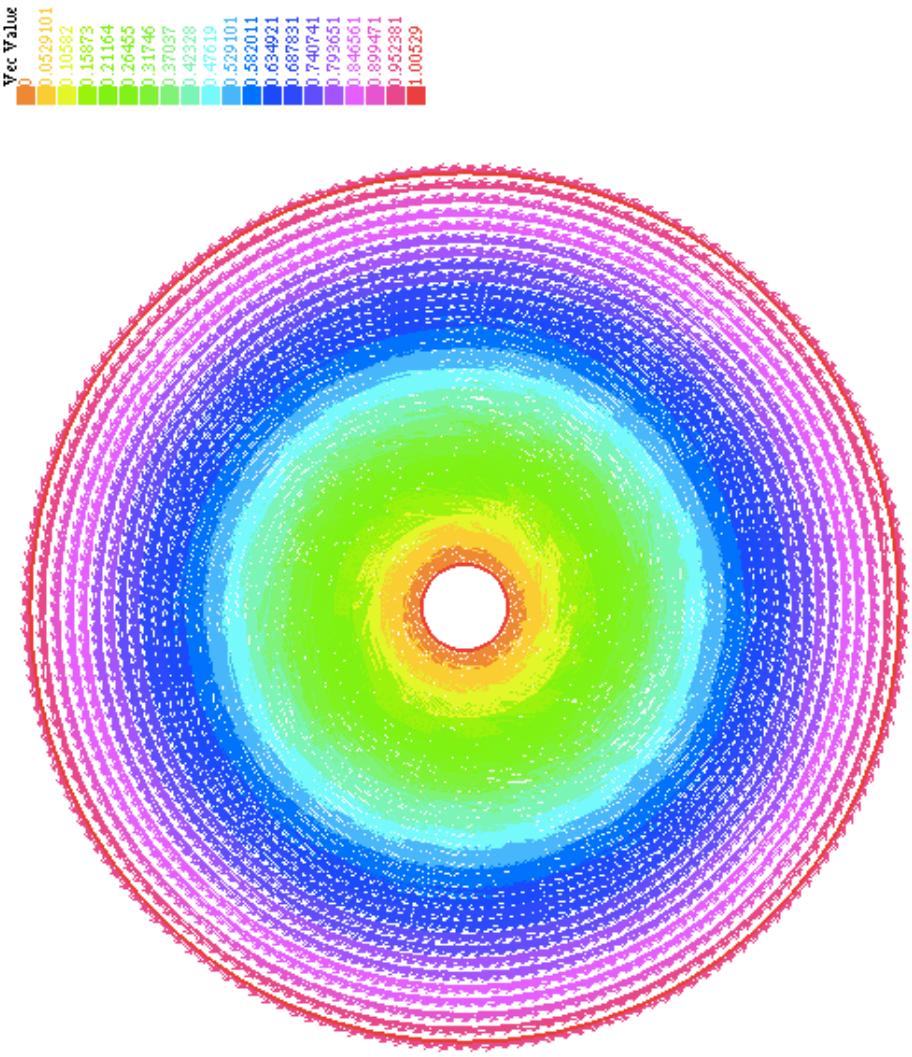

Figure 12: SM where $\delta = h^{\frac{1}{6}}$ for any $C_s > 0$; Flow reaches nonphysical equilibrium.

4.0 DAMPING FUNCTIONS CORRECT OVER-DISSIPATION OF THE SMAGORINSKY MODEL

Experience with the Smagorinsky model (SM) indicates it over dissipates (p.247 of Sagaut [71]). This extra dissipation can laminarize the numerical approximation of a turbulent flow and prevents the transition to turbulence (p.192 of [47]). Model refinements aim at reducing model dissipation occur as early as 1975 [72] and continues with dynamic parameter selection (Germano, Piomelli, Moin and Cabot [24] and Swierczewska [80]), structural sensors (Hughes, Oberai and Mazzei [34]) and near wall models (e.g., Piomelli and Balaras [65], John, Layton and Sahin [40] and John and Liakos [41]). The classical approach is to multiply the turbulent viscosity with damping function $\beta(x)$ (such as van Driest damping [83]) with $\beta(x) \to 0$ as $x \to$ walls. There have been many numerical tests but little analytic support of this combination. This paper analyzes this combination of the SM with damping function $\beta(x)$ in the flow domain $\Omega = (0, L)^3$,

$$u_t + u \cdot \nabla u - \nu \Delta u + \nabla p - \nabla \cdot (\beta(x)(C_s \delta)^2 |\nabla u| \nabla u) = 0 \quad \text{and} \quad \nabla \cdot u = 0 \quad \text{in } \Omega. \tag{4.0.1}$$

In (4.0.1) u is the velocity, p is the pressure, ν is the kinematic viscosity, $\delta << 1$ is a model length scale and $C_s \simeq 0.1$ is the standard model parameter (Lilly [50]). To evaluate the effect of a damping function in the near wall region, we study the time-averaged energy dissipation rate of (4.0.1) for shear flow. L-periodic boundary conditions in x and y directions are imposed. $z = 0$ is a fixed wall and the wall $z = L$ moves with velocity U (Figure 13),

$$u(x, y, 0, t) = (0, 0, 0)^\top \quad \text{and} \quad u(x, y, L, t) = (U, 0, 0)^\top. \tag{4.0.2}$$

The Reynolds number is $\mathcal{R}e = \frac{UL}{\nu}$. The time-averaged energy dissipation rate for model (4.0.1) includes dissipation due to the viscous forces and turbulent diffusion reduced by the damping function $\beta(x)$. It is given by

$$\langle \varepsilon_{SMD}(u) \rangle = \limsup_{T\to\infty} \frac{1}{T} \int_0^T \left(\frac{1}{|\Omega|} \int_\Omega \nu |\nabla u|^2 + (c_s \delta)^2 \beta(x) |\nabla u|^3 dx \right) dt. \tag{4.0.3}$$

This chapter estimates $\langle \varepsilon_{SMD}(u) \rangle$ (Theorem 4.2.1) for a damping function $\beta(x)$ in terms of its integral on an $\gamma = \mathcal{O}(\mathcal{R}e^{-1})$ strip along the moving wall as

$$\langle \varepsilon_{SMD}(u) \rangle \leq \left[C_1 + C_2 \left(\frac{C_s \delta}{L} \right)^2 \mathcal{R}e^3 \, \frac{1}{L} \int_{L-\gamma L}^{L} \beta(z) \, dz \right] \frac{U^3}{L}.$$

For an algebraic approximation of van Driest damping, Corollary 4.2.2 shows

$$\langle \varepsilon_{SMD}(u) \rangle \leq \left[C_2 + C_2 \left(\frac{C_s \delta}{L} \right)^2 \mathcal{R}e^2 \right] \frac{U^3}{L}.$$

The above estimate goes to $\frac{U^3}{L}$ for fixed $\mathcal{R}e$ as $\delta \to 0$, but blows up as $\mathcal{R}e \to \infty$ for fixed δ, suggesting over-dissipation. On the other hand, damping with a classical mixing length formula (4.2.19) of Prandtl, we obtain in Corollary 4.2.4

$$\langle \varepsilon_{SMD}(u) \rangle \leq C \, \frac{U^3}{L},$$

which is consistent with Kolmogorov phenomenology.

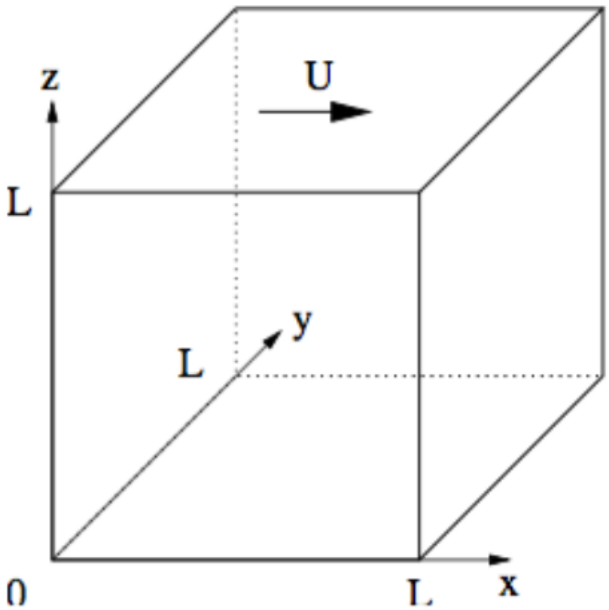

Figure 13: Shear flow.

4.0.1 Related Work

In the theory of turbulence, the time-averaged energy dissipation rate is a fundamental quantity (Sreenivasan [76], Pope [67], Lesieur [49], and Frisch [20]) determines the smallest persistent length scales and the dimension of any global attractor [46]. Moreover, the smallest length scale of turbulent flow simulation can be estimated by using upper bounds of the energy dissipation rate. In turbulent flows, the energy dissipation is often observed to approach a limit independent of the viscosity [43]. No rigorous proof of this fact has been given. For shear flow between parallel plates, Busse [10] and Howard [33] estimated $\langle \varepsilon(u) \rangle$ under the assumption that the flow is statistically stationary. Doering and Constantin [15] proved an upper bound on the time-averaged energy dissipation rate for general weak solutions of the Navier-Stokes equations (NSE), $\langle \varepsilon(u) \rangle \leq C \frac{U^3}{L}$. Similar estimates have been proven by Marchiano [53], Wang [85] and Kerswell [42] in more generality.

The Smagorinsky model [77], $\beta(x) \equiv 1$ in (4.0.1), is a common turbulence model used in

Large Eddy Simulation (e.g., [5], [71], [38], [59], [64] and [25]). The extra term with respect to the NSE can be generally justified as follows. In turbulence, dissipation occurs non-negligibly only at very small scales, smaller than the typical mesh. The balance between energy input at the largest scales and the energy dissipation at the smallest is a critical selection mechanism for determining the statistics of turbulent flows. To get an accurate simulation, once a mesh is selected, an extra dissipative term must be introduced to model the effect of the unresolved fluctuations, which are smaller than the mesh width, upon the resolved velocity.

The energy dissipation rate of the Smagorinsky model for shear flow with boundary layers was estimated in [45] as:

$$\langle \varepsilon_s(u) \rangle \leq [1 + C_s^2 (\frac{\delta}{L})^2 (1 + \mathcal{R}e)^2] \frac{U^3}{L}. \tag{4.0.4}$$

This estimate blows up for δ fixed as $\mathcal{R}e \to \infty$, which is consistent with the numerical evidence (e.g., Iliescu and Fischer [35] and Moin and Kim [57]). Surprisingly, it was shown in [45] that the energy dissipation rate of the Smagorinsky model in the absence of boundary layers satisfies:

$$\langle \varepsilon_s(u) \rangle \leq C \frac{U^3}{L}. \tag{4.0.5}$$

Comparing these two results (4.0.4) and (4.0.5) suggests that the model over-dissipation is due to the action of the model viscosity in boundary layers rather than in interior small scales generated by the turbulent cascade. To reduce the effect of model viscosity in the boundary layers damping functions $\beta(x)$, which go to zero at the walls, are often used (Pope [67]). In this case most of the tools of analysis, such as Körn's inequality, the Poincaré-Friederichs inequality, and Sobolev's inequality, no longer hold. Thus, the mathematical development of the SM under no-slip boundary conditions with damping function is cited in [5] p.78 as an important open problem.

4.1 MATHEMATICAL PRELIMINARIES

We use the standard notations $L^p(\Omega), W^{k,p}(\Omega), H^k(\Omega) = W^{k,2}(\Omega)$ for the Lebesgue and Sobolev spaces respectively. The inner product in the space $L^2(\Omega)$ will be denoted by $(\cdot,\cdot)$ and its norm by $||\cdot||$ for scalar, vector and tensor quantities. Norms in Sobolev spaces $H^k(\Omega), k > 0$, are denoted by $||\cdot||_{H^k}$ and the usual L^p norm is denoted by $||\cdot||_p$. The symbols C and C_i for $i = 1, 2, 3$ stand for generic positive constant independent of the ν, L and U. In addition, ∇u is the gradient tensor $(\nabla u)_{ij} = \frac{\partial u_j}{\partial x_i}$ for $i, j = 1, 2, 3$.

Definition 4.1.1. The velocity at a given time t is sought in the space

$$\mathbb{X}(\Omega) := \{u \in H^1(\Omega) : u(x, y, 0) = (0, 0, 0)^\top,\ u(x, y, L) = (U, 0, 0)^\top,$$
$$u \text{ is } L\text{-periodic in } x \text{ and } y \text{ direction}\}.$$

The test function space is

$$\mathbb{X}_0(\Omega) := \{u \in H^1(\Omega) : u(x, y, 0) = (0, 0, 0)^\top,\ u(x, y, L) = (0, 0, 0)^\top,$$
$$u \text{ is } L\text{-periodic in } x \text{ and } y \text{ direction}\}.$$

The pressure at time t is sought in

$$Q(\Omega) := L^2_0(\Omega) = \{q \in L^2(\Omega) :\ \textstyle\int_\Omega q dx = 0\}.$$

And the space of divergence-free functions is denoted by

$$V(\Omega) := \{u \in \mathbb{X}(\Omega) :\ (\nabla \cdot u, q) = 0\ \forall q \in Q\}.$$

Definition 4.1.2. (Trilinear from) Define $b : \mathbb{X} \times \mathbb{X} \times \mathbb{X} \to \mathbb{R}$ as $b(u, v, w) := (u \cdot \nabla v, w)$.

Lemma 4.1.1. The nonlinear term $b(\cdot,\cdot,\cdot)$ is continuous on $\mathbb{X}\times\mathbb{X}\times\mathbb{X}$ (and thus on $V \times V \times V$ as well). Moreover, we have the following skew-symmetry property for b

$$b(u, v, v) = 0 \quad \forall u \in V, v \in \mathbb{X}.$$

Proof. The proof is standard and the one with zero boundary conditions can be found in p.114 of Girault and Raviart [27]. □

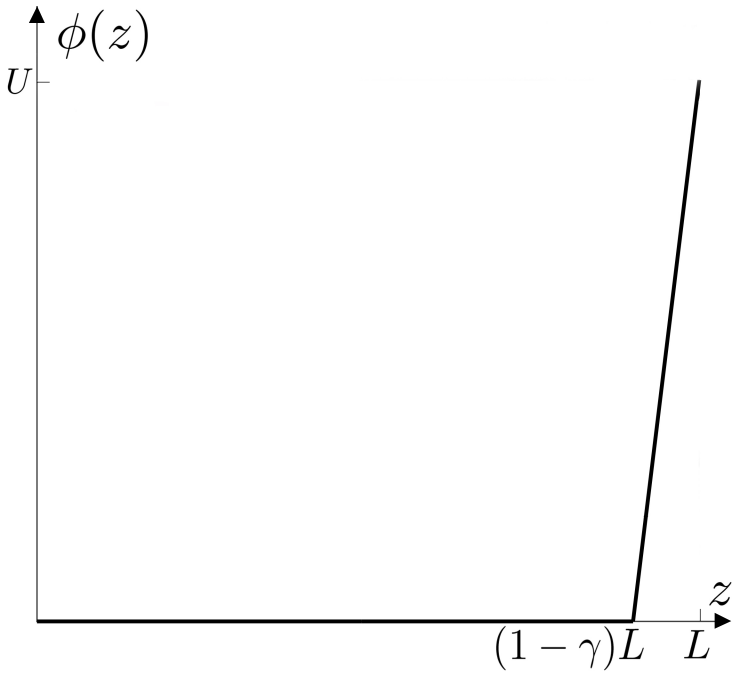

Figure 14: The background flow.

4.1.1 Construction of Background Flow

One key step to the upper bound on $\langle \varepsilon_{SMD}(u) \rangle$ is to construct an appropriate background flow, $\Phi \in \mathbb{X}(\Omega)$, following Hopf [32] and Doering and Constantin [15]. This is a divergence-free function extending the boundary condition (4.0.2) to the interior of Ω. Moreover, $u - \Phi \in \mathbb{X}_0(\Omega)$ and will be used as a test function in the weak form (4.2.1). The choice of $\gamma \in (0,1)$ will be determined by the needs of the estimates in (4.2.16) and it will be chosen to be $\gamma = \frac{1}{5.1} (\mathcal{R}e)^{-1}$.

Definition 4.1.3. (The background flow) Define $\Phi(x,y,z) := (\phi(z), 0, 0)^\top$, where

$$\phi(z) = \begin{cases} 0 & \text{if } z \in [0, L-\gamma L] \\ \frac{U}{\gamma L}(z - (L-\gamma L)) & \text{if } z \in [L-\gamma L, L] \end{cases}.$$

$\phi(z)$ is sketched in Figure 14. We collect two properties for Φ in Lemmas 4.1.2 and 4.1.3.

Lemma 4.1.2. Φ satisfies

a) $\|\Phi\|_\infty \leq U$, b) $\|\nabla\Phi\|_\infty \leq \frac{U}{\gamma L}$, c) $\|\Phi\|^2 \leq \frac{U^2\gamma L^3}{3}$, d) $\|\nabla\Phi\|^2 \leq \frac{U^2 L}{\gamma}$.

Proof. They all are the immediate consequence of the Definition 4.1.3. We show (c) here as an example.

$$\|\Phi\|^2 = L^2 \int_0^L |\phi(z)|^2 dz = L^2 \int_{L-\gamma L}^L \tfrac{U^2}{(\gamma L)^2}(z-(L-\gamma L))^2 dz = \tfrac{U^2\gamma L^3}{3}.$$

□

We will need the well-known dependence of the Poincaré -Friedrichs inequality constant on the domain. A straightforward argument in the thin domain $\mathcal{O}_{\gamma L}$ implies Lemma 4.1.3.

Lemma 4.1.3. Let $\mathcal{O}_{\gamma L} = \{(x,y,z) \in \Omega : L - \gamma L \leq z \leq L\}$ be the region close to the upper boundary. Then we have

$$\|u - \Phi\|_{L^2(\mathcal{O}_{\gamma L})} \leq \gamma L \|\nabla(u-\Phi)\|_{L^2(\mathcal{O}_{\gamma L})}. \tag{4.1.1}$$

Proof. First let v be a C^1 function on $\mathcal{O}_{\gamma L}$ that vanishes for $z = L$. Then component-wise $(i = 1, 2, 3)$, we have

$$v_i(x,y,z) = v_i(x,y,L) - \int_z^L \frac{dv_i}{d\xi}(x,y,\xi)d\xi.$$

Observing that $v_i(x,y,L) = 0$, squaring both sides, and using the Cauchy-Schwarz inequality, we get

$$v_i^2(x,y,z) \leq \gamma L \int_{L-\gamma L}^L (\frac{dv_i}{d\xi}(x,y,\xi))^2 d\xi.$$

Integrating both sides with respect to z gives

$$\int_{L-\gamma L}^L v_i^2(x,y,z)dz \leq (\gamma L)^2 \int_{L-\gamma L}^L (\frac{dv_i}{d\xi}(x,y,\xi))^2 d\xi.$$

Then integrating with respect to x and y and summing from $i = 1$ to 3, we obtain

$$\|v\|^2_{L^2(\mathcal{O}_{\gamma L})} \leq (\gamma L)^2 \|\nabla v\|^2_{L^2(\mathcal{O}_{\gamma L})}.$$

This proves the lemma for $v \in C^1$. Finally use a density argument and take $v = u - \Phi$. □

4.1.2 The Kinetic Energy

Before proving the main theorem, we prove boundedness of the kinetic energy, $\frac{1}{2}||u||^2$, and that $\langle \varepsilon_{SMD}(u) \rangle$ is well-defined. The proof of the model (4.0.1) is similar to the NSE case first presented in Hopf [32]. We need the following proposition first.

Proposition 4.1.4. Let $\nabla v \in L^p(\mathcal{O}_{\gamma L})$ and $0 < p < \infty$. If $v(x, y, L, t) = 0$ then

$$||\frac{v(x,y,z)}{L-z}||_{L^p(\mathcal{O}_{\gamma L})} \leq \frac{p}{p-1} ||\frac{\partial v}{\partial z}(x,y,z)||_{L^p(\mathcal{O}_{\gamma L})}.$$

Proof. Using B. Hardy's inequality (P.313 of Brezis [8]) when $z \in [L - \gamma L, L]$ for fixed x and y gives

$$||\frac{v(x,y,z)}{L-z}||_{L^p([L-\gamma L,L])} \leq \frac{p}{p-1} ||\frac{\partial v}{\partial z}(x,y,z)||_{L^p([L-\gamma L,L])}.$$

Raising both sides to power p, then taking a double integral with respect to x and y for $x, y \in [0, L]$ implies the result,

$$||\frac{v(x,y,z)}{L-z}||^p_{L^p(\mathcal{O}_{\gamma L})} \leq (\frac{p}{p-1})^p ||\frac{\partial v}{\partial z}(x,y,z)||^p_{L^p(\mathcal{O}_{\gamma L})} \leq (\frac{p}{p-1})^p ||\nabla v||^p_{L^p(\mathcal{O}_{\gamma L})}.$$

□

Lemma 4.1.5. The kinetic energy and the time averages of the energy dissipation of the solution to (4.0.1) with the boundary conditions (4.0.2) are uniformly bounded in time, i.e.

$$\sup_{t\in(0,\infty)} ||u(t)|| \leq C < \infty \quad \text{and} \quad \sup_{t\in(0,\infty)} \frac{1}{T} \int_0^T (\frac{1}{|\Omega|} \int_\Omega \nu |\nabla u|^2 + (c_s\delta)^2 \beta(x) |\nabla u|^3 dx)\, dt \leq C < \infty.$$

Proof. The strategy is to subtract off the inhomogeneous boundary conditions (4.0.2). Consider $v = u - \Phi$, then v satisfies homogeneous boundary conditions. Substituting $u = v + \Phi$ in the equation (4.0.1) yields

$$v_t + v \cdot \nabla v - \nu \Delta v + \nabla p + \phi(z) \frac{\partial v}{\partial x} + v_3 \phi'(z)(1,0,0) - \nabla \cdot (\beta(x)(C_s\delta)^2 |\nabla(v+\Phi)| \nabla(v+\Phi)) = 0, \tag{4.1.2}$$

$$\nabla \cdot v = 0.$$

with boundary conditions

$$v(x,y,0,t) = (0,0,0)^\top \quad \text{and} \quad v(x,y,L,t) = (0,0,0)^\top, \tag{4.1.3}$$

and

$$v(x+L,y,z,t) = v(x,y,z,t) \quad \text{and} \quad v(x,y+L,z,t) = v(x,y,z,t). \tag{4.1.4}$$

Taking the inner product with $v = (v_1, v_2, v_3)$ and integrating over Ω give

$$\frac{1}{2}\frac{\partial}{\partial t}||v||^2 + \nu||\nabla v||^2 + \int_\Omega \left(\phi(z)\frac{\partial v}{\partial x}\cdot v + v_1 v_3 \phi'(z)\right) dx + (\beta(x)(C_s\delta)^2|\nabla(v+\Phi)|\nabla(v+\Phi), \nabla v) = 0. \tag{4.1.5}$$

Since any integral containing ϕ and ϕ' will be zero outside the strip $\mathcal{O}_{\gamma L}$, by integrating by parts we have a

$$\begin{aligned}\int_\Omega \phi(z)\frac{\partial v}{\partial x}\cdot v\, dx = \frac{1}{2}\int_{\mathcal{O}_{\gamma L}} \phi(z)\frac{\partial}{\partial x}|v|^2\, dx &= \frac{1}{2}\int_{\mathcal{O}_{\gamma L}} \frac{\partial}{\partial x}(\phi(z)|v|^2)\, dx - \frac{1}{2}\int_{\mathcal{O}_{\gamma L}} \phi'(z)|v|^2\, dx \\ &= -\frac{1}{2}\frac{U}{\gamma L}\int_{\mathcal{O}_{\gamma L}} |v|^2\, dx.\end{aligned} \tag{4.1.6}$$

Inserting this identity in (4.1.5) and using the triangle inequality on the last term gives

$$\begin{aligned}&\frac{\partial}{\partial t}||v||^2 + 2\nu||\nabla v||^2 + \frac{U}{\gamma L}\int_{\mathcal{O}_{\gamma L}} \left(2v_1v_3 - |v|^2\right) dx + 2\int_\Omega \beta(x)(C_s\delta)^2|\nabla v|^3\, dx \\ &\leq 4\int_\Omega (\beta(x)(C_s\delta)^2|\nabla v|^2\,|\nabla\Phi|\, dx + 2\int_\Omega (\beta(x)(C_s\delta)^2|\nabla v|\,|\nabla\Phi|^2\, dx.\end{aligned} \tag{4.1.7}$$

The rest of analysis requires approximating various terms in the above. Let $p = 2$ in Proposition 4.1.4 and the two terms on the LHS of (4.1.7) can be bounded above as

$$\begin{aligned}\frac{U}{\gamma L}\int_{\mathcal{O}_{\gamma L}} |v|^2\, dx = \frac{U}{\gamma L}\int_{\mathcal{O}_{\gamma L}} d(z)^2|\frac{v}{d(z)}|^2\, dx &\leq \frac{U}{\gamma L}(\gamma L)^2\int_{\mathcal{O}_{\gamma L}} |\frac{v}{d(z)}|^2\, dx \\ &\leq 2U\gamma L\int_{\mathcal{O}_{\gamma L}} |\nabla v|^2\, dx \leq 2U\gamma L||\nabla v||^2.\end{aligned} \tag{4.1.8}$$

Similarly

$$\frac{U}{\gamma L}\int_{\mathcal{O}_{\gamma L}} 2|v_1 v_3|\,dx \le 4U\gamma L||\nabla v||^2. \tag{4.1.9}$$

To bound the two terms on the RHS of (4.1.7), use Hölder's inequality and Young's inequality $||fg||_{L^1} \le ||f||_{L^p}\,||g||_{L^q} \le \frac{\epsilon}{p}|f||^p_{L^p} + \frac{\epsilon^{-\frac{q}{p}}}{q}||g||^q_{L^q}$. Consider the first term, for $p=\frac{3}{2}$, $q=3$ and $\epsilon = 0.6$ we have

$$\begin{aligned} 4\int_\Omega (\beta(x)(C_s\delta)^2|\nabla v|^2\,|\nabla\Phi|\,dx &\le 4(C_s\delta)^2\Big(\int_\Omega \beta(x)|\nabla v|^3\,dx\Big)^{\frac{2}{3}}\Big(\int_\Omega \beta(x)|\nabla\Phi|^3\,dx\Big)^{\frac{1}{3}} \\ &\le 1.6\int_\Omega \beta(x)(C_s\delta)^2|\nabla v|^3\,dx + 4\int_\Omega \beta(x)(C_s\delta)^2|\nabla\Phi|^3\,dx. \end{aligned} \tag{4.1.10}$$

The second term is estimated exactly like the last term for $p=3$, $q=\frac{3}{2}$ and $\epsilon = 0.6$ as

$$\begin{aligned} 2\int_\Omega (\beta(x)(C_s\delta)^2|\nabla v|\,|\nabla\Phi|^2\,dx &\le 2(C_s\delta)^2\Big(\int_\Omega \beta(x)|\nabla v|^3\,dx\Big)^{\frac{1}{3}}\Big(\int_\Omega \beta(x)|\nabla\Phi|^3\,dx\Big)^{\frac{2}{3}} \\ &\le 0.4\int_\Omega \beta(x)(C_s\delta)^2|\nabla v|^3\,dx + 2\int_\Omega \beta(x)(C_s\delta)^2|\nabla\Phi|^3\,dx. \end{aligned} \tag{4.1.11}$$

Inserting these last four estimates into the energy inequality (4.1.7) for v gives

$$\frac{\partial}{\partial t}||v||^2 + (2\nu - 6U\gamma L)||\nabla v||^2 \le 6\int_\Omega \beta(x)(C_s\delta)^2|\nabla\Phi|^3\,dx.$$

Thus, if γ is chosen small enough that

$$\gamma < \frac{1}{3}(\mathcal{R}e)^{-1},$$

then $(2\nu - 6U\gamma L)$ becomes positive. Applying the Poincaré-Friedrichs inequality $||v|| \le C||\nabla v||$ gives

$$\frac{\partial}{\partial t}||v||^2 + C||v||^2 \le 6\int_\Omega \beta(x)(C_s\delta)^2|\nabla\Phi|^3\,dx.$$

Since RHS is uniformly bounded in time, a standard Grönwall's inequality shows that

$$\sup_{t\in(0,\infty)} ||v(t)|| \le C < \infty,$$

which proves the boundedness of the kinetic energy, $\frac{1}{2}||u||^2$. From this and standard arguments it follows that

$$\frac{1}{T}\int_0^T (\frac{1}{|\Omega|}\int_\Omega \nu|\nabla u|^2 + (c_s\delta)^2\beta(x)|\nabla u|^3 dx)\ dt \leq C < \infty,$$

which means $\langle \varepsilon_{SMD}(u)\rangle$ is well-defined. □

4.1.3 van Driest Damping

To modify the mixing-length model van Driest proposed [83], with some theoretical support but mainly as a good fit to data (p.77 of Wilcox [86]), that the mixing length ℓ should be multiplied by the damping function so that $\ell(x) \to 0$ as $x \to$ wall. The van Driest damping function is

$$f_w(z) = 1 - e^{\frac{-z^+}{A^+}}, \tag{4.1.12}$$

where $A^+ = 26$ is the van Driest constant and z^+ is the non-dimensional distance from the wall (p.76 of Wilcox [86])

$$z^+ = \frac{u_\tau(L-z)}{\nu}, \tag{4.1.13}$$

which determines the relative importance of viscous and turbulent phenomena. u_τ is the wall shear velocity given by

$$u_\tau = \sqrt{\nu \frac{\partial u}{\partial z}\Big|_{\text{wall}}}. \tag{4.1.14}$$

u_τ is still unknown, the analysis herein will require a specific value for u_τ. To this end, it can be estimated as follows. Near the wall $\nabla u \simeq \frac{\partial u}{\partial z}$, then

$$u_\tau = \sqrt{\nu \frac{\partial u}{\partial z}\Big|_{\text{wall}}} \simeq \sqrt{\nu\ \nabla u|_{\text{wall}}} = \sqrt[4]{\nu^2(\nabla u|_{\text{wall}})^2} \simeq \sqrt[4]{\nu\langle\bar{\epsilon}_w\rangle}, \tag{4.1.15}$$

where $\bar{\epsilon}_w$ is a spatial-average energy dissipation rate near the wall. After assuming a non-zero fraction occurs in near-wall region [83] and therefore neglecting the effects of viscosity far from the boundary layer, dissipation occurs mainly in the boundary layers near the bottom and top walls which both have a volume of $L^3\,\gamma$. Hence

$$\langle\epsilon\rangle = 2\frac{1}{L^3}\,(L^3\,\gamma)\langle\bar{\epsilon}_w\rangle = 2\gamma\langle\bar{\epsilon}_w\rangle.$$

On the other hand, based on the statistical equilibrium $\langle\epsilon\rangle = \frac{U^3}{L}$, therefore

$$\langle\epsilon\rangle = \frac{U^3}{L} = 2\gamma\langle\bar{\epsilon}_w\rangle.$$

Using $\gamma = \mathcal{O}(\mathcal{R}e^{-1})$ gives

$$\langle\bar{\epsilon}_w\rangle \simeq \frac{1}{2}\frac{U^4}{\nu}. \tag{4.1.16}$$

Then u_τ is estimated by inserting (4.1.16) in (4.1.15) to be

$$u_\tau \simeq \frac{U}{\sqrt[4]{2}}. \tag{4.1.17}$$

Hence van Driest damping function is approximated as (Figure 15)

$$f_w(z) \simeq 1 - \exp(\frac{-U(L-z)}{26\sqrt[4]{2}\ \nu}). \tag{4.1.18}$$

Using Taylor series to approximate (4.1.18) in the boundary layer $\mathcal{O}_{\gamma L}$ gives

$$f_w(z) \simeq \sum_{n=1}^{k}[\frac{1}{26\ \sqrt[4]{2}\ n!}\,\mathcal{R}e\,(1-\frac{z}{L})]^n + \mathcal{O}(\mathcal{R}e^{k+1}\,(1-\frac{z}{L})^{k+1}). \tag{4.1.19}$$

Note that the above approximation (4.1.19) is valid when the reminder $\mathcal{R}e\,(1-\frac{z}{L})$ is less than 1, and this occurs when $L - \gamma L \leq z \leq L$. Moreover, approximation (4.1.19) suggests $(\mathcal{R}e)^\alpha(1-\frac{z}{L})^\alpha$ for $\alpha \geq 1$ as a damping function only on the top layer. Thus (4.1.20) is an algebraic approximation to the van Driest damping on the whole symmetric domain (Figure 16, for $\alpha = 2$).

$$\beta_w(z) = \begin{cases} (\mathcal{R}e)^\alpha(\frac{z}{L})^\alpha & \text{if } z \in [0, \gamma L] \\ 1 & \text{if } z \in [\gamma L, L-\gamma L] \\ (\mathcal{R}e)^\alpha(1-\frac{z}{L})^\alpha & \text{if } z \in [L-\gamma L, L] \end{cases}. \tag{4.1.20}$$

Remark 4.1.6. β_w plays the role of β in (4.0.1).

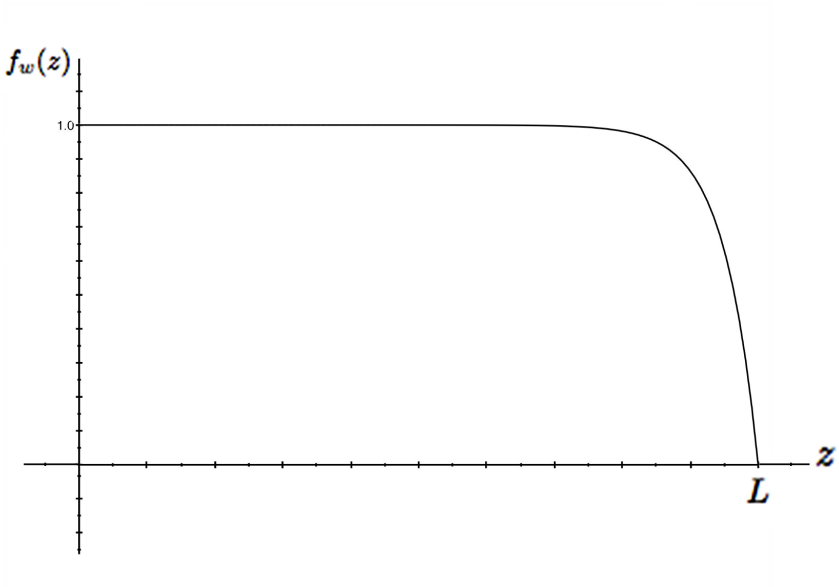

Figure 15: van Driest.

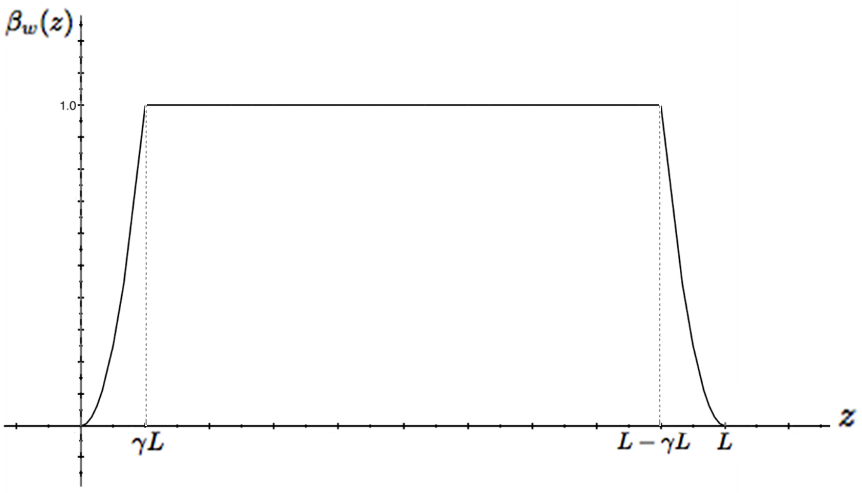

Figure 16: Algebraic approximation of van Driest.

4.2 ANALYSIS OF THE SMAGORINSKY WITH DAMPING FUNCTION

Theorem 4.2.1. Suppose $u_0 \in L^2(\Omega)$ and let [1] $\gamma = \frac{1}{5.1}\mathcal{R}e^{-1}$, then for any positive damping function $\beta(z) \in L^1(\Omega)$, $\langle \varepsilon_{SMD}(u) \rangle$ satisfies

$$\langle \varepsilon_{SMD}(u) \rangle \leq \left[C_1 + C_2 \, (\frac{C_s \delta}{L})^2 \, \mathcal{R}e^3 \, \frac{1}{L} \int_{L-\gamma L}^{L} \beta(z) \, dz \right] \frac{U^3}{L}.$$

Proof. The weak form of (4.0.1) is obtained by taking the scalar product $v \in \mathbb{X}_0$ and $q \in L_0^2$ with (4.0.1) and integrating over the space Ω:

$$\begin{aligned} (u_t, v) + \nu(\nabla u, \nabla v) + b(u, u, v) - (p, \nabla \cdot v) + (\beta(x)(C_s\delta)^2 |\nabla u| \nabla u, \nabla v) = 0 \quad \forall v \in \mathbb{X}_0, \\ (\nabla \cdot u, q) = 0 \quad \forall q \in L_0^2, \\ (u(x,0) - u_0(x), v) = 0 \quad \forall v \in \mathbb{X}_0. \end{aligned} \tag{4.2.1}$$

Take $v = u - \Phi$ in (4.2.1). Using the skew-symmetry of $b(\cdot, \cdot, \cdot)$ (Lemma 4.1.1) and $\nabla \cdot \Phi = 0$ gives:

$$(u_t, u - \Phi) + \nu(\nabla u, \nabla u - \nabla \Phi) + b(u, u, u - \Phi) + (\beta(x)(C_s\delta)^2 |\nabla u| \nabla u, \nabla u - \nabla \Phi) = 0,$$

which is equivalent to the following

$$\begin{aligned} \frac{1}{2}\frac{d}{dt}\|u\|^2 + \nu\|\nabla u\|^2 + (C_s\delta)^2(\beta(x)|\nabla u|\nabla u, \nabla u) = \frac{d}{dt}(u, \Phi) + b(u, u, \Phi) + \nu(\nabla u, \nabla \Phi) \\ + (C_s\delta)^2(\beta(x)|\nabla u|\nabla u, \nabla \Phi). \end{aligned} \tag{4.2.2}$$

Integrating with respect to time from above equation gives

$$\begin{aligned} &\frac{1}{2}\|u(T)\|^2 - \frac{1}{2}\|u(0)\|^2 + \nu \int_0^T \|\nabla u\|^2 dt + \int_0^T (\int_\Omega (C_s\delta)^2 \beta(x)|\nabla u|^3 dx) dt = (u(T), \Phi) \\ &- (u(0), \Phi) + \int_0^T b(u, u, \Phi) dt + \nu \int_0^T (\nabla u, \nabla \Phi) dt + (C_s\delta)^2 \int_0^T (\beta(x)|\nabla u|\nabla u, \nabla \Phi) dt. \end{aligned} \tag{4.2.3}$$

[1] In fact γ can be $\kappa(\frac{1}{5}\mathcal{R}e^{-1})$ for any $\kappa \in (0, 1)$. Without loss of generality, γ is taken to be $\frac{1}{5.1}\mathcal{R}e^{-1}$ for simplicity in calculations.

The proof continues by bounding, term by term, each term on the right-hand side of the energy equality (4.2.3). Using the Cauchy-Schwarz-Young's inequality and Lemma 4.1.2, the first three terms are estimated as follows.

$$(u(T),\Phi) \le \frac{1}{2}\|u(T)\|^2 + \frac{1}{2}\|\Phi\|^2 = \frac{1}{2}\|u(T)\|^2 + \frac{U^2\gamma L^3}{6}. \tag{4.2.4}$$

$$(u(0),\Phi) \le \|u(0)\|\|\Phi\| = \sqrt{\frac{\gamma}{3}} U L^{\frac{3}{2}} \|u(0)\|. \tag{4.2.5}$$

$$\nu\int_0^T (\nabla u, \nabla\Phi)dt \le \frac{\nu}{2}\int_0^T \|\nabla u\|^2 + \|\nabla\Phi\|^2 dt = \frac{\nu}{2}\int_0^T \|\nabla u\|^2 dt + \frac{\nu}{2}\frac{U^2 L}{\gamma}T. \tag{4.2.6}$$

For the nonlinear term $b(\cdot,\cdot,\cdot)$ in (4.2.3) add and subtract terms and then use skew-symmetry. This gives

$$\begin{aligned} b(u,u,\Phi) &= b(u-\Phi, u-\Phi, \Phi) + b(\Phi, u-\Phi, \Phi) \\ &= \frac{1}{2}b(u-\Phi, u-\Phi, \Phi) - \frac{1}{2}b(u-\Phi, \Phi, u-\Phi) \\ &+ \frac{1}{2}b(\Phi, u-\Phi, \Phi) - \frac{1}{2}b(\Phi, \Phi, u-\Phi). \end{aligned} \tag{4.2.7}$$

To estimate the four terms in (4.2.7), use Lemma 4.1.2, Lemma 4.1.3, the Cauchy-Schwarz-Young's inequality. Moreover, apply the fact that $b(u,u,\Phi)$ is an integration on $\mathcal{O}_{\gamma L}$ since $\text{supp}(\Phi) = \overline{\mathcal{O}}_{\gamma L}$. For the first term in (3.7) we have

$$\begin{aligned} &b(u-\Phi, u-\Phi, \Phi) \le \|\Phi\|_{L^\infty(\mathcal{O}_{\gamma L})}\|u-\Phi\|_{L^2(\mathcal{O}_{\gamma L})}\|\nabla(u-\Phi)\|_{L^2(\mathcal{O}_{\gamma L})} \le \gamma L U\|\nabla(u-\Phi)\|^2_{L^2(\mathcal{O}_{\gamma L})} \\ &\le \gamma L U\|\nabla u - \nabla\Phi\|^2_{L^2} \le UL\gamma(\|\nabla u\| + \|\nabla\Phi\|)^2 \le UL\gamma(2\|\nabla u\|^2 + 2\|\nabla\Phi\|^2) \\ &\le UL\gamma(2\|\nabla u\|^2 + 2\frac{U^2L}{\gamma}) = 2UL\gamma\|\nabla u\|^2 + 2U^3L^2. \end{aligned} \tag{4.2.8}$$

For the second term we have

$$\begin{aligned} &b(u-\Phi, \Phi, u-\Phi) \le \|\nabla\Phi\|_{L_\infty(\mathcal{O}_{\gamma L})}\|u-\Phi\|^2_{L^2(\mathcal{O}_{\gamma L})} \le \frac{U}{\gamma L}\gamma^2L^2\|\nabla(u-\Phi)\|^2_{L^2(\mathcal{O}_{\gamma L})} \\ &\le \gamma^2L^2\frac{U}{\gamma L}(2\|\nabla u\|^2 + 2\frac{U^2L}{\gamma}) = 2\gamma LU\|\nabla u\|^2 + 2U^3L^2. \end{aligned} \tag{4.2.9}$$

The third one is estimated as

$$
\begin{aligned}
&b(\Phi, u-\Phi, \Phi) \leq \|\Phi\|_{L^\infty(\mathcal{O}_{\gamma L})}\|\nabla(u-\Phi)\|_{L^2(\mathcal{O}_{\gamma L})}\|\Phi\|_{L^2(\mathcal{O}_{\gamma L})} \leq U\sqrt{\frac{U^2\gamma L^3}{3}}(\|\nabla u\| + \|\nabla\Phi\|)\\
&\leq U\sqrt{\frac{U^2\gamma L^3}{3}}(\|\nabla u\| + \sqrt{\frac{U^2 L}{\gamma}}) \leq \frac{U^2\gamma^{\frac{1}{2}}L^{\frac{3}{2}}}{\sqrt{3}}\|\nabla u\| + \frac{U^3L^2}{\sqrt{3}}\\
&= [\frac{U^{\frac{3}{2}}L}{\sqrt{3}}]\ [(U\gamma L)^{\frac{1}{2}}\|\nabla u\|] + \frac{U^3L^2}{\sqrt{3}} \leq (\frac{U^3L^2}{6}) + \frac{1}{2}UL\gamma\|\nabla u\|^2 + \frac{U^3L^2}{\sqrt{3}}\\
&= \frac{1}{2}UL\gamma\|\nabla u\|^2 + (\frac{\sqrt{3}}{3} + \frac{1}{6})U^3L^2.
\end{aligned}
\tag{4.2.10}
$$

And finally the last one satisfies

$$
\begin{aligned}
&b(\Phi, \Phi, u-\Phi) \leq \|\Phi\|_{L^\infty(\mathcal{O}_{\gamma L})}\|\nabla\Phi\|_{L^2(\mathcal{O}_{\gamma L})}\|u-\Phi\|_{L^2(\mathcal{O}_{\gamma L})} \leq U\sqrt{\frac{U^2L}{\gamma}}\gamma L\|\nabla(u-\Phi)\|_{L^2(\mathcal{O}_{\gamma L})}\\
&\leq U^2\gamma^{\frac{1}{2}}L^{\frac{3}{2}}(\|\nabla u\| + \|\nabla\Phi\|) \leq U^2\gamma^{\frac{1}{2}}L^{\frac{3}{2}}(\|\nabla u\| + (\frac{U^2L}{\gamma})^{\frac{1}{2}})\\
&= U^2\gamma^{\frac{1}{2}}L^{\frac{3}{2}}\|\nabla u\| + U^3L^2 = [U^{\frac{3}{2}}L]\ [(UL\gamma)^{\frac{1}{2}}\|\nabla u\|] + U^3L^2\\
&\leq \frac{1}{2}(U^3L^2) + \frac{1}{2}UL\gamma\|\nabla u\|^2 + U^3L^2 = \frac{1}{2}UL\gamma\|\nabla u\|^2 + \frac{3}{2}U^3L^2.
\end{aligned}
\tag{4.2.11}
$$

Using (4.2.8), (4.2.9), (4.2.10) and (4.2.11) in (4.2.7) gives the final estimation for the nonlinear term as below.

$$
|b(u, u, \Phi)| \leq \frac{5}{2}UL\gamma\|\nabla u\|^2 + \frac{19}{6}U^3L^2. \tag{4.2.12}
$$

Finally the last term on the RHS of (4.2.3) can be estimated as the follows. Using Hölder's inequality and Young's inequality for $p = \frac{3}{2}$ and $q = 3$ gives

$$
\begin{aligned}
|(\beta(x)|\nabla u|\nabla u, \nabla\Phi)| &\leq \int_\Omega |\beta(x)||\nabla u|^2|\nabla\Phi|dx\\
&= \int_\Omega (\beta^{\frac{2}{3}}|\nabla u|^2)\ (|\beta|^{\frac{1}{3}}|\nabla\Phi|)dx\\
&\leq\ [\int_\Omega \beta|\nabla u|^3dx]^{\frac{2}{3}}\ [\int_\Omega \beta|\nabla\Phi|^3dx]^{\frac{1}{3}} \leq\ \frac{2}{3}\int_\Omega \beta|\nabla u|^3dx + \frac{1}{3}\int_\Omega \beta|\nabla\Phi|^3dx.
\end{aligned}
\tag{4.2.13}
$$

Inserting (4.2.4), (4.2.5), (4.2.6), (4.2.12) and (4.2.13) in (4.2.3) implies

$$\frac{1}{2}\|u(T)\|^2 - \frac{1}{2}\|u(0)\|^2 + \nu\int_0^T \|\nabla u\|^2 dt + (C_s\delta)^2\int_0^T (\int_\Omega \beta(x)|\nabla u|^3 dx)dt \leq \frac{1}{2}\|u(T)\|^2 + \frac{U^2\gamma L^3}{6} + \sqrt{\frac{\gamma}{3}}UL^{\frac{3}{2}}\|u(0)\| + \frac{5}{2}UL\gamma\int_0^T \|\nabla u\|^2 dt + \frac{19}{6}U^3L^2T + \frac{\nu}{2}\int_0^T \|\nabla u\|^2 dt + \frac{\nu}{2}\frac{U^2L}{\gamma}T + \frac{2}{3}(C_s\delta)^2\int_0^T (\int_\Omega \beta(x)|\nabla u|^3 dx)dt + \frac{1}{3}(C_s\delta)^2\int_0^T (\int_\Omega \beta(x)|\nabla \Phi|^3 dx)dt. \tag{4.2.14}$$

Since the kinetic energy is bounded (Lemma 4.1.5), the above inequality becomes

$$(\frac{1}{2} - \frac{5}{2\nu}\gamma LU)\int_0^T \nu\|\nabla u\|^2 dt + \frac{1}{3}(C_s\delta)^2\int_0^T (\int_\Omega \beta(x)|\nabla u|^3 dx)dt \leq \frac{1}{2}\|u(0)\|^2 + \frac{1}{6}U^2\gamma L^3 + \sqrt{\frac{\gamma}{3}}UL^{\frac{3}{2}}\|u(0)\| + \frac{19}{6}U^3L^2T + \frac{\nu}{2\gamma}LU^2T + \frac{1}{3}(C_s\delta)^2\int_0^T (\int_\Omega \beta(x)|\nabla \Phi|^3 dx)dt. \tag{4.2.15}$$

Finally dividing both sides of (4.2.15) by T and $|\Omega| = L^3$ and taking the limit superior leads to

$$min\{\frac{1}{2} - \frac{5}{2}\frac{\gamma LU}{\nu}, \frac{1}{3}\}\langle\varepsilon_{SMD}(u)\rangle \leq \frac{19}{6}\frac{U^3}{L} + \frac{\nu}{2\gamma}\frac{U^2}{L^2} + \frac{1}{3}\frac{1}{L^3}(C_s\delta)^2\int_\Omega \beta(x)|\nabla\Phi|^3 dx. \tag{4.2.16}$$

The above inequality leads to the last step when C_1 and C_2 are positive and independent of viscosity, diam(Ω) and lid velocity. Take $\gamma = \frac{1}{5.1}\mathcal{R}e^{-1}$, then $(\frac{1}{2} - \frac{5}{2\nu}\gamma LU)$ becomes positive and therefore

$$\langle\varepsilon_{SMD}(u)\rangle \leq C_1\frac{U^3}{L} + C_2\frac{1}{L^3}(C_s\delta)^2\int_\Omega \beta(x)|\nabla\Phi|^3 dx. \tag{4.2.17}$$

Because the background flow Φ vanishes on $(\Omega\backslash\mathcal{O}_{\gamma L})$, we have

$$\int_\Omega \beta(x)|\nabla\Phi|^3 dx = (\frac{U}{\gamma L})^3\int_0^L\int_0^L\int_{L-\gamma L}^L \beta(x,y,z)dxdydz = \frac{U^3}{\gamma^3 L}\int_{L-\gamma L}^L \beta(z)dz. \tag{4.2.18}$$

Inserting (4.2.18) in (4.2.17) proves Theorem 4.2.1. □

4.2.1 Evaluation of Damping Functions

Theorem 4.2.1 is the starting point for the evaluation of damping functions. It is next applied to two damping functions in Corollaries 4.2.2 and 4.2.4 and the results will be compared.

Corollary 4.2.2. For the algebraic approximation of the van Driest damping function, $\beta_w(z)$ in (4.1.20), we have

$$\langle \varepsilon_{SMD}(u) \rangle \leq \left[C_1 + C_2 \frac{1}{\alpha+1} (\frac{C_s \delta}{L})^2 \mathcal{R}e^2 \right] \frac{U^3}{L}.$$

Proof. The result is a direct calculation by applying $\beta_w(z)$ in (4.1.20) to the Theorem 4.2.1. □

The upper bound in Corollary 4.2.2 is a function of the global velocity U, domain diameter L, the eddy size δ, and surprisingly, the Reynolds number. Moreover, it blows up as $\mathcal{R}e \to \infty$. Due to this fact one can propose the following modification to $\beta_w(z)$. Consider $\beta_d(z) \in C^1(\Omega)$ in (4.2.19) which is based on a connection of the algebraic damping near the wall smoothly to the no damping in the interior by Hermite interpolation. It is given by

$$\beta_d(z) = \begin{cases} (\frac{z}{L})^\alpha (1-\frac{z}{L})^\alpha & \text{if } z \in [0, \gamma L] \\ a_1(z-\gamma L)^3 + b_1(z-\gamma L)^2 + c_1(z-\gamma L) + d_1 & \text{if } z \in [\gamma L, 2\gamma L] \\ 1 & \text{if } z \in [2\gamma L, L-2\gamma L] \\ a_2(z+2\gamma L - L)^3 + b_2(z+2\gamma L - L)^2 + 1 & \text{if } z \in [L-2\gamma L, L-\gamma L] \\ (\frac{z}{L})^\alpha (1-\frac{z}{L})^\alpha & \text{if } z \in [L-\gamma L, L] \end{cases}, \tag{4.2.19}$$

where $\alpha \geq 0$ and a_1, a_2, b_1, b_2, c_1 and d_1 are constant such that

- $a_1 = \frac{-2}{\gamma^3 L^3} + \frac{1}{L^3}\alpha\gamma^{\alpha-3}(1-\gamma)^{\alpha-1}(1-2\gamma) + \frac{2}{L^3}\gamma^{\alpha-3}(1-\gamma)^\alpha$,
- $b_1 = \frac{3}{\gamma^2 L^2} - \frac{2}{L^2}\alpha\gamma^{\alpha-2}(1-\gamma)^{\alpha-1}(1-2\gamma) - \frac{3}{L^2}\gamma^{\alpha-2}(1-\gamma)^\alpha$,
- $c_1 = \frac{1}{L}\alpha\gamma^{\alpha-1}(1-\gamma)^{\alpha-1}(1-2\gamma)$,
- $d_1 = \gamma^\alpha(1-\gamma)^\alpha$,
- $a_2 = -a_1$,
- $b_2 = -\frac{3}{\gamma^2 L^2} + \frac{1}{L^2}\alpha\gamma^{\alpha-2}(1-\gamma)^{\alpha-1}(1-2\gamma) + \frac{3}{L^2}\gamma^{\alpha-2}(1-\gamma)^\alpha$.

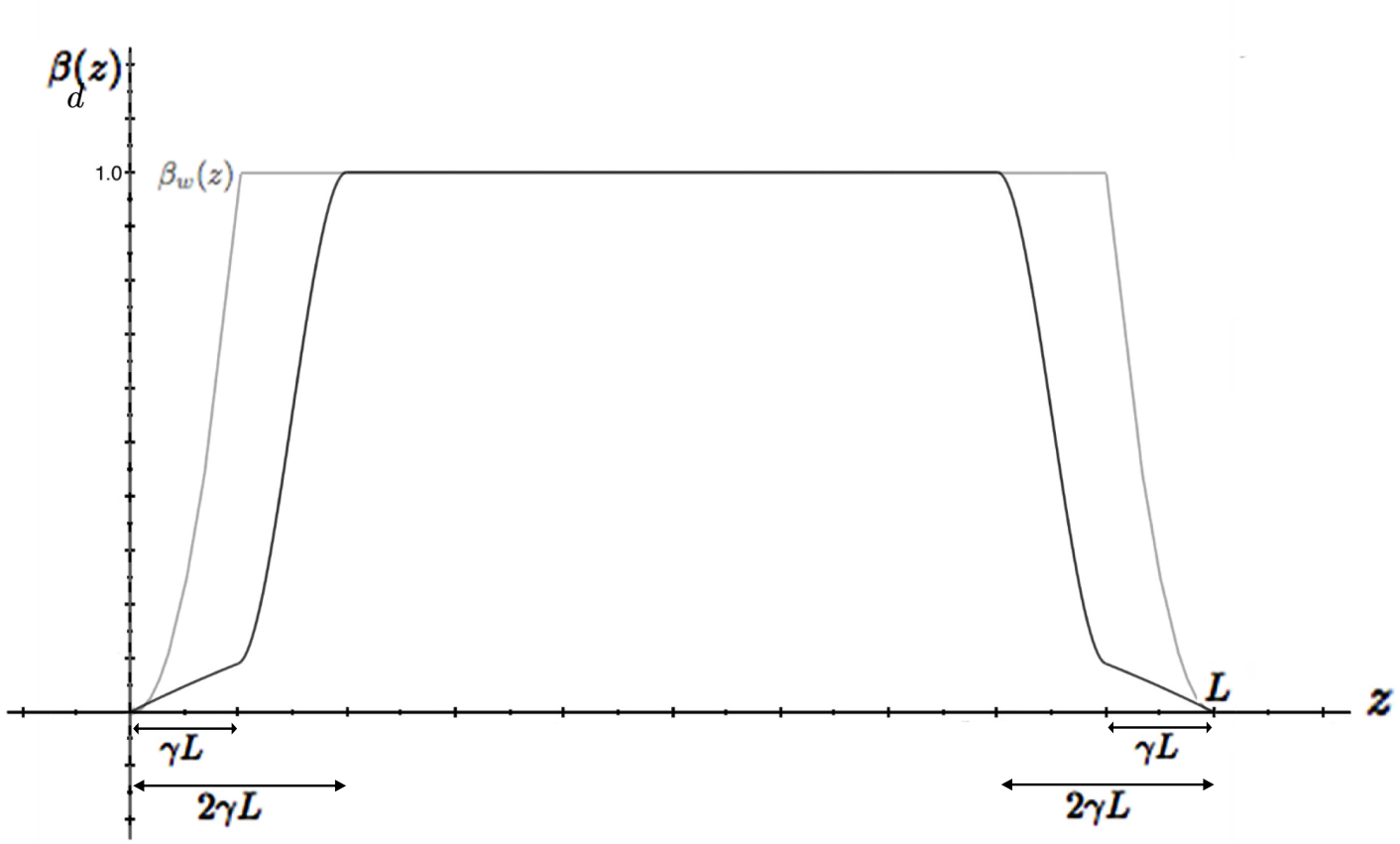

Figure 17: Proposed damping function (3.19).

Remark 4.2.3. All the constants above are calculated such that $\beta_d(z) \in C^1$. β_d, which plays the role of β in (4.0.1), is sketched in Figure 5 and compared to β_w. They both are symmetric, bounded and vanish at $z = 0$ and $z = L$. Moreover, they are almost 1 on the whole domain except on the thin boundary layers.

Corollary 4.2.4. Suppose $u_0 \in L^2(\Omega)$ and β_d given by (4.2.19) with $2 \leq \alpha \in \mathbb{N}$. Then, for any $\mathcal{R}e \geq 1$ we have

$$\langle \varepsilon_{SMD}(u) \rangle \leq \left[C_1 + C_2 (\frac{C_s \delta}{L})^2 \right] \frac{U^3}{L}.$$

Proof. Considering β_d is symmetric on the whole domain implies

$$\int_{L-\gamma L}^{L} \beta_d(z) dz = \int_0^{\gamma L} (\frac{z}{L})^\alpha (1 - \frac{z}{L})^\alpha dz.$$

Now applying the Binomial Theorem on $(1 - \frac{z}{L})^\alpha$ and then taking the integral gives

$$\begin{aligned} \int_{L-\gamma L}^{L} \beta_d(z) dz = L\gamma^{\alpha+1} \big(& \frac{1}{\alpha+1} - \frac{1}{\alpha+2}\alpha\gamma + \frac{1}{\alpha+3}\frac{\alpha(\alpha-1)}{2}\gamma^2 \\ & + \ldots + (-1)^\alpha \frac{1}{2\alpha}\alpha\gamma^{\alpha-1} + (-1)^\alpha \frac{1}{2\alpha+1}\gamma^\alpha \big). \end{aligned} \tag{4.2.20}$$

After dropping negative terms, since $\gamma = \frac{1}{5.1}(\mathcal{R}e)^{-1} \ll 1$ the RHS of (4.2.20) can be bounded above by a constant, C_α, which depends on α. Therefore

$$\int_{L-\gamma L}^{L} \beta_d(z) dz \leq C_\alpha L \gamma^{\alpha+1}, \tag{4.2.21}$$

Using $\gamma = \frac{1}{5.1}(\mathcal{R}e)^{-1}$ and inserting the above in the Theorem 4.2.1 imply

$$\langle \varepsilon_{SMD}(u) \rangle \leq \left[C_1 + C_2 \, (\frac{C_s \delta}{L})^2 \, (\frac{1}{5.1})^3 \, C_\alpha \, \gamma^{\alpha-2} \right] \frac{U^3}{L}.$$

Use the assumptions $\alpha \geq 2$ and $\gamma = \frac{1}{5.1}(\mathcal{R}e)^{-1} \ll 1$ imply $\gamma^{\alpha-2} \leq 1$ and now the corollary is proved.

□

Corollary 4.2.4 is in accordance with the Kolmogorov theory of turbulence. It establishes that the combination of SM with damping function $\beta_d(z)$ given by (4.2.19) does not over dissipate, and the energy input rate $\frac{U^3}{L}$ is balanced by $\langle \varepsilon_{SMD}(u) \rangle$. This estimate is consistent with the rate proven for the NSE in [15] and [17]; it is also dimensionally consistent.

The assumption $\alpha \geq 2$ is a significant one in the analysis. When $\alpha = 1$ we obtain the following corollary.

Corollary 4.2.5. Suppose $\alpha = 1$ in Corollary 4.2.4, then

$$\langle \varepsilon_{SMD}(u) \rangle \leq \left[C_1 + C_2 (\frac{C_s \delta}{L})^2 \mathcal{R}e \right] \frac{U^3}{L}.$$

Proof. The proof follows that of $\alpha \geq 2$ in the Corollary 4.2.4 except the inequality (4.2.21) is modified to

$$\int_{L-\gamma L}^{L} \beta_d(z)\, dz \leq C\, L\, (\mathcal{R}e)^{-2},$$

for $\alpha = 1$. □

4.3 CONCLUSION

The key parameter is $\alpha =$ the order of contact of the damping function at the wall. Comparing $\langle \varepsilon_{SMD}(u) \rangle \simeq \frac{U^3}{L}$ for $\alpha \geq 2$ in Corollary 4.2.4 with $\langle \varepsilon_{SMD}(u) \rangle \simeq \left[C_1 + C_2 (\frac{C_s \delta}{L})^2 \mathcal{R}e \right] \frac{U^3}{L}$ for $\alpha = 1$ in Corollary 4.2.5 suggests that the model over dissipates flows for $\alpha = 1$. If the upper bounds are sharp (an open problem), the accurate simulation would need $\alpha \geq 2$. The next logical step is to study $\langle \varepsilon_{SMD}(u^h) \rangle$ after discretization by fixed mesh h and extend the results in this paper, especially when the mesh does not resolve the boundary layers.

5.0 A DISCRETE HOPF INTERPOLANT AND STABILITY OF THE FINITE ELEMENT METHOD FOR NATURAL CONVECTION

Natural convection of a fluid driven by heating a side wall or the bottom wall is a classic problem in fluid mechanics that is still of technological and scientific importance [11]. The temperature in this problem is uniformly bounded in time ($\|T(t)\| \leq C < \infty$) under mild data assumptions. However, when this often analyzed problem is approximated by standard FEM, all available stability bounds, e.g. [78,79,87], for the temperature exhibit exponential growth in time unless the heat transfer through the solid container is included in the model, e.g. [6]. Moreover, even in the stationary case, stability estimates can yield extremely restrictive mesh conditions ($h = \mathcal{O}(Ra^{-30/(6-d)})$), e.g. [12].

In this chapter we prove that, without the aforementioned restrictions, the temperature approximation is bounded sub-linearly in terms of the simulation time t^* provided that the first mesh line in the finite element mesh is within $\mathcal{O}(Ra^{-1})$ of the heated wall; that is, $\|T_h^n\| \leq C\sqrt{t^*}$ [19]. In practice, numerical simulations are carried out on a graded mesh [11,36,52,55] due to the interaction between the boundary layer, which is $\mathcal{O}(Ra^{-1/4})$ in the laminar regime [26], and the core flow. In particular, several mesh points are placed within the boundary layer, which encompasses the internal core flow. Although our condition is more restrictive, this may be due to a gap in the analysis and, nonetheless, it is indicative of the value of graded meshes for stability as well as accuracy.

Consider natural convection within an enclosed cavity. Let $\Omega \subset \mathbb{R}^d$ (d=2,3) be a convex polyhedral domain with boundary $\partial\Omega$. Here n denotes the usual outward normal, $\xi = g/|g|$ denotes the unit vector in the direction of gravity, Pr is the Prandtl number, and Ra is the Rayleigh number. Further, f and γ are the body force and heat source, respectively. The boundary is partitioned such that $\partial\Omega = \overline{\Gamma_1} \cup \overline{\Gamma_2}$ with $\Gamma_1 \cap \Gamma_2 = \emptyset$ and $|\Gamma_H \cup \Gamma_N| = |\Gamma_1| > 0$.

Given $u(x,0) = u^0(x)$ and $T(x,0) = T^0(x)$, let $u(x,t) : \Omega \times (0,t^*] \to \mathbb{R}^d$, $p(x,t) : \Omega \times (0,t^*] \to \mathbb{R}$, and $T(x,t) : \Omega \times (0,t^*] \to \mathbb{R}$ satisfy

$$u_t + u \cdot \nabla u - Pr\Delta u + \nabla p = PrRa\xi T + f \ \ in\ \Omega, \tag{5.0.1}$$

$$\nabla \cdot u = 0 \ \ in\ \Omega, \tag{5.0.2}$$

$$T_t + u \cdot \nabla T - \Delta T = \gamma \ \ in\ \Omega, \tag{5.0.3}$$

$$u = 0 \ \ on\ \partial\Omega, \quad T = 1 \ \ on\ \Gamma_N, \ \ T = 0 \ \ on\ \Gamma_H, \quad n \cdot \nabla T = 0 \ \ on\ \Gamma_2. \tag{5.0.4}$$

In Sections 5.1 and 5.2, we collect necessary mathematical tools and present common numerical schemes. In Section 5.3, the major results are proven. In particular, it is shown that provided the first mesh line in the finite element mesh is within $\mathcal{O}(Ra^{-1})$ of the heated wall, then the computed velocity, pressure, and temperature are stable allowing for sub-linear growth in t^* (Theorems 5.3.1 and 5.3.2). Conclusions are presented in Section 5.4.

5.1 MATHEMATICAL PRELIMINARIES

The $L^2(\Omega)$ inner product is $(\cdot,\cdot)$ and the induced norm is $\|\cdot\|$. Moreover, for any subset $\Omega \neq O \subset \mathbb{R}^d$ we define the L^2 inner product $(\cdot,\cdot)_{L^2(O)}$ and norm $\|\cdot\|_{L^2(O)}$. Define the Hilbert spaces,

$$X := H_0^1(\Omega)^d = \{v \in H^1(\Omega)^d : v = 0 \ on\ \partial\Omega\}, \ Q := L_0^2(\Omega) = \{q \in L^2(\Omega) : \int_\Omega q dx = 0\},$$
$$W_{\Gamma_1} := \{S \in H^1(\Omega) : S = 0 \ on\ \Gamma_1\}, \ W := H^1(\Omega), \ V := \{v \in X : (q, \nabla \cdot v) = 0 \ \forall q \in Q\}.$$

The explicitly skew-symmetric trilinear forms are denoted:

$$b(u,v,w) = \frac{1}{2}(u \cdot \nabla v, w) - \frac{1}{2}(u \cdot \nabla w, v) \quad \forall u,v,w \in X,$$
$$b^*(u,T,S) = \frac{1}{2}(u \cdot \nabla T, S) - \frac{1}{2}(u \cdot \nabla S, T) \quad \forall u \in X, \ T,S \in W.$$

They enjoy the following useful properties.

Lemma 5.1.1. There are constants C_1 and C_2 such that for all $u, v, w \in X$ and $T, S \in W$, $b(u, v, w)$ and $b^*(u, T, S)$ satisfy

$$\begin{aligned} b(u, v, w) &= (u \cdot \nabla v, w) + \frac{1}{2}((\nabla \cdot u)v, w), \\ b^*(u, T, S) &= (u \cdot \nabla T, S) + \frac{1}{2}((\nabla \cdot u)T, S), \\ b(u, v, w) &\leq C_1 \|\nabla u\| \|\nabla v\| \|\nabla w\|, \\ b^*(u, T, S) &\leq C_2 \|\nabla u\| \|\nabla T\| \|\nabla S\|. \end{aligned}$$

Proof. See Lemma 18 p. 123 of [47]. □

5.1.1 Finite Element Preliminaries

Consider a regular mesh $\Omega_h = \{K\}$ of Ω with maximum triangle diameter length h. Let $X_h \subset X$, $Q_h \subset Q$, $W_h \subset W$, and $W_{\Gamma_1,h} \subset W_{\Gamma_1}$ be conforming finite element spaces consisting of continuous piecewise polynomials of degrees j, l, j, and j, respectively. Furthermore, we consider those spaces for which the discrete inf-sup condition is satisfied,

$$\inf_{q_h \in Q_h} \sup_{v_h \in X_h} \frac{(q_h, \nabla \cdot v_h)}{\|q_h\| \|\nabla v_h\|} \geq \beta > 0, \tag{5.1.1}$$

where β is independent of h. The space of discretely divergence free functions is defined by

$$V_h := \{v_h \in X_h : (q_h, \nabla \cdot v_h) = 0, \forall q_h \in Q_h\}$$

and accompanying dual norm

$$\|w\|_{V_h^*} = \sup_{v_h \in V_h} \frac{(w, v_h)}{\|\nabla v_h\|}.$$

The continuous time, finite element in space weak formulation of the system (5.0.1) - (5.0.4) is: Find $u_h : [0, t^*] \to X_h$, $p_h : [0, t^*] \to Q_h$, $T_h : [0, t^*] \to W_h$ for a.e. $t \in (0, t^*]$ satisfying:

$$(u_{h,t}, v_h) + b(u_h, u_h, v_h) + Pr(\nabla u_h, \nabla v_h) - (p_h, \nabla \cdot v_h) = PrRa(\gamma T_h, v_h) + (f, v_h) \ \ \forall v_h \in X_h, \tag{5.1.2}$$

$$(q_h, \nabla \cdot u_h) = 0 \ \ \forall q_h \in Q_h, \tag{5.1.3}$$

$$(T_{h,t}, S_h) + b^*(u_h, T_h, S_h) + (\nabla T_h, \nabla S_h) = (\gamma, S_h) \ \ \forall S_h \in W_{h,\Gamma_1}. \tag{5.1.4}$$

5.1.2 Construction of the Discrete Hopf Extension

The mesh condition $h = \mathcal{O}(Ra^{-30/(6-d)})$ from [12] arises from the use of the Scott-Zhang interpolant of degree j. To improve upon this condition, we develop a special interpolant for the upcoming analysis. We construct it as follows:

Step one: Consider those mesh elements K such that $K \cap \Gamma_1 \neq \emptyset$. Enumerate these mesh elements from 1 to l'.

Step two: $\forall\, 1 \leq l \leq l'$, let $\{\phi_k^l\}_{k=1}^{d+1}$ be the usual piecewise linear hat functions with $supp\ \phi_k^l \subset K_l$.

Step three: Fix l, select those ϕ_k^l such that $\phi_k^l(x) = 1$ for $x \in K_l \cap \Gamma_1$.

Step four: Define ψ_i such that $\{\psi^i\}_{i=1}^{i'} = \{\phi_k^l\}_{k,l=1}^{k',l'}$.

Step five: Define $\tau = \sum_{i=1}^{i'} \tilde{T}^i \psi^i$ where $-\infty < \tilde{T}_{min} \leq \tilde{T}^i \leq \tilde{T}_{max} < \infty$ are arbitrary constants.

Then,

Theorem 5.1.2. Suppose $\tilde{T} : \Gamma_1 \to \mathbb{R}$ is a piecewise linear function defined on Γ_1. The discrete Hopf extension $\tau : \Omega \to \mathbb{R}$ satisfies

$$\tau(x) = \tilde{T}\ on\ \Gamma_1,$$
$$\tau(x) = 0\ on\ \Omega - \cup_{l=1}^{l'} K_l.$$

Moreover, let $\delta = \max_{1\leq l\leq l'} h_l$. Then, the following estimate holds: $\forall \epsilon > 0$, $\forall (\chi_1, \chi_2) \in (X_h, W_h)$

$$|b^*(\chi_1, \tau, \chi_2)| \leq C\delta\Big(\epsilon^{-1}\|\nabla\chi_1\|^2 + \epsilon\|\nabla\chi_2\|^2\Big). \tag{5.1.5}$$

Proof. The properties are a consequence of the construction. For the estimate (5.1.5), it suffices to consider $|b^*(\chi_1, \tilde{T}^i\psi^i, \chi_2)|$ where $\tilde{T}^i = \tilde{T}(x_i)$ is the corresponding nodal value of $\tilde{T}$. For each ψ^i there is a corresponding mesh element K_l such that $supp\ \psi^i \subset K_l$. Let $\hat{K} \subset \mathbb{R}^d$ be the reference element and $F_{K_l} : \hat{K} \to K_l$ the associated affine transformation given by $x = F_{K_l}\hat{x} = B_{K_l}\hat{x} + b_{K_l}$. We will utilize the operator norm $\|\cdot\|_{op}$ and the Euclidean norm $|\cdot|_2$ below.

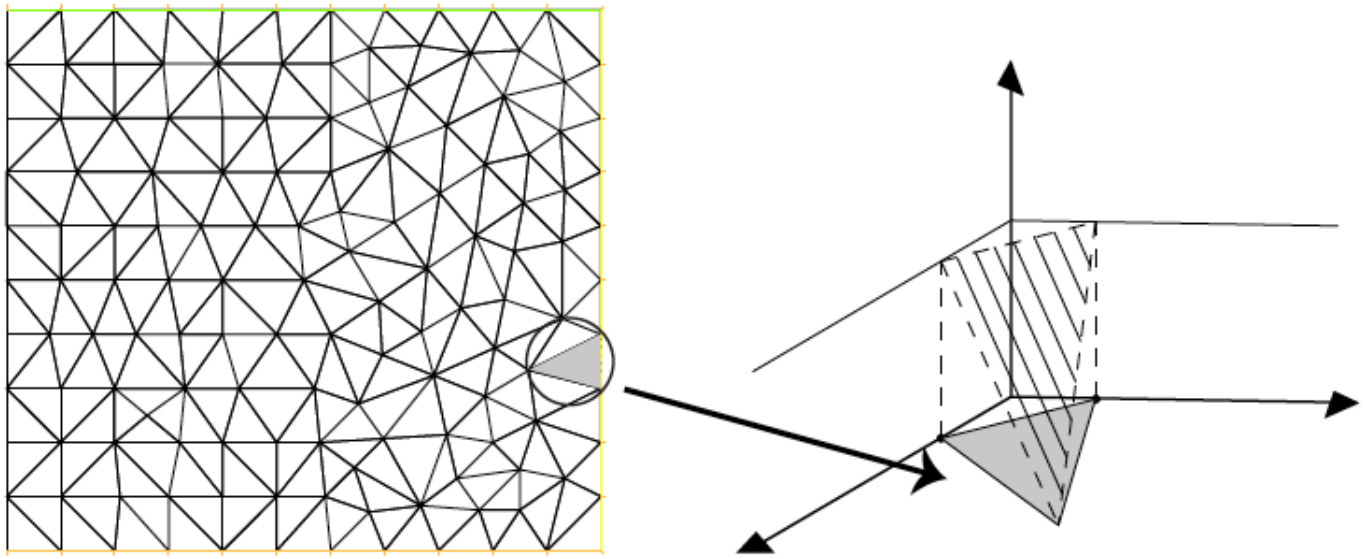

Figure 18: The discrete Hopf interpolant on one mesh element.

Consider $\frac{1}{2}|(\chi_1 \cdot \nabla \tilde{T}^i \psi^i, \chi_2)|$, the estimate for $\frac{1}{2}|(\chi_1 \cdot \nabla \chi_2, \tilde{T}^i \psi^i)|$ follows analogously. Transform to the reference element, use standard FEM estimates, the Cauchy-Schwarz inequality, and equivalence of norms. Then,

$$\begin{aligned}
\frac{1}{2}|(\chi_1 \cdot \nabla \tilde{T}^i \psi^i, \chi_2)| &= \frac{|\tilde{T}^i||det(B_{K_l})|}{2} \left| \int_{\hat{K}} \hat{\chi_1} \cdot B_{K_l}^{-T} \hat{\nabla} \hat{\psi^i} \hat{\chi_2} d\hat{x} \right| \\
&\leq \frac{|\tilde{T}^i||det(B_{K_l})|}{2} \|B_{K_l}^{-T}\|_{op} |\hat{\nabla} \hat{\psi^i}|_2 \int_{\hat{K}} |\hat{\chi_1}|_2 |\hat{\chi_2}| d\hat{x} \\
&\leq C h_l^{d-1} \|\hat{\chi_1}\|_{L2(\hat{K})} \|\hat{\chi_2}\|_{L2(\hat{K})} \\
&\leq C h_l^{d-1} \|\hat{\nabla} \hat{\chi_1}\|_{L2(\hat{K})} \|\hat{\nabla} \hat{\chi_2}\|_{L2(\hat{K})}.
\end{aligned} \tag{5.1.6}$$

Consider $\|\hat{\nabla} \hat{\chi_2}\|_{L2(\hat{K})}$ and $\|\hat{\nabla} \hat{\chi_1}\|_{L2(\hat{K})}$. Transforming back to the mesh element and using

standard FEM estimates yields

$$\begin{aligned}
\|\hat{\nabla}\hat{\chi_2}\|^2_{L2(\hat{K})} &= |det(B^{-1}_{K_l})| \int_{K_l} B^T_{K_l}\nabla\chi_2 \cdot B^T_{K_l}\nabla\chi_2 dx \qquad (5.1.7)\\
&\leq |det(B^{-1}_{K_l})| \|B^T_{K_l}\|^2_{op} \|\nabla\chi_2\|^2_{L2(K_l)}\\
&\leq Ch_l^{2-d}\|\nabla\chi_2\|^2_{L2(K_l)}\\
&\leq Ch_l^{2-d}\|\nabla\chi_2\|^2,\\
\|\hat{\nabla}\hat{\chi_1}\|^2_{L2(\hat{K})} &\leq Ch_l^{2-d}\|\nabla\chi_1\|^2. \qquad (5.1.8)
\end{aligned}$$

Use (5.1.7) and (5.1.8) in (5.1.6) and Young's inequality. This yields

$$\frac{1}{2}|(\chi_1 \cdot \nabla\tilde{T}^i\psi^i, \chi_2)| \leq Ch_l\Big(\epsilon\|\nabla\chi_1\|^2 + \epsilon^{-1}\|\nabla\chi_2\|^2\Big).$$

Summing from $i = 1$ to $i = i'$ and taking the maximum h_l yields the result. □

Remark: If we allow the interpolant to be constructed with the basis elements of W_h, we can reconstruct any function $\upsilon_h \in W_h$ exactly on the boundary Γ_1 with the same properties.
Remark: For square and cubic domains we can define such an interpolant explicitly, e.g.,

$$\tau(x) = \begin{cases} \frac{1}{2\delta}(2\delta - x_\alpha) & 0 \leq x_\alpha \leq \delta,\\ \frac{1}{2} & \delta \leq x_\alpha \leq 1-\delta,\\ \frac{1}{2\delta}(1 - x_\alpha) & 1-\delta \leq x_\alpha \leq 1, \end{cases}$$

where α is in the direction orthogonal to the differentially heated walls or in the direction of gravity for the differentially heated vertical wall problem and Rayleigh-Bénard problem, respectively. This function was introduced first by Hopf [32] and has been useful in estimating the energy dissipation rates for shear-driven flows and convection [16].

5.2 NUMERICAL SCHEMES

In this section, we consider the following popular temporal discretizations: BDF1, linearly implicit BDF1, BDF2, and linearly implicit BDF2; see [3, 37] regarding linearly implicit variants. Let $\eta(\chi) = a_{-1}\chi^{n+1} + a_0\chi^n$. Denote the fully discrete solutions by u_h^n, p_h^n, and T_h^n at time levels $t^n = n\Delta t$, $n = 0, 1, ..., N$, and $t^* = N\Delta t$. Given $(u_h^n, T_h^n) \in (X_h, W_h)$, find $(u_h^{n+1}, p_h^{n+1}, T_h^{n+1}) \in (X_h, Q_h, W_h)$ satisfying, for every $n = 0, 1, ..., N-1$, the fully discrete approximation of the system (5.0.1) - (5.0.4) is

BDF1 and linearly implicit BDF1:

$$(\frac{u_h^{n+1} - u_h^n}{\Delta t}, v_h) + b(\eta(u_h), u_h^{n+1}, v_h) + Pr(\nabla u_h^{n+1}, \nabla v_h) - (p_h^{n+1}, \nabla \cdot v_h) = PrRa(\xi\eta(T_h), v_h) + (f^{n+1}, v_h) \ \ \forall v_h \in X_h, \quad (5.2.1)$$

$$(\nabla \cdot u_h^{n+1}, q_h) = 0 \ \ \forall q_h \in Q_h, \quad (5.2.2)$$

$$(\frac{T_h^{n+1} - T_h^n}{\Delta t}, S_h) + b^*(\eta(u_h), T_h^{n+1}, S_h) + (\nabla T_h^{n+1}, \nabla S_h) = (\gamma^{n+1}, S_h) \ \ \forall S_h \in W_{h,\Gamma_1}, \quad (5.2.3)$$

where BDF1 is given by $a_{-1} = a_0 + 1 = 1$ and linearly implicit BDF1 by $a_{-1} + 1 = a_0 = 1$. Moreover, given (u_h^{n-1}, T_h^{n-1}) and $(u_h^n, T_h^n) \in (X_h, Q_h, W_h)$, find $(u_h^{n+1}, p_h^{n+1}, T_h^{n+1}) \in (X_h, Q_h, W_h)$ satisfying, for every $n = 1, 2, ..., N-1$, the fully discrete approximation of the system (5.0.1) - (5.0.4) is

BDF2 and linearly implicit BDF2:

$$(\frac{3u_h^{n+1} - 4u_h^n + u_h^{n-1}}{2\Delta t}, v_h) + b(\eta(u_h), u_h^{n+1}, v_h) + Pr(\nabla u_h^{n+1}, \nabla v_h) - (p_h^{n+1}, \nabla \cdot v_h) = PrRa(\xi\eta(T_h), v_h) + (f^{n+1}, v_h) \ \ \forall v_h \in X_h, \quad (5.2.4)$$

$$(\nabla \cdot u_h^{n+1}, q_h) = 0 \ \ \forall q_h \in Q_h, \quad (5.2.5)$$

$$(\frac{3T_h^{n+1} - 4T_h^n + T_h^{n-1}}{2\Delta t}, S_h) + b^*(\eta(u_h), T_h^{n+1}, S_h) + (\nabla T_h^{n+1}, \nabla S_h) = (\gamma^{n+1}, S_h) \ \ \forall S_h \in W_{h,\Gamma_1}, \quad (5.2.6)$$

where BDF2 is given by $a_{-1} = a_0 + 1 = 1$ and linearly implicit BDF2 by $1 - a_{-1} = a_0 = -1$.

5.3 NUMERICAL ANALYSIS

We present stability results for the aforementioned algorithms provided the first meshline in the finite element mesh is within $\mathcal{O}(Ra^{-1})$ of the heated wall.

5.3.1 Stability Analysis

Theorem 5.3.1. Consider **BDF1** or **linearly implicit BDF1**. Suppose $f \in L^2(0,t^*;H^{-1}(\Omega)^d)$, and $\gamma \in L^2(0,t^*;H^{-1}(\Omega))$. If $\delta = \mathcal{O}(Ra^{-1})$, then there exist $C>0$, independent of t^*, such that

BDF1:

$$\frac{1}{2}\|T_h^N\|^2 + \|u_h^N\|^2 + \sum_{n=0}^{N-1}\|T_h^{n+1}-T_h^n\|^2 + \sum_{n=0}^{N-1}\|u_h^{n+1}-u_h^n\|^2 + \frac{\Delta t}{4}\sum_{n=0}^{N-1}\|\nabla T_h^{n+1}\|^2 + \frac{Pr\Delta t}{4}\sum_{n=0}^{N-1}\|\nabla u_h^{n+1}\|^2 \leq Ct^*,$$

linearly implicit BDF1:

$$\frac{1}{2}\|T_h^N\|^2 + \|u_h^N\|^2 + \sum_{n=0}^{N-1}\|T_h^{n+1}-T_h^n\|^2 + \sum_{n=0}^{N-1}\|u_h^{n+1}-u_h^n\|^2 + \frac{\Delta t}{4}\sum_{n=0}^{N-1}\|\nabla T_h^{n+1}\|^2 + \frac{Pr\Delta t}{8}\sum_{n=0}^{N-1}\|\nabla u_h^{n+1}\| + \frac{Pr\Delta t}{8}\|\nabla u_h^N\|^2 \leq Ct^*.$$

Further,

$$\beta\Delta t\sum_{n=0}^{N-1}\|p_h^{n+1}\| \leq C\sqrt{t^*}.$$

Proof. Our strategy is to first estimate the temperature approximation in terms of the velocity approximation and data. We then bound the velocity approximation in terms of data yielding stability of both approximations. Denote $\theta_h^{n+1} = T_h^{n+1} - \tau$. Consider **BDF1**. Let $S_h = \theta_h^{n+1} \in W_{\Gamma_1,h}$ in equation (5.2.3) and use the polarization identity. Multiply by Δt

on both sides, rewrite all quantities in terms of θ_h^k, $k = n,\ n+1$, and rearrange. Since $(\nabla\tau, \nabla\theta_h^{n+1}) = 0$ we have,

$$\frac{1}{2}\Big\{\|\theta_h^{n+1}\|^2 - \|\theta_h^n\|^2 + \|\theta_h^{n+1} - \theta_h^n\|^2\Big\} + \Delta t\|\nabla\theta_h^{n+1}\|^2 = -\Delta t b^*(u_h^{n+1}, \theta_h^{n+1} + \tau, \theta_h^{n+1}) \quad (5.3.1)$$
$$+\Delta t(\gamma^{n+1}, \theta_h^{n+1}).$$

Consider $-\Delta t b^*(u_h^{n+1}, \theta_h^{n+1} + \tau, \theta_h^{n+1})$. Use skew-symmetry and apply Lemma 5.1.1,

$$-\Delta t b^*(u_h^{n+1}, \theta_h^{n+1} + \tau, \theta_h^{n+1}) = -\Delta t b^*(u_h^{n+1}, \tau, \theta_h^{n+1}) \le C\Delta t\,\delta\ \big(\epsilon_1^{-1}\|\nabla u_h^{n+1}\|^2 + \epsilon_1\|\nabla\theta_h^{n+1}\|^2\big). \quad (5.3.2)$$

Use Cauchy-Schwarz-Young's on $\Delta t(\gamma^{n+1}, \theta_h^{n+1})$,

$$\Delta t(\gamma^{n+1}, \theta_h^{n+1}) \le \frac{\Delta t}{2\epsilon_2}\|\gamma^{n+1}\|_{-1}^2 + \frac{\Delta t\epsilon_2}{2}\|\nabla\theta_h^{n+1}\|^2. \quad (5.3.3)$$

Using (5.3.2) and (5.3.3) in (5.3.1) leads to

$$\frac{1}{2}\Big\{\|\theta_h^{n+1}\|^2 - \|\theta_h^n\|^2 + \|\theta_h^{n+1} - \theta_h^n\|^2\Big\} + \Delta t\|\nabla\theta_h^{n+1}\|^2 \le C\Delta t\,\delta\,\big(\epsilon_1^{-1}\|\nabla u_h^{n+1}\|^2 + \epsilon_1\|\nabla\theta_h^{n+1}\|^2\big)$$
$$+\frac{\Delta t}{2\epsilon_2}\|\gamma^{n+1}\|_{-1}^2 + \frac{\Delta t\epsilon_2}{2}\|\nabla\theta_h^{n+1}\|^2.$$

Let $\epsilon_1 = \frac{1}{2C\delta}$ and $\epsilon_2 = 1/2$. Regrouping terms leads to

$$\frac{1}{2}\Big\{\|\theta_h^{n+1}\|^2 - \|\theta_h^n\|^2 + \|\theta_h^{n+1} - \theta_h^n\|^2\Big\} + \frac{\Delta t}{4}\|\nabla\theta_h^{n+1}\|^2 \le 2C^2\Delta t\,\delta^2\,\|\nabla u_h^{n+1}\|^2 + \Delta t\|\gamma^{n+1}\|_{-1}^2.$$

Sum from $n = 0$ to $n = N-1$ and put all data on the right hand side. This yields bounds on the temperature approximation in terms of the velocity approximation and data as follows,

$$\frac{1}{2}\|\theta_h^N\|^2 + \frac{1}{2}\sum_{n=0}^{N-1}\|\theta_h^{n+1} - \theta_h^n\|^2 + \frac{\Delta t}{4}\sum_{n=0}^{N-1}\|\nabla\theta_h^{n+1}\|^2 \le 2C^2\Delta t\,\delta^2\sum_{n=0}^{N-1}\|\nabla u_h^{n+1}\|^2 \quad (5.3.4)$$
$$+\Delta t\sum_{n=0}^{N-1}\|\gamma^{n+1}\|_{-1}^2 + \frac{1}{2}\|\theta_h^0\|^2.$$

Next, let $v_h = u_h^{n+1} \in V_h$ in (5.2.1) and use the polarization identity. Multiply by Δt on both sides and rearrange terms. Then,

$$\frac{1}{2}\Big\{\|u_h^{n+1}\|^2 - \|u_h^n\|^2 + \|u_h^{n+1} - u_h^n\|^2\Big\} + Pr\Delta t\|\nabla u_h^{n+1}\|^2 = \Delta t PrRa(\xi(\theta_h^{n+1} + \tau), u_h^{n+1}) \\ + \Delta t(f^{n+1}, u_h^{n+1}). \tag{5.3.5}$$

Use the Cauchy-Schwarz-Young's and Poincaré-Friedrichs inequalities on $\Delta t PrRa(\xi(\theta_h^{n+1} + \tau), u_h^{n+1})$ and $\Delta t(f^{n+1}, u_h^{n+1})$, in addition note that $\|\xi\|_{L^\infty} = 1$,

$$\Delta t PrRa(\xi\theta_h^{n+1}, u_h^{n+1}) \leq \frac{\Delta t Pr^2 Ra^2 C_{PF,1}^2 C_{PF,2}^2}{2\epsilon_3}\|\nabla\theta_h^{n+1}\|^2 + \frac{\Delta t\epsilon_3}{2}\|\nabla u_h^{n+1}\|^2, \tag{5.3.6}$$

$$\Delta t PrRa(\xi\tau, u_h^{n+1}) \leq \frac{\Delta t}{2\epsilon_4} Pr^2 Ra^2\|\tau\|_{-1}^2 + \frac{\Delta t\epsilon_4}{2}\|\nabla u_h^{n+1}\|^2, \tag{5.3.7}$$

$$\Delta t(f^{n+1}, u_h^{n+1}) \leq \frac{\Delta t}{2\epsilon_5}\|f^{n+1}\|_{-1}^2 + \frac{\Delta t\epsilon_5}{2}\|\nabla u_h^{n+1}\|^2. \tag{5.3.8}$$

Using (5.3.6), (5.3.7), and (5.3.8) in (5.3.5) leads to

$$\frac{1}{2}\Big\{\|u_h^{n+1}\|^2 - \|u_h^n\|^2 + \|u_h^{n+1} - u_h^n\|^2\Big\} + Pr\Delta t\|\nabla u_h^{n+1}\|^2 \leq \frac{\Delta t Pr^2 Ra^2 C_{PF,1}^2 C_{PF,2}^2}{2\epsilon_3}\|\nabla\theta_h^{n+1}\|^2 \\ + \frac{\Delta t Pr^2 Ra^2}{2\epsilon_4}\|\tau\|_{-1}^2 + \frac{\Delta t}{2\epsilon_5}\|f^{n+1}\|_{-1}^2 + (\epsilon_3 + \epsilon_4 + \epsilon_5)\frac{\Delta t}{2}\|\nabla u_h^{n+1}\|^2.$$

Let $\epsilon_3 = \epsilon_4 = 4\epsilon_5 = Pr/2$. Then,

$$\frac{1}{2}\Big\{\|u_h^{n+1}\|^2 - \|u_h^n\|^2 + \|u_h^{n+1} - u_h^n\|^2\Big\} + \frac{Pr\Delta t}{4}\|\nabla u_h^{n+1}\| \leq \Delta t PrRa^2 C_{PF,1}^2 C_{PF,2}^2\|\nabla\theta_h^{n+1}\|^2 \\ + \Delta t PrRa^2\|\tau\|_{-1}^2 + \frac{\Delta t}{Pr}\|f^{n+1}\|_{-1}^2.$$

Summing from $n = 0$ to $n = N - 1$ and putting all data on r.h.s. yields

$$\frac{1}{2}\|u_h^N\|^2 + \frac{1}{2}\sum_{n=0}^{N-1}\|u_h^{n+1} - u_h^n\|^2 + \frac{Pr\Delta t}{4}\sum_{n=0}^{N-1}\|\nabla u_h^{n+1}\| \leq \Delta t PrRa^2 C_{PF,1}^2 C_{PF,2}^2\sum_{n=0}^{N-1}\|\nabla\theta_h^{n+1}\|^2 \\ + \frac{\Delta t}{Pr}\sum_{n=0}^{N-1}\Big(Pr^2 Ra^2\|\tau\|_{-1}^2 + \|f^{n+1}\|_{-1}^2\Big) + \frac{1}{2}\|u_h^0\|^2. \tag{5.3.9}$$

Now, from equation (5.3.4), we have

$$\Delta t Pr Ra^2 C_{PF,1}^2 C_{PF,2}^2 \sum_{n=0}^{N-1} \|\nabla \theta_h^{n+1}\|^2 \leq 8\, C^2 C_{PF,1}^2 C_{PF,2}^2 Pr Ra^2\, \delta^2\, \Delta t \sum_{n=0}^{N-1} \|\nabla u_h^{n+1}\|^2$$
$$+ 4 Pr Ra^2 C_{PF,1}^2 C_{PF,2}^2 \Delta t \sum_{n=0}^{N-1} \|\gamma^{n+1}\|_{-1}^2 + 2 Pr Ra^2 C_{PF,1}^2 C_{PF,2}^2 \|\theta_h^0\|^2. \quad (5.3.10)$$

Using the above in (5.3.9) with $\delta = \frac{1}{8 C C_{PF,1} C_{PF,2}} Ra^{-1}$ leads to

$$\frac{1}{2}\|u_h^N\|^2 + \frac{1}{2}\sum_{n=0}^{N-1} \|u_h^{n+1} - u_h^n\|^2 + \frac{Pr\Delta t}{8} \sum_{n=0}^{N-1} \|\nabla u_h^{n+1}\|$$
$$\leq 4 Pr Ra^2 C_{PF,1}^2 C_{PF,2}^2 \Delta t \sum_{n=0}^{N-1} \|\gamma^{n+1}\|_{-1}^2 + 2 Pr Ra^2 C_{PF,1}^2 C_{PF,2}^2 \|\theta_h^0\|^2$$
$$+ \frac{\Delta t}{Pr} \sum_{n=0}^{N-1} \left(Pr^2 Ra^2 \|\tau\|_{-1}^2 + \|f^{n+1}\|_{-1}^2 \right) + \frac{1}{2}\|u_h^0\|^2. \quad (5.3.11)$$

Thus, the velocity approximation is bounded above by data and therefore the temperature approximation as well; that is, both the velocity and temperature approximations are stable. Adding (5.3.4) and (5.3.11), multiplying by 2, and using the identity $T_h^n = \theta_h^n + \tau$ together with the triangle inequality yields the result.

Next, consider **linearly implicit BDF1**. We apply similar techniques as in the above. This leads to

$$\frac{1}{2}\|\theta_h^N\|^2 + \frac{1}{2}\sum_{n=0}^{N-1} \|\theta_h^{n+1} - \theta_h^n\|^2 + \frac{\Delta t}{4} \sum_{n=0}^{N-1} \|\nabla \theta_h^{n+1}\|^2 \leq \quad (5.3.12)$$
$$4C^2 \Delta t \delta^2 \sum_{n=0}^{N-1} \|\nabla u_h^n\|^2 + \Delta t \sum_{n=0}^{N-1} \|\gamma^{n+1}\|_{-1}^2 + \frac{1}{2}\|\theta_h^0\|^2,$$

and

$$\frac{1}{2}\|u_h^N\|^2 + \frac{1}{2}\sum_{n=0}^{N-1} \|u_h^{n+1} - u_h^n\|^2 + \frac{Pr\Delta t}{8} \sum_{n=0}^{N-1} \|\nabla u_h^{n+1}\| + \frac{Pr\Delta t}{8}\|\nabla u_h^N\|$$
$$\leq 4 Pr Ra^2 C_{PF,1}^2 C_{PF,2}^2 \Delta t \sum_{n=0}^{N-1} \|\gamma^{n+1}\|_{-1}^2 + 2 Pr Ra^2 C_{PF,1}^2 C_{PF,2}^2 \|\theta_h^0\|^2$$
$$+ \frac{\Delta t}{Pr} \sum_{n=0}^{N-1} \left(\|\tau\|_{-1}^2 + \|f^{n+1}\|_{-1}^2 \right) + \frac{1}{2}\|u_h^0\|^2 + \frac{Pr\Delta t}{8}\|\nabla u_h^0\|. \quad (5.3.13)$$

The result follows. We now prove stability of the pressure approximation. Consider (5.2.1), isolate $(\frac{u_h^{n+1}-u_h^n}{\Delta t}, v_h)$, let $0 \neq v_h \in V_h$, and multiply by Δt. Then,

$$\begin{aligned}(u_h^{n+1} - u_h^n, v_h) = &- \Delta t b(\eta(u_h), u_h^{n+1}, v_h) - \Delta t Pr(\nabla u_h^{n+1}, \nabla v_h) \\ &+ \Delta t PrRa(\xi\eta(T_h), v_h) + \Delta t(f^{n+1}, v_h).\end{aligned} \tag{5.3.14}$$

Applying Lemma 5.1.2 to the skew-symmetric trilinear term and the Cauchy-Schwarz and Poincaré-Friedrichs inequalities to the remaining terms yields

$$|-\Delta t b(\eta(u_h), u_h^{n+1}, v_h)| \leq C_1 \Delta t \|\nabla\eta(u_h)\| \|\nabla u_h^{n+1}\| \|\nabla v_h\|, \tag{5.3.15}$$

$$|-\Delta t Pr(\nabla u_h^{n+1}, \nabla v_h)| \leq Pr\Delta t \|\nabla u_h^{n+1}\| \|\nabla v_h\|, \tag{5.3.16}$$

$$|\Delta t PrRa(\xi\eta(T_h), v_h)| \leq PrRaC_{PF,1}\Delta t \|\eta(T_h)\| \|\nabla v_h\|, \tag{5.3.17}$$

$$|\Delta t(f^{n+1}, v_h)| \leq \Delta t \|f^{n+1}\|_{-1} \|\nabla v_h\|. \tag{5.3.18}$$

Apply the above estimates in (5.3.14), divide by the common factor $\|\nabla v_h\|$ on both sides, and take the supremum over all $0 \neq v_h \in V_h$. Then,

$$\begin{aligned}\|u_h^{n+1} - u_h^n\|_{V_h^*} \leq &\, C_1 \Delta t \|\nabla\eta(u_h)\| \|\nabla u_h^{n+1}\| + Pr\Delta t \|\nabla u_h^{n+1}\| \\ &+ PrRaC_{PF,1}\Delta t \|\eta(T_h)\| + \Delta t \|f^{n+1}\|_{-1}.\end{aligned} \tag{5.3.19}$$

Reconsider equations (5.2.1). Multiply by Δt and isolate the pressure term,

$$\begin{aligned}\Delta t(p_h^{n+1}, \nabla \cdot v_h) = &(u_h^{n+1} - u_h^n, v_h) + \Delta t b(\eta(u_h), u_h^{n+1}, v_h) + Pr\Delta t(\nabla u_h^{n+1}, \nabla v_h) \\ &- PrRa\Delta t(\xi\eta(T_h), v_h) - \Delta t(f^{n+1}, v_h).\end{aligned} \tag{5.3.20}$$

Apply (5.3.15), (5.3.16), (5.3.17), and (5.3.18) on the r.h.s terms. Then,

$$\begin{aligned}\Delta t(p_h^{n+1}, \nabla \cdot v_h) \leq (u_h^{n+1} - u_h^n, v_h) + \Big(&C_1 \Delta t \|\nabla\eta(u_h)\| \|\nabla u_h^{n+1}\| + Pr\Delta t \|\nabla u_h^{n+1}\| \\ &+ PrRaC_{PF,1}\Delta t \|\eta(T_h)\| + \Delta t \|f^{n+1}\|_{-1}\Big) \|\nabla v_h\|.\end{aligned} \tag{5.3.21}$$

Divide by $\|\nabla v_h\|$ and note that $\frac{(u_h^{n+1}-u_h^n, v_h)}{\|\nabla v_h\|} \leq \|u_h^{n+1} - u_h^n\|_{V_h^*}$. Take the supremum over all $0 \neq v_h \in X_h$,

$$\begin{aligned}\Delta t \sup_{0 \neq v_h \in X_h} \frac{(p_h^{n+1}, \nabla \cdot v_h)}{\|\nabla v_h\|} \leq 2\Big(&C_1 \Delta t \|\nabla\eta(u_h)\| \|\nabla u_h^{n+1}\| + Pr\Delta t \|\nabla u_h^{n+1}\| \\ &+ PrRaC_{PF,1}\Delta t \|\eta(T_h)\| + \Delta t \|f^{n+1}\|_{-1}\Big).\end{aligned} \tag{5.3.22}$$

Use the inf-sup condition (5.1.1),

$$\begin{aligned}\beta\Delta t\|p_h^{n+1}\| \leq 2\Big(&C_1\Delta t\|\nabla\eta(u_h)\|\|\nabla u_h^{n+1}\| + Pr\Delta t\|\nabla u_h^{n+1}\| \\ &+ PrRaC_{PF,1}\Delta t\|\eta(T_h)\| + \Delta t\|f^{n+1}\|_{-1}\Big).\end{aligned} \tag{5.3.23}$$

Summing from $n = 0$ to $n = N - 1$ yields stability of the pressure approximation, built on the stability of the temperature and velocity approximations. □

Theorem 5.3.2. Consider **BDF2** or **linearly implicit BDF2**. Suppose $f \in L^2(0,\infty;H^{-1}(\Omega)^d)$, and $\gamma \in L^2(0,\infty;H^{-1}(\Omega))$. If $\delta = \mathcal{O}(Ra^{-1})$, then there exists $C > 0$, independent of t^*, such that

BDF2:

$$\begin{aligned}&\frac{1}{2}\|T_h^N\|^2 + \frac{1}{2}\|2T_h^N - T_h^{N-1}\|^2 + \|u_h^N\|^2 + \|2u_h^N - u_h^{N-1}\|^2 + \sum_{n=1}^{N-1}\|T_h^{n+1} - 2T_h^n + T_h^{n-1}\|^2 \\ &\quad + \sum_{n=1}^{N-1}\|u_h^{n+1} - 2u_h^n + u_h^{n-1}\|^2 + \frac{\Delta t}{2}\sum_{n=1}^{N-1}\|\nabla T_h^{n+1}\|^2 + \frac{Pr\Delta t}{2}\sum_{n=1}^{N-1}\|\nabla u_h^{n+1}\|^2 \leq Ct^*.\end{aligned}$$

linearly implicit BDF2:

$$\begin{aligned}&\frac{1}{2}\|T_h^N\|^2 + \frac{1}{2}\|2T_h^N - T_h^{N-1}\|^2 + \|u_h^N\|^2 + \|2u_h^N - u_h^{N-1}\|^2 + \sum_{n=1}^{N-1}\|T_h^{n+1} - 2T_h^n + T_h^{n-1}\|^2 \\ &\quad + \sum_{n=1}^{N-1}\|u_h^{n+1} - 2u_h^n + u_h^{n-1}\|^2 + \frac{\Delta t}{2}\sum_{n=1}^{N-1}\|\nabla T_h^{n+1}\|^2 + \frac{Pr\Delta t}{2}\sum_{n=1}^{N-1}\|\nabla u_h^{n+1}\|^2 \\ &\quad + \frac{Pr\Delta t}{2}\Big(\|\nabla u_h^N\|^2 + \|\nabla u_h^{N-1}\|^2\Big) \leq Ct^*.\end{aligned}$$

Further,

$$\beta\Delta t\sum_{n=0}^{N-1}\|p_h^{n+1}\| \leq C\sqrt{t^*}.$$

Proof. We follow the general strategy in Theorem 5.3.1. Consider **linearly implicit BDF2** first. Let $S_h = \theta_h^{n+1} \in W_{\Gamma_1,h}$ in equation (5.2.6) and use the polarization identity. Multiply by Δt on both sides, rewrite all quantities in terms of θ_h^k, $k = n,\ n+1$, and rearrange. Then,

$$\frac{1}{4}\Big\{\|\theta_h^{n+1}\|^2 + \|2\theta_h^{n+1} - \theta_h^n\|^2\Big\} - \frac{1}{4}\Big\{\|\theta_h^n\|^2 + \|2\theta_h^n - \theta_h^{n-1}\|^2\Big\} + \frac{1}{4}\|\theta_h^{n+1} - 2\theta_h^n + \theta_h^{n-1}\|^2 + \Delta t\|\nabla\theta_h^{n+1}\|^2 = -\Delta t b^*(2u_h^n - u_h^{n-1}, \tau, \theta_h^{n+1}) + \Delta t(\gamma^{n+1}, \theta_h^{n+1}). \quad (5.3.24)$$

Consider $-\Delta t b^*(2u_h^n - u_h^{n-1}, \tau, \theta_h^{n+1}) = -2\Delta t b^*(u_h^n, \tau, \theta_h^{n+1}) + \Delta t b^*(u_h^{n-1}, \tau, \theta_h^{n+1})$. Use Lemma 5.3.2, then

$$-2\Delta t b^*(u_h^n, \tau, \theta_h^{n+1}) \le C\,\delta\,\Delta t\Big(4\epsilon_6^{-1}\|\nabla u_h^n\|^2 + \epsilon_6\|\nabla\theta_h^{n+1}\|^2\Big), \quad (5.3.25)$$

$$\Delta t b^*(u_h^{n-1}, \tau, \theta_h^{n+1}) \le C\,\delta\,\Delta t\Big(\epsilon_7^{-1}\|\nabla u_h^{n-1}\|^2 + \epsilon_7\|\nabla\theta_h^{n+1}\|^2\Big). \quad (5.3.26)$$

Use above estimates and (5.3.3) in equation (5.3.24). Let $\epsilon_6 = \epsilon_7 = \frac{1}{4C\delta}$ and $\epsilon_2 = 1/4$. This leads to

$$\frac{1}{4}\Big\{\|\theta_h^{n+1}\|^2 + \|2\theta_h^{n+1} - \theta_h^n\|^2\Big\} - \frac{1}{4}\Big\{\|\theta_h^n\|^2 + \|2\theta_h^n - \theta_h^{n-1}\|^2\Big\} + \frac{1}{4}\|\theta_h^{n+1} - 2\theta_h^n + \theta_h^{n-1}\|^2 + \frac{\Delta t}{4}\|\nabla\theta_h^{n+1}\|^2 \le 16C^2\Delta t\,\delta^2\,\|\nabla u_h^n\|^2 + 4C^2\Delta t\,\delta^2\,\|\nabla u_h^{n-1}\|^2 + 2\Delta t\|\gamma^{n+1}\|_{-1}^2. \quad (5.3.27)$$

Sum from $n = 1$ to $n = N-1$ and put all data on the right hand side. This yields

$$\frac{1}{4}\|\theta_h^N\|^2 + \frac{1}{4}\|2\theta_h^N - \theta_h^{N-1}\|^2 + \frac{1}{4}\sum_{n=1}^{N-1}\|\theta_h^{n+1} - 2\theta_h^n + \theta_h^{n-1}\|^2 + \frac{\Delta t}{4}\sum_{n=1}^{N-1}\|\nabla\theta_h^{n+1}\|^2 \le 16C^2\Delta t\,\delta^2\sum_{n=1}^{N-1}\|\nabla u_h^n\|^2 + 4C^2\Delta t\,\delta^2\sum_{n=1}^{N-1}\|\nabla u_h^{n-1}\|^2 + 2\Delta t\sum_{n=1}^{N-1}\|\gamma^{n+1}\|_{-1}^2 + \frac{1}{4}\|\theta_h^0\|^2 + \frac{1}{4}\|\theta_h^1 - \theta_h^0\|^2. \quad (5.3.28)$$

Now, let $v_h = u_h^{n+1} \in V_h$ in (5.2.4) and use the polarization identity. Multiply by Δt on both sides and rearrange terms. Then,

$$\frac{1}{4}\Big\{\|u_h^{n+1}\|^2 + \|2u_h^{n+1} - u_h^n\|^2\Big\} - \frac{1}{4}\Big\{\|u_h^n\|^2 + \|2u_h^n - u_h^{n-1}\|^2\Big\} + \frac{1}{4}\|u_h^{n+1} - 2u_h^n + u_h^{n-1}\|^2 + Pr\Delta t\|\nabla u_h^{n+1}\|^2 = \Delta t Pr Ra(\xi(2\theta_h^n - \theta_h^{n-1} + \tau), u_h^{n+1}) + \Delta t(f^{n+1}, u_h^{n+1}). \quad (5.3.29)$$

Use the Cauchy-Schwarz-Young's and Poincaré-Friedrichs inequalities on $\Delta t Pr Ra(\xi(2\theta_h^n - \theta_h^{n-1} + \tau), u_h^{n+1})$,

$$2\Delta t Pr Ra(\xi\theta_h^n, u_h^{n+1}) \leq \frac{4\Delta t Pr^2 Ra^2 C_{PF,1}^2 C_{PF,2}^2}{2\epsilon_8}\|\nabla\theta_h^n\|^2 + \frac{\Delta t\epsilon_8}{2}\|\nabla u_h^{n+1}\|^2, \tag{5.3.30}$$

$$-\Delta t Pr Ra(\xi\theta_h^{n-1}, u_h^{n+1}) \leq \frac{\Delta t Pr^2 Ra^2 C_{PF,1}^2 C_{PF,2}^2}{2\epsilon_9}\|\nabla\theta_h^{n-1}\|^2 + \frac{\Delta t\epsilon_9}{2}\|\nabla u_h^{n+1}\|^2. \tag{5.3.31}$$

Using (5.3.7), (5.3.8), (5.3.30), and (5.3.31) in (5.3.29) leads to

$$\begin{aligned}\frac{1}{4}\Big\{\|u_h^{n+1}\|^2 + \|2u_h^{n+1} - u_h^n\|^2\Big\} - \frac{1}{4}\Big\{\|u_h^n\|^2 + \|2u_h^n - u_h^{n-1}\|^2\Big\} + \frac{1}{4}\|u_h^{n+1} - 2u_h^n + u_h^{n-1}\|^2 \\ + Pr\Delta t\|\nabla u_h^{n+1}\|^2 \leq \frac{2\Delta t Pr^2 Ra^2 C_{PF,1}^2 C_{PF,2}^2}{\epsilon_8}\|\nabla\theta_h^n\|^2 + \frac{\Delta t Pr^2 Ra^2 C_{PF,1}^2 C_{PF,2}^2}{2\epsilon_9}\|\nabla\theta_h^{n-1}\|^2 \\ + \frac{\Delta t}{2\epsilon_4}\|\tau\|_{-1}^2 + \frac{\Delta t}{2\epsilon_5}\|f^{n+1}\|_{-1}^2 + \frac{\Delta t}{2}(\epsilon_4 + \epsilon_5 + \epsilon_8 + \epsilon_9)\|\nabla u_h^{n+1}\|^2.\end{aligned}$$

Let $2\epsilon_4 = 2\epsilon_5 = \epsilon_8 = \epsilon_9 = Pr/2$. Then,

$$\begin{aligned}\frac{1}{4}\Big\{\|u_h^{n+1}\|^2 + \|2u_h^{n+1} - u_h^n\|^2\Big\} - \frac{1}{4}\Big\{\|u_h^n\|^2 + \|2u_h^n - u_h^{n-1}\|^2\Big\} + \frac{1}{4}\|u_h^{n+1} - 2u_h^n + u_h^{n-1}\|^2 \\ + \frac{Pr\Delta t}{4}\|\nabla u_h^{n+1}\|^2 \leq 4\Delta t Pr Ra^2 C_{PF,1}^2 C_{PF,2}^2\|\nabla\theta_h^n\|^2 + \Delta t Pr^2 Ra^2 C_{PF,1}^2 C_{PF,2}^2\|\nabla\theta_h^{n-1}\|^2 \\ + \frac{2\Delta t}{Pr}\|\tau\|_{-1}^2 + \frac{2\Delta t}{Pr}\|f^{n+1}\|_{-1}^2.\end{aligned}$$

Summing from $n = 1$ to $n = N-1$ and putting all data on r.h.s. yields

$$\begin{aligned}\frac{1}{4}\|u_h^N\|^2 + \frac{1}{4}\|2u_h^N - u_h^{N-1}\|^2 + \frac{1}{4}\sum_{n=1}^{N-1}\|u_h^{n+1} - 2u_h^n + u_h^{n-1}\|^2 \\ + \frac{Pr\Delta t}{4}\sum_{n=1}^{N-1}\|\nabla u_h^{n+1}\|^2 \leq \Delta t Pr Ra^2 C_{PF,1}^2 C_{PF,2}^2\sum_{n=1}^{N-1}\Big(4\|\nabla\theta_h^n\|^2 + \|\nabla\theta_h^{n-1}\|^2\Big) \\ + \frac{2\Delta t}{Pr}\sum_{n=1}^{N-1}\Big(\|\tau\|_{-1}^2 + \|f^{n+1}\|_{-1}^2\Big) + \frac{1}{4}\|u_h^1\|^2 + \frac{1}{4}\|2u_h^1 - u_h^0\|^2.\end{aligned} \tag{5.3.32}$$

Now, from equation (5.3.28), we have

$$\begin{aligned}&\Delta t Pr Ra^2 C_{PF,1}^2 C_{PF,2}^2\sum_{n=1}^{N-1}\|\nabla\theta_h^{n+1}\|^2 \\ &\leq 64\, C^2\, C_{PF,1}^2 C_{PF,2}^2 Pr Ra^2\, \delta^2\, \Delta t\sum_{n=0}^{N-1}\Big(\|\nabla u_h^n\|^2 + \|\nabla u_h^{n-1}\|^2\Big) \\ &+ 8Pr Ra^2 C_{PF,1}^2 C_{PF,2}^2\Delta t\sum_{n=1}^{N-1}\|\gamma^{n+1}\|_{-1}^2 + Pr Ra^2 C_{PF,1}^2 C_{PF,2}^2\Big(\|\theta_h^1\|^2 + \|2\theta_h^1 - \theta_h^0\|^2\Big).\end{aligned} \tag{5.3.33}$$

Add and subtract $\frac{Pr\Delta t}{8}\sum_{n=1}^{N-1}\|\nabla u_h^n\|$ and $\frac{Pr\Delta t}{8}\sum_{n=1}^{N-1}\|\nabla u_h^{n-1}\|$ in (5.3.32) and use the above estimate with $\delta = \frac{1}{16\sqrt{2}\,C\,C_{PF,1}C_{PF,2}}\,Ra^{-1}$. Then,

$$\frac{1}{4}\|u_h^N\|^2+\frac{1}{4}\|2u_h^N-u_h^{N-1}\|^2+\frac{1}{4}\sum_{n=1}^{N-1}\|u_h^{n+1}-2u_h^n+u_h^{n-1}\|^2+\frac{Pr\Delta t}{8}\sum_{n=1}^{N-1}\|\nabla u_h^{n+1}\|+\frac{Pr\Delta t}{8}\|\nabla u_h^N\|$$
$$+\frac{Pr\Delta t}{8}\|\nabla u_h^{N-1}\| \leq 8PrRa^2C_{PF,1}^2C_{PF,2}^2\Delta t\sum_{n=1}^{N-1}\|\gamma^{n+1}\|_{-1}^2+PrRa^2C_{PF,1}^2C_{PF,2}^2\Big(\|\theta_h^1\|^2+\|2\theta_h^1-\theta_h^0\|^2\Big)$$
$$+\frac{2\Delta t}{Pr}\sum_{n=0}^{N-1}\Big(\|\tau\|_{-1}^2+\|f^{n+1}\|_{-1}^2\Big)+\frac{1}{4}\|u_h^1\|^2+\frac{1}{4}\|2u_h^1-u_h^0\|^2+\frac{Pr\Delta t}{8}\|\nabla u_h^1\|+\frac{Pr\Delta t}{8}\|\nabla u_h^0\|. \tag{5.3.34}$$

The result follows. Applying similar techniques as in the above and Theorem 5.3.1 yields the result for **BDF2**. Pressure stability follows by similar arguments in Theorem 5.3.1. □

5.4 CONCLUSION

The coupling terms $b^*(\eta(u_h), T_h^{n+1}, S_h)$ and $PrRa(\xi\eta(T), v_h)$ that arise in stability analyses of FEM discretizations of natural convection problems with sidewall heating are the major source of difficulty. The former term forces the stability of the temperature approximation to be dependent on the velocity approximation and vice versa for the latter term. Standard techniques fail to overcome this imposition, in the absence of a discrete Grönwall inequality.

The authors introduced a new discrete Hopf interpolant that was able to overcome this issue. Fully discrete stability estimates were proven which improve upon previous estimates. In particular, it was shown that provided that the first mesh line in the finite element mesh is within $\mathcal{O}(Ra^{-1})$ of the nonhomogeneous Dirichlet boundary, the velocity, pressure and temperature approximations are stable allowing for sub-linear growth in t^*.

A uniform in time stability estimate was not able to be achieved due to the term $PrRa(\xi\tau, v_h)$, which arises when an interpolant of the boundary is introduced. The authors conjecture that the results proven herein may be improved, owing to a gap in the analysis. **Open problems include:** Is it possible to improve the current results with a

less restrictive mesh condition? Moreover, can these results be improved to uniform in time stability? An important next step would be reanalyzing stability for natural convection problems, with sidewall heating, where a turbulence model is incorporated.

6.0 CONCLUSIONS AND FUTURE WORK

In turbulence, dissipation occurs non-negligibly only at very small scales, smaller than a typical mesh [67]. Turbulence models are introduced to account for sub-mesh scale effects, when solving fluid flow problems numerically [47]. One key in getting a good approximation for a turbulence model is to correctly calibrate the energy dissipation in the model on an under-resolved mesh [46]. The energy dissipation rate is a fundamental quantity in the theory of turbulence ([76], [67], [49], and [20]), which is employed as the benchmark to investigate the accuracy of a turbulence model (e.g. [58] and [35]). In this thesis, we presented the analysis and numerical analysis of the energy dissipation rate of a turbulence model. In this direction, this research is the first connection between computational experience and mathematical analysis.

Analytic estimates of the energy dissipation rates of a few turbulence models have recently appeared (e.g. [15]. [16], [17], [46] and [45]), but none (yet) study energy dissipation restricted to resolved scales, i.e. after spatial discretization with $h \geq$ Kolmogorov microscale. Since turbulence models are considered to model the energy lost from resolved to under-resolved scales h, the practical question is: What is the energy dissipation rate associated with the coarse mesh size h. In this direction in Chapter 3, upper bounds are derived on the computed time-averaged energy dissipation rate, for an under-resolved mesh for turbulent shear flow. The Smagorinsky model is used as the turbulence model. The upper bound is independent of the viscosity at the high Reynolds number (as $\mathcal{R}e \to \infty$), in accord with the Statistical Equilibrium Law. The analysis indicates that the turbulent boundary layer is a more important length scale for shear flow than the Kolmogorov microscale. Moreover, this estimate suggests over-dissipation for any model's artificial parameters, consistent with numerical evidence on the effects of model viscosity. Therefore the next natural question is:

How to fix the over-dissipation of the model? This question was answered in Chapter 4.

Experience with the Smagorinsky model indicates it over dissipates [71]. This extra dissipation laminarizes the numerical approximation of a turbulent flow and prevents the transition to turbulence [47]. Motivated from Chapter 3 and comparing results in [46] and [45] suggests that the model over-dissipation is due to the action of the model viscosity in boundary layers rather than in interior small scales generated by the turbulent cascade. To reduce the effect of model viscosity in the boundary layers damping functions $\beta(x)$, which go to zero at the walls, are often used (Pope [67]). In this case most of the tools of analysis, such as Körn's inequality, the Poincaré-Friederichs inequality, and Sobolev's inequality, no longer hold. Thus, the mathematical development of the Smagorinsky model under no-slip boundary conditions with damping function is cited in [5] as an important open problem. Mathematical analysis was given in Chapter 4 that allows evaluation of statistics of the turbulence model for any damping function. Moreover, it was proven that the combination of the Smagorinsky model with the van- Driest damping function does not over dissipate and is also consistent with Kolmogorov phenomenology.

In this line of research there are many questions and challenges which are still open. The following are a few ideas for future research.

- **3D simulation:** 3D simulation is required to verify the result in Chapters 3 and 4.
- **Other modern turbulence models:** Following this research, one can calibrate the dissipation of a modern turbulence model used in engineering. The dissipation for the model can be investigated for both continuous and discrete cases. The goal is not only to understand the dissipation of the model on the under-resolved mesh, but also to find a sufficient condition on the model's artificial parameters in order to get the correct amount of a dissipation.
- **Fully discrete case:** Extending the results and investigating the properties of the energy dissipation rate for the fully discrete turbulence models is an important problem.

Natural convection of a fluid driven by heating a wall is a classical problem in fluid mechanics that is still of technological and scientific importance (e.g. [11] and [26]). Calculating the dissipation of the fully discrete Natural Convection is a very interesting problem.

Motivated from here, we study the stability of fully discrete Natural Convection Problems in Chapter 5. The temperature in natural convection problems is, under mild data assumptions, uniformly bounded in time. This property has not yet been proven for the standard finite element method approximation of natural convection problems with nonhomogeneous partitioned Dirichlet boundary conditions, e.g., the differentially heated vertical wall and Rayleigh-Bénard problems. For these problems, only stability in time, allowing for possible exponential growth of $\|T_h^n\|$, has been proven using Grönwall's inequality (e.g. [78, 79, 87]). In Chapter 5, we proved that the temperature approximation can grow at most sub-linearly in time provided a mild restriction on the first mesh line in the finite element mesh. In this line, there are many interesting questions remain to be answered.

- Is it possible to improve the current results with a less restrictive mesh condition?
- Can the results be improved to uniform in time stability?
- What is the stability for natural convection problems, with sidewall heating, where a turbulence model is incorporated?

BIBLIOGRAPHY

[1] R. A. Antonia and B. R. Pearson, *Effect of initial conditions on the mean energy dissipation rate and the scaling exponent*, Physical Review E **62** (2000), 8086-8090.

[2] R. A. Antonia, B. R. Satyaprakash, and A. K. M. F. Hussain, *Measurements of dissipation rate and some other characteristics of turbulent plane and circular jets*, Physics of Fluids **23** (1980), 695–700.

[3] U. M. Ascher, S. J. Ruuth, and B. T. R. Wetton, *Implicit-Explicit Methods for Time-Dependent Partial Differential Equations*, Siam J. Numer. Anal. **32** (1995), 797–823.

[4] G. K. Batchelor, *The theory of homogeneous turbulence*, Cambridge University Press, Cambridge, England, 1953.

[5] L. C. Berselli, T. Iliescu, and W. J. Layton, *Mathematics of large eddy simulation of turbulent flows*, Scientific Computation, Springer-Verlag, Berlin, 2006.

[6] J. Boland and W. J. Layton, *An analysis of the finite element method for natural convection problems*, Numer. Methods Partial Diferential Equations **2** (1990), 115–126.

[7] W. Bos, L. Shao, and J. P. Bertoglio, *Spectral imbalance and the normalized dissipation rate of turbulence*, Physics of Fluids **19** (2007).

[8] H. Brezis, *Functional analysis, Sobolev spaces and partial differential equations*, Universitext, Springer, New York, 2011.

[9] P. Burattini, P. Lavoie, and R. A. Antonia, *On the normalized turbulent energy dissipation rate*, Physics of Fluids **17** (2005).

[10] F. H. Busse, *Bounds for turbulent shear flow*, Journal of Fluid Mechanics **41** (1970), 4219–240.

[11] M. A. Christon, P. M. Gresho, and S. B. Sutton, *Computational predictability of time-dependent natural convection flows in enclosures (including a benchmark solution)*, Int. J. Numer. Meth. Fluids **40** (2002), 953–980.

[12] E. Colmenares and M. Neilan, *Dual-mixed finite element methods for the stationary Boussinesq problem*, Computers and Mathematics with Applications **72** (2016), 1828–1850.

[13] P. Constantin and C. Foias, *The Navier-Stokes equations*, Chicago lectures in mathematics series (1988).

[14] J. Davila and J. C. Vassilicos, *Richardsons Pair Diffusion and the Stagnation Point Structure of Turbulence*, Physical review letters **91** (2003).

[15] C .R. Doering and P. Constantin, *Energy dissipation in shear driven turbulence*, Physical review letters **69** (1992), 1648.

[16] C. R. Doering and P. Constantin, *Variational bounds on energy dissipation in incompressible flows. III. Convection*, Phys. Rev. E **53** (1996), 5957–5981.

[17] C. R. Doering and C. Foias, *Energy dissipation in body-forced turbulence*, J. Fluid Mech. **467** (2002), 289–306.

[18] Q. Du and M. D. Gunzburger, *Finite-element approximations of a Ladyzhenskaya model for stationary incompressible viscous flow*, SIAM J. Numer. Anal. **27** (1990), no. 1, 1–19.

[19] J. A. Fiordilino and A. Pakzad, *A Discrete Hopf Interpolant and Stability of the Finite Element Method for Natural Convection*, Submitted to Mathematics of Computation, arXiv:1710.02509.

[20] U. Frisch, *Turbulence*, Cambridge University Press, Cambridge, 1995. The legacy of A. N. Kolmogorov.

[21] M. Gad-el-Hak and S. Corrsin, *Measurements of the nearly isotropic turbulence behind a uniform jet grid*, Journal of Fluid Mechanics **62** (1974), 115-143.

[22] B. Galperin and S. A. Orszag, *Large eddy simulation of complex engineering and geophysical flows*, Cambridge University Press, 1993.

[23] T. Gelhard, G. Lube, M. A. Olshanskii, and J. Starcke, *Stabilized finite element schemes with LBB-stable elements for incompressible flows*, Journal of Computational and Applied Mathematics **177** (2005).

[24] M. Germano, U. Piomelli, P. Moin, and W. H. Cabot, *A dynamic subgrid-scale eddy viscosity model*, Physics of Fluids A **3** (1991), 1760.

[25] B. J. Geurts, *Inverse modeling for large-eddy simulation*, Physics of Fluids **9**, 3585.

[26] A. E. Gill, *The boundary-layer regime for convection in a rectangular cavity*, Journal of Fluid Mechanics **26** (1966), 515-536.

[27] V. Girault and P. A. Raviart, *Finite element approximation of the Navier-Stokes equations*, Lecture Notes in Mathematics, vol. 749, Springer-Verlag, Berlin-New York, 1979.

[28] S. Goto and J. C. Vassilicos, *The dissipation rate coefficient of turbulence is not universal and depends on the internal stagnation point structure*, Physics of Fluids **21** (2009).

[29] M. D. Gunzburger, *Finite Element Methods for Viscous Incompressible Flows: A Guide to Theory, Practice, and Algorithms*, Academic Press Boston, 1989.

[30] F. Hecht, *New development in FreeFEM++*, J. Numer. Math. **20** (2012), 251265.

[31] C. Horgan, *Korns Inequalities and Their Applications in Continuum Mechanics*, SIAM Review **37** (1995), no. 4, 491–511.

[32] E. Hopf, *Lecture series of the symposium on partial differential equations*, Berkeley, 1955.

[33] L. N. Howard, *Bounds on flow quantities*, Annual Review of Fluid Mechanics **4** (1972), 473–494.

[34] T. J. Hughes, A. Oberai, L. Mazzei, and J. Starcke, *Large eddy simulation of turbulent channel flows by the variational multiscale method*, Physics of Fluids **13** (2001), 1784–1799.

[35] T. Iliescu and P. Fischer, *Backscatter in the rational LES model*, Computers and Fluids **33** (2004), 783–790.

[36] N. Z. Ince and B. E. Launder, *On the computation of buoyancy-driven turbulent flows in rectangular enclosures*, Int. J. Heat and Fluid Flow **10** (1989), 110–117.

[37] R. Ingram, *A new linearly extrapolated Crank-Nicolson time-stepping scheme for the Navier-Stokes equations*, Mathematics of Computation **82** (2013), 1953–1973.

[38] V. John, *Large eddy simulation of turbulent incompressible flows*, Lecture Notes in Computational Science and Engineering, vol. 34, Springer-Verlag, Berlin, 2004. Analytical and numerical results for a class of LES models.

[39] V. John, W. J. Layton, and C. C. Manica, *Convergence of Time-Averaged Statistics of Finite Element Approximations of the NavierStokes Equations*, SIAM J. Numer. Anal. **46(1)** (2007), 151–179.

[40] V. John, W. J. Layton, and N. Sahin, *Derivation and analysis of near wall models for channel and recirculating flows*, Comput. Math. Appl. **48** (2004), no. 7-8, 1135–1151.

[41] V. John and A. Liakos, *Time-dependent flow across a step: the slip with friction boundary condition*, Internat. J. Numer. Methods Fluids **50** (2006), no. 6, 713–731.

[42] R. R. Kerswell, *Variational bounds on shear-driven turbulence and turbulent Boussinesq convection*, Physica D **100** (1997), 355–376.

[43] A. N. Kolmogorov, *The local structure of turbulence in incompressible viscous fluid for very large Reynolds numbers*, Proc. Roy. Soc. London Ser. A **434** (1991), no. 1890, 9–13. Translated from the Russian by V. Levin; Turbulence and stochastic processes: Kolmogorov's ideas 50 years on.

[44] D. P. Lathrop, J. Fineberg, and H. L. Swinney, *Turbulent flow between concentric rotating cylinders at large Reynolds number*, Physical review letters **68** (1992), no. 10, 1515.

[45] W. J. Layton, *Energy dissipation in the Smagorinsky model of turbulence*, Appl. Math. Lett. **59** (2016), 56–59.

[46] W. J. Layton, *Energy dissipation bounds for shear flows for a model in large eddy simulation*, Math. Comput. Modelling **35** (2002), no. 13, 1445–1451.

[47] W. J. Layton, *Introduction to the numerical analysis of incompressible viscous flows*, Computational Science & Engineering, vol. 6, Society for Industrial and Applied Mathematics (SIAM), Philadelphia, PA, 2008.

[48] J. Leray, *Sur le mouvement dun liquide visqueux emplissant lespace*, Acta Math. **63** (1934), 193-248.

[49] M. Lesieur, *Turbulence in fluids*, 3rd ed., Fluid Mechanics and its Applications, vol. 40, Kluwer Academic Publishers Group, Dordrecht, 1997.

[50] D. K. Lilly, *The representation of small-scale turbulence in numerical simulation experiments*, IBM Scientific Computing Symposium on Environmental Sciences (1967).

[51] J. L. Lumley, *Some comments on turbulence*, Physics of Fluids A **4** (1992), 203-211.

[52] M. T. Manzari, *An explicit finite element algorithm for convection heat transfer problems*, International Journal of Numerical Methods for Heat and Fluid Flow **9** (1999), 860–877.

[53] C. Marchioro, *Remark on the energy dissipation in shear driven turbulence*, Phys. D **74** (1994), no. 3-4, 395–398.

[54] N. MazellierJ and C. Vassilicos, *The turbulence dissipation constant is not universal because of its universal dependence on large-scale flow topology*, Physics of Fluids **20** (2008).

[55] N. Massarott, P. Nithiarasu, and O. C. Zienkiewicz, *Characteristic-based-split(CBS) algorithm for incompressible flow problems with heat transfer*, nternational Journal of Numerical Methods for Heat and Fluid Flow **8** (1998), 969–990.

[56] W. D. McComb, A. Berera, S. R. Yoffe, and M. F. Linkmann, *Energy transfer and dissipation in forced isotropic turbulence*, Phys. Rev. E **91** (2015).

[57] P. Moin and J. Kim, *Numerical investigation of turbulent channel flow*, Journal of Fluid Mechanics **118** (1982), 341–377.

[58] R. Moser, J. Kim, and N. Mansour, *Direct Numerical Simulation of Turbulent Channel Flow up to $\mathcal{R}e_\tau$=590*, Phys. Fluids **11** (1998), 943945.

[59] A. Muschinski, *A similarity theory of locally homogeneous and isotropic turbulence generated by a Smagorinsky-type LES*, JFM **325** (1996), 239–260.

[60] R. Nicodemus, S. Grossmann, and M. Holthaus, *Towards lowering dissipation bounds for turbulent flows*, The European Physical Journal B **10** (1999), no. 2, 385–396.

[61] R. Nicodemus, S. Grossmann, and M. Holthaus, *Variational bound on energy dissipation in plane Couette flow*, Physical Review E **56** (1997), no. 6, 6774.

[62] A. Pakzad, *Damping functions correct over-dissipation of the Smagorinsky Model*, Mathematical Methods in the Applied Sciences **40** (2017), no. 16, 5933–5945.

[63] A. Pakzad, *Analysis of mesh effects on turbulence statistics,* Journal of Mathematical Analysis and Applications, arXiv:1804.00745 (2018).

[64] C. Parés, *Approximation de la solution des équations d'un modèle de turbulence par une méthode de Lagrange-Galerkin*, Rev. Mat. Apl. **15** (1994), no. 2, 63–124.

[65] U. Piomelli and E. Balaras, *Wall-layer models for largeeddy simulations*, Annual Review of Fluid Mechanics **34** (2002), 349–374.

[66] S. B. Pope, *Ten questions concerning the large-eddy simulation of turbulent flows*, New Journal of Physics **6** (2004).

[67] S. B. Pope, *Turbulent flows*, Cambridge University Press, Cambridge, 2000.

[68] H. Reichardt, *Gesetzmassigkeiten der geradlinigen turbulenten Couettestromung*, Report No. 22 of the Max-Planck-Institut fur Stromungsforschung und Aerodynamische versuchsanstalt, Gottingen (1959).

[69] L. F. Richardson, *weather prediction by numerical process*, Cambridge, UK: Cambridge Univ. Press, 1922.

[70] P. G. Saffman, *485-614 in: Topics in Nonlinear Physics, N. Zabusky (ed.)*, Springer-Verlag, New York, 1968.

[71] P. Sagaut, *Large eddy simulation for incompressible flows*, Scientific Computation, Springer-Verlag, Berlin, 2001. An introduction; With an introduction by Marcel Lesieur; Translated from the 1998 French original by the author.

[72] U. Schumann, *Subgrid scale model for finite difference simulations of turbulent flows in plane channels and annuli*, Journal of Computational Physics **18** (1975), 376–404.

[73] C. Seis, *Scaling bounds on dissipation in turbulent flows*, J. Fluid Mech. **777** (2015), 591-603.

[74] K. R. Sreenivasan, *The energy dissipation in turbulent shear flows*, Symposium on Developments in Fluid Dynamics and Aerospace Engineering, 1995, pp. 159–190.

[75] K. R. Sreenivasan, *An update on the energy dissipation rate in isotropic turbulence*, Phys. Fluids **10** (1998), no. 2, 528–529.

[76] K. R. Sreenivasan, *On the scaling of the turbulent energy dissipation rate*, Phys. Fluids **27** (1984), 1048–1051.

[77] J. Smagorinsky, *General circulation experiments with the primitive equations. I. The basic experiment*, Mon, Weather Rev. **91** (1963), 99–164.

[78] Z. Si, X. Song, and P. Huang, *Modified Characteristics GaugeUzawa Finite Element Method for Time Dependent Conduction-Convection Problems*, J. Sci. Comput. **58** (2014), 1–24.

[79] Z. Si, Y. He, and K. Wang, *A defect-correction method for unsteady conduction convection problems I: spatial discretization*, Science China Mathematics **54** (2011), 185–204.

[80] A. Swierczewska, *A dynamical approach to large eddy simulation of turbulent flows: existence of weak solutions*, Mathematical Methods in the Applied Sciences **29** (2006), 99–121.

[81] G. I. Taylor, *statistical theory of turbulence*, Proc. R. Soc. Lond A 151:421-44 (1935).

[82] D. J. Tritton, *Physical Fluid Dynamics, 2nd edition*, Oxford Science Publications, 1988.

[83] E. R. van Driest, *On turbulent flow near a wall*, Journal of the Aeronautical Science **23** (1956), 1007.

[84] X. Wang, *Approximation of stationary statistical properties of dissipative dynamical systems: time discretization*, Mathematics of Computation **79** (2010), no. 269, 259-280.

[85] X. Wang, *Time-averaged energy dissipation rate for shear driven flows in* $\mathbf{R}^n$, Phys. D **99** (1997), no. 4, 555–563.

[86] D. C. Wilcox, *Turbulence modeling for CFD*, DCW Industries, Inc., 2006.

[87] J. Wu, D. Gui, D. Liu, and X. Feng, *The characteristic variational multiscale method for time dependent conduction-convection problems*, Int. Comm. Heat Mass Trans. **68** (2015), 58–68.